Supporting information: Histogram-free reweighting with grand canonical Monte Carlo: Post-simulation optimization of non-bonded potentials for phase equilibria

Richard A. Messerly,*,† Mohammad S. Barhaghi,‡ Jeffrey J. Potoff,‡ and Michael R. Shirts¶

†Thermodynamics Research Center, National Institute of Standards and Technology, Boulder, Colorado, 80305, United States

‡Department of Chemical Engineering and Materials Science, Wayne State University, Detroit, Michigan 48202, United States

¶Department of Chemical and Biological Engineering, University of Colorado, Boulder, Colorado, 80309, United States

E-mail: richard.messerly@nist.gov

S1 Bonded parameters

Table S1: Equilibrium (fixed) bond lengths (r_{eq}). CH_x and CH_y represent CH_3 , $CH_2(sp^3)$, $CH(sp^3)$, or $C(sp^3)$ sites.

Bond sites	$r_{ m eq}$ (nm)				
	TraPPE MiPPE NERD				
$CH_x\text{-}CH_y$	0.154	0.154	0.154		
$C(sp)$ - CH_x	_	0.146	_		
CH≡CH	_	0.121	_		
C≡CH	_	0.121	_		

Table S2: Equilibrium bond angles (θ_{eq}) and force constants (k_{θ}/k_{B}) , where k_{B} is the Boltzmann constant.

Bending sites	$\theta_{ m eq}$ (degrees)			$k_{ heta}/k_{ m B}$ (K/rad ²)
	TraPPE	MiPPE	NERD	
CH_x - CH_2 - CH_y	114.0	114.0	114.0	62500
CH_x - CH - CH_y	112.0	112.0	109.5	62500
$CH_x\text{-}C\text{-}CH_y$	109.5	109.5	109.5	62500
CH_x - CH_2 - $C(sp)$	_	112	_	62500
CH_x - $C(sp)\equiv CH$	_	180	_	30800
CH_x - $C(sp)\equiv C$	_	180	_	30800

Table S3: Fourier constants (c_n/k_B) in units of K.

Torsion sites	$c_0/k_{ m B}$	$c_1/k_{ m B}$	$c_2/k_{ m B}$	$c_3/k_{ m B}$
CH_x - CH_2 - CH_y	0.0	355.03	-68.19	791.32
CH_x - CH_2 - CH - CH_y	-251.06	428.73	-111.85	441.27
CH_x - CH_2 - C - CH_y	0.0	0.0	0.0	461.29
$CH_x\text{-}CH\text{-}CH\text{-}CH_y$	-251.06	428.73	-111.85	441.27
CH_x - CH_2 - $C(sp)$	94.88	162.00	-205.40	980.40
CH_x - CH_2 - $C(sp)\equiv C(sp)$	0	0	0	0
CH_x - CH_2 - $C(sp)$ $\equiv CH(sp)$	0	0	0	0
CH_x - $C(sp)\equiv C(sp)$ - CH_y	0	0	0	0

S2 Fixed vs. flexible bonds

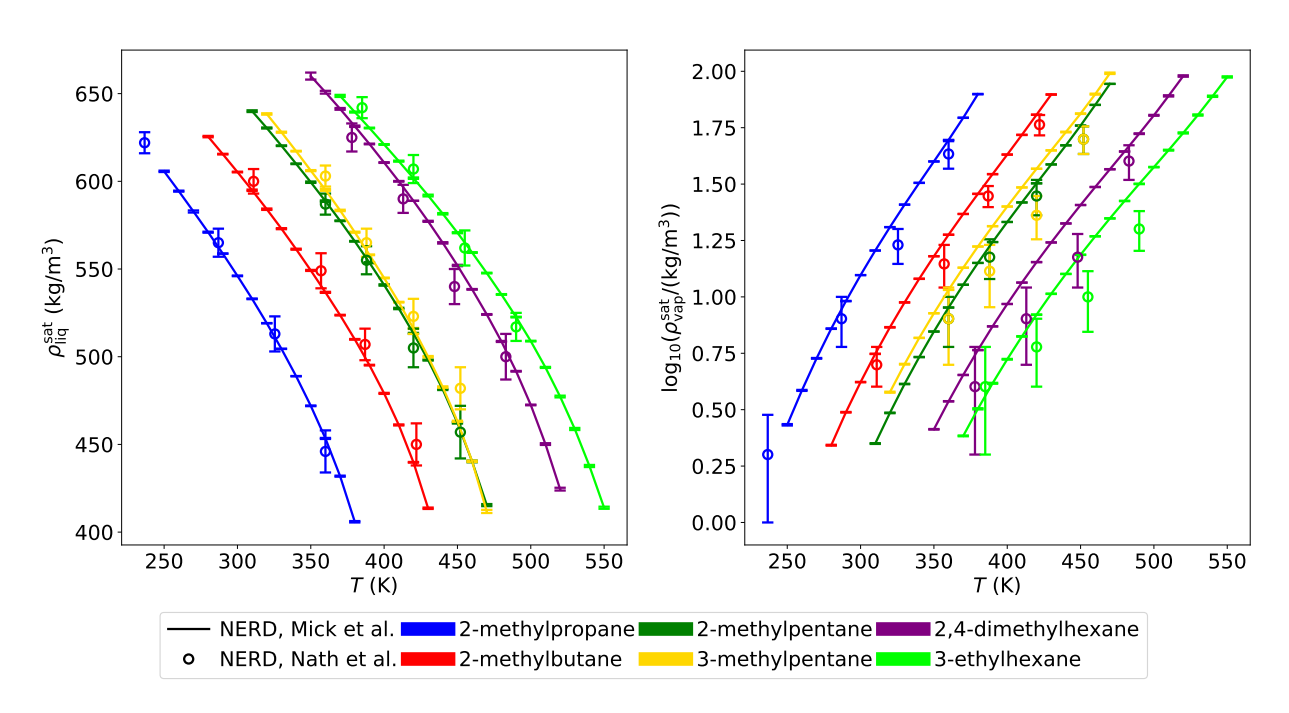


Figure S1: Comparison of saturated liquid (left panel) and vapor (right panel) densities for fixed (Mick et al.) and flexible (Nath et al.) bonds. Mick et al. used GCMC-HR while Nath et al. utilized GEMC. Note that Nath et al. did not report tabulated values for vapor pressure or enthalpy of vaporization.

S3 CBMC acceptance rates

Table S4: Percentage acceptance of CBMC moves for cyclohexane with MiPPE force field. Averages were computed from 20 replicate simulations with $L_{\rm box}$ = 3.0 nm.

T(K)	μ (K)	Acceptance (%)
450	-4370	68.8
500	-4370	75.1
550	-4370	39.5
500	-4135	5.50
460	-4025	2.20
410	-3890	1.11
360	-3790	0.19

S4 Compiler and hardware

With the exception of the 20 replicates performed for MiPPE cyclohexane (3.0 and 3.5 nm box length) and TAMie cyclohexane, all simulations are run on a Linux 4.4.0-112-generic x86_64 on an Intel(R) Xeon(R) CPU E5-2699 v4 @ 2.20GHz machine. On this machine, GOMC was erroneously compiled using the sub-optimal GNU compiler collection (GCC) instead of the preferred Intel compiler. GOMC compiled with the Intel compiler typically runs approximately twice as fast as GOMC compiled with the GCC compiler.

The 20 replicate simulations for MiPPE cyclohexane (3.0 and 3.5 nm box length) and TAMie cyclohexane utilize several different machine hardware architectures, listed in Table S5. GOMC was compiled with the Intel compiler on each of these machines.

Table S5: Machine hardware for 20 replicate simulations of MiPPE cyclohexane

Intel(R) Core(TM) i7-4790K CPU @ 4.00GHz Intel(R) Core(TM) i5-3570 CPU @ 3.40GHz Intel(R) Core(TM) i5-2500K CPU @ 3.30GHz Intel(R) Xeon(R) CPU X5450 @ 3.00GHz Intel(R) Xeon(R) CPU X5355 @ 2.66GHz Intel(R) Xeon(R) CPU E5-2640 v3 @ 2.60GHz Intel(R) Core(TM)2 Quad CPU Q6600 @ 2.40GHz

S5 ϵ -scaling

S5.1 Tabulated ψ values

Table S6: Optimal ϵ -scaling parameter (ψ) values and corresponding scoring function. Abbreviations correspond to those in Figure 2.

Molecular name	Abbreviation	Optimal ψ	Optimal score
	Branched alka	nes	
2-methylpropane	$2MC_3$	1.0015	0.3883
2-methylbutane	$2MC_4$	1.0025	0.4281
2-methylpentane	$2MC_5$	1.0020	0.4770
3-methylpentane	$3MC_5$	1.0103	0.4050
2,2-dimethylpropane	$22DMC_3$	1.0035	0.5132
2,2-dimethylbutane	$22DMC_4$	0.9985	0.5445
2,3-dimethylbutane	$23DMC_4$	1.0000	0.4724
2,2,4-trimethylpentane	$234TMC_5$	1.0005	0.4367
	Alkynes		
1-ethyne	C_2	1.0005	0.2931
1-propyne	C_3	0.9965	0.3307
1-butyne	$1C_4$	1.0063	1.143
2-butyne	$2C_4$	1.0031	0.3191
1-pentyne	$1C_5$	1.0087	1.8505
2-pentyne	$2C_5$	1.0186	1.3801
1-hexyne	$1C_6$	1.0063	1.908
2-hexyne	$2C_6$	1.0228	1.0594
1-heptyne	$1C_7$	1.0066	0.8415
1-octyne	$1C_8$	1.0034	0.9777
1-nonyne	1C ₉	1.0000	0.9128

S5.2 Tabulated phase equilibria for optimal ψ

S5.2.1 Branched alkanes

Table S7: GCMC-MBAR results for 2-methylpropane with the iMiPPE force field (optimal ψ value from Table S6). Subscripts correspond to the 95% confidence interval computed with bootstrap re-sampling.

$T^{\mathrm{sat}}(K)$	$ ho_{ m liq}^{ m sat}$ (kg/m ³)	$ ho_{ m vap}^{ m sat}$ (kg/m ³)	$P_{\mathrm{vap}}^{\mathrm{sat}}$ (MPa)	$\Delta H_{\rm v}$ (kJ/mol)	$Z_{ m vap}^{ m sat}$
390	$390.5_{4.5}$	$85.7_{2.5}$	$2.718_{0.030}$	$9.90_{0.20}$	$0.569_{0.011}$
380	$418.0_{2.3}$	$65.5_{2.0}$	$2.272_{0.017}$	$11.81_{0.14}$	$0.639_{0.016}$
370	$440.86_{0.43}$	$51.3_{1.3}$	$1.8856_{0.0088}$	$13.31_{0.11}$	$0.695_{0.015}$
360	$460.16_{0.83}$	$40.72_{0.64}$	$1.5515_{0.0048}$	$14.524_{0.080}$	$0.740_{0.011}$
350	$477.25_{0.86}$	$32.43_{0.28}$	$1.2638_{0.0038}$	$15.559_{0.056}$	$0.78_{0.01}$
340	$492.86_{0.74}$	$25.78_{0.16}$	$1.0177_{0.0034}$	$16.473_{0.048}$	$0.81_{0.01}$
330	$507.34_{0.80}$	$20.38_{0.14}$	$0.8090_{0.0033}$	$17.292_{0.053}$	$0.84_{0.01}$
320	$521.13_{0.61}$	$15.97_{0.11}$	$0.6336_{0.0034}$	$18.042_{0.053}$	$0.87_{0.01}$
310	$534.54_{0.29}$	$12.374_{0.074}$	$0.4881_{0.0036}$	$18.745_{0.042}$	$0.89_{0.01}$
300	$547.12_{0.22}$	$9.452_{0.060}$	$0.3690_{0.0035}$	$19.389_{0.035}$	$0.910_{0.010}$
290	$558.97_{0.19}$	$7.101_{0.076}$	$0.2732_{0.0032}$	$19.980_{0.039}$	$0.927_{0.012}$
280	$570.80_{0.34}$	$5.230_{0.094}$	$0.1975_{0.0027}$	$20.552_{0.048}$	$0.943_{0.019}$
270	$582.96_{0.45}$	$3.76_{0.10}$	$0.1389_{0.0025}$	$21.122_{0.071}$	$0.956_{0.034}$
260	$593.85_{0.25}$	$2.63_{0.10}$	$0.0946_{0.0027}$	$21.62_{0.12}$	$0.966_{0.060}$
250	$603.32_{0.94}$	$1.787_{0.089}$	$0.0623_{0.0034}$	$22.06_{0.24}$	$0.97_{0.10}$

Table S8: GCMC-MBAR results for 2-methylbutane with the iMiPPE force field (optimal ψ value from Table S6). Subscripts correspond to the 95% confidence interval computed with bootstrap re-sampling.

$T^{\mathrm{sat}}\left(\mathbf{K}\right)$	$ ho_{ m liq}^{ m sat}$ (kg/m ³)	$ ho_{ m vap}^{ m sat}$ (kg/m ³)	$P_{ m vap}^{ m sat}$ (MPa)	$\Delta H_{\rm v}$ (kJ/mol)	$Z_{ m vap}^{ m sat}$
440	$403.0_{2.4}$	$84.5_{1.4}$	$2.490_{0.015}$	$11.80_{0.11}$	$0.58_{0.01}$
430	$429.5_{1.4}$	$67.3_{1.1}$	$2.1160_{0.0099}$	$13.658_{0.094}$	$0.63_{0.01}$
420	$451.56_{0.83}$	$53.86_{0.75}$	$1.7868_{0.0058}$	$15.259_{0.071}$	$0.69_{0.01}$
410	$470.40_{0.84}$	$43.55_{0.44}$	$1.4985_{0.0031}$	$16.608_{0.052}$	$0.73_{0.01}$
400	$487.2_{1.1}$	$35.38_{0.25}$	$1.2466_{0.0017}$	$17.769_{0.044}$	$0.76_{0.01}$
390	$502.5_{1.3}$	$28.74_{0.17}$	$1.0277_{0.0016}$	$18.796_{0.044}$	$0.80_{0.01}$
380	$516.7_{1.4}$	$23.25_{0.13}$	$0.8385_{0.0025}$	$19.723_{0.041}$	$0.82_{0.01}$
370	$530.1_{1.2}$	$18.699_{0.091}$	$0.6765_{0.0033}$	$20.574_{0.033}$	$0.85_{0.01}$
360	$542.77_{0.83}$	$14.917_{0.061}$	$0.5388_{0.0038}$	$21.360_{0.027}$	$0.87_{0.01}$
350	$554.94_{0.49}$	$11.782_{0.058}$	$0.4234_{0.0039}$	$22.094_{0.027}$	$0.89_{0.01}$
340	$566.86_{0.43}$	$9.196_{0.079}$	$0.3274_{0.0037}$	$22.793_{0.033}$	$0.91_{0.01}$
330	$578.69_{0.60}$	$7.08_{0.10}$	$0.2489_{0.0032}$	$23.467_{0.052}$	$0.925_{0.011}$
320	$589.78_{0.55}$	$5.36_{0.12}$	$0.1856_{0.0027}$	$24.087_{0.073}$	$0.939_{0.019}$
310	$599.68_{0.39}$	$3.99_{0.12}$	$0.1354_{0.0024}$	$24.634_{0.10}$	$0.951_{0.031}$
300	$609.37_{0.41}$	$2.90_{0.11}$	$0.0965_{0.0025}$	$25.16_{0.14}$	$0.961_{0.050}$
290	$619.67_{0.47}$	$2.065_{0.092}$	$0.0670_{0.0030}$	$25.71_{0.20}$	$0.971_{0.076}$

Table S9: GCMC-MBAR results for 2-methylpentane with the iMiPPE force field (optimal ψ value from Table S6). Subscripts correspond to the 95% confidence interval computed with bootstrap re-sampling.

$T^{\mathrm{sat}}(\mathbf{K})$	$ ho_{ m liq}^{ m sat}$ (kg/m ³)	$ ho_{ m vap}^{ m sat}$ (kg/m ³)	$P_{\mathrm{vap}}^{\mathrm{sat}}$ (MPa)	$\Delta H_{\rm v}$ (kJ/mol)	$Z_{ m vap}^{ m sat}$
470	$424.43_{0.72}$	$75.06_{0.98}$	$2.0415_{0.0063}$	$14.355_{0.063}$	$0.60_{0.01}$
460	$446.63_{0.44}$	$59.92_{0.85}$	$1.7383_{0.0032}$	$16.259_{0.079}$	$0.65_{0.01}$
450	$466.02_{0.34}$	$48.40_{0.58}$	$1.4722_{0.0024}$	$17.883_{0.082}$	$0.70_{0.01}$
440	$483.12_{0.37}$	$39.46_{0.30}$	$1.2388_{0.0030}$	$19.257_{0.075}$	$0.74_{0.01}$
430	$498.62_{0.46}$	$32.30_{0.13}$	$1.0347_{0.0032}$	$20.456_{0.064}$	$0.77_{0.01}$
420	$513.07_{0.46}$	$26.404_{0.097}$	$0.8567_{0.0028}$	$21.538_{0.049}$	$0.80_{0.01}$
410	$526.79_{0.34}$	$21.50_{0.12}$	$0.7026_{0.0021}$	$22.536_{0.031}$	$0.83_{0.01}$
400	$539.84_{0.33}$	$17.39_{0.13}$	$0.5701_{0.0016}$	$23.462_{0.027}$	$0.85_{0.01}$
390	$552.17_{0.47}$	$13.96_{0.12}$	$0.4573_{0.0015}$	$24.320_{0.043}$	$0.87_{0.01}$
380	$563.75_{0.44}$	$11.10_{0.10}$	$0.3622_{0.0018}$	$25.113_{0.052}$	$0.890_{0.011}$
370	$574.77_{0.27}$	$8.738_{0.085}$	$0.2829_{0.0022}$	$25.853_{0.051}$	$0.907_{0.015}$
360	$585.55_{0.30}$	$6.794_{0.076}$	$0.2177_{0.0027}$	$26.562_{0.058}$	$0.922_{0.021}$
350	$596.34_{0.30}$	$5.208_{0.079}$	$0.1647_{0.0031}$	$27.257_{0.083}$	$0.936_{0.030}$
340	$606.99_{0.31}$	$3.928_{0.084}$	$0.1222_{0.0035}$	$27.93_{0.12}$	$0.948_{0.045}$
330	$617.01_{0.30}$	$2.909_{0.083}$	$0.0888_{0.0039}$	$28.55_{0.18}$	$0.959_{0.067}$
320	$626.41_{0.21}$	$2.111_{0.076}$	$0.0631_{0.0043}$	$29.13_{0.26}$	$0.968_{0.099}$

Table S10: GCMC-MBAR results for 3-methylpentane with the iMiPPE force field (optimal ψ value from Table S6). Subscripts correspond to the 95% confidence interval computed with bootstrap re-sampling.

$T^{\mathrm{sat}}(\mathbf{K})$	$ ho_{ m liq}^{ m sat}$ (kg/m ³)	$ ho_{ m vap}^{ m sat}$ (kg/m ³)	$P_{\mathrm{vap}}^{\mathrm{sat}}$ (MPa)	$\Delta H_{\rm v}$ (kJ/mol)	$Z_{ m vap}^{ m sat}$
480	$428.2_{1.5}$	75_{12}	$2.171_{0.060}$	$14.81_{0.93}$	$0.625_{0.090}$
470	$449.9_{1.6}$	$61.1_{8.5}$	$1.863_{0.021}$	$16.56_{0.84}$	$0.672_{0.089}$
460	$468.1_{1.3}$	$50.3_{4.0}$	$1.5910_{0.0071}$	$18.01_{0.53}$	$0.712_{0.060}$
450	$484.5_{1.2}$	$41.6_{1.1}$	$1.350_{0.014}$	$19.28_{0.23}$	$0.747_{0.027}$
440	$500.3_{1.1}$	$34.45_{0.21}$	$1.137_{0.015}$	$20.464_{0.074}$	$0.78_{0.01}$
430	$515.5_{1.0}$	$28.41_{0.46}$	$0.950_{0.013}$	$21.563_{0.068}$	$0.81_{0.01}$
420	$529.38_{0.62}$	$23.34_{0.40}$	$0.786_{0.010}$	$22.556_{0.054}$	$0.83_{0.01}$
410	$541.89_{0.69}$	$19.07_{0.30}$	$0.6449_{0.0079}$	$23.443_{0.043}$	$0.85_{0.01}$
400	$553.62_{0.90}$	$15.49_{0.24}$	$0.5233_{0.0062}$	$24.264_{0.049}$	$0.88_{0.01}$
390	$565.07_{0.63}$	$12.48_{0.20}$	$0.4198_{0.0048}$	$25.051_{0.039}$	$0.89_{0.01}$
380	$575.97_{0.45}$	$9.95_{0.17}$	$0.3326_{0.0039}$	$25.789_{0.043}$	$0.912_{0.014}$
370	586_{95}	$7.8_{1.6}$	$0.260_{0.066}$	$26.5_{4.1}$	$0.93_{0.18}$
360	$597.06_{0.27}$	$6.10_{0.13}$	$0.2001_{0.0035}$	$27.178_{0.094}$	$0.945_{0.029}$
350	$607.29_{0.23}$	$4.67_{0.12}$	$0.1514_{0.0039}$	$27.83_{0.14}$	$0.959_{0.043}$

Table S11: GCMC-MBAR results for 2,2-dimethylpropane with the iMiPPE force field (optimal ψ value from Table S6). Subscripts correspond to the 95% confidence interval computed with bootstrap re-sampling.

T ^{sat} (K)	$ ho_{ m liq}^{ m sat}$ (kg/m ³)	$ ho_{ m vap}^{ m sat}$ (kg/m ³)	P _{vap} (MPa)	$\Delta H_{\rm v}$ (kJ/mol)	$Z_{ m vap}^{ m sat}$
410	$413.2_{2.6}$	$75.9_{2.6}$	$2.173_{0.029}$	$11.65_{0.11}$	$0.606_{0.013}$
400	$437.1_{2.3}$	$59.3_{1.8}$	$1.831_{0.018}$	$13.410_{0.083}$	$0.669_{0.014}$
390	$457.4_{1.5}$	$47.4_{1.1}$	$1.532_{0.010}$	$14.814_{0.051}$	$0.719_{0.013}$
380	$474.6_{1.1}$	$38.29_{0.72}$	$1.2725_{0.0056}$	$15.944_{0.045}$	$0.759_{0.011}$
370	$489.78_{0.98}$	$31.00_{0.48}$	$1.0468_{0.0035}$	$16.909_{0.045}$	$0.792_{0.011}$
360	$504.12_{0.89}$	$25.02_{0.33}$	$0.8520_{0.0036}$	$17.785_{0.044}$	$0.821_{0.012}$
350	$518.05_{0.86}$	$20.05_{0.21}$	$0.6853_{0.0043}$	$18.604_{0.046}$	$0.847_{0.011}$
340	$531.32_{0.93}$	$15.93_{0.18}$	$0.5437_{0.0045}$	$19.363_{0.057}$	$0.871_{0.011}$
330	$543.65_{0.96}$	$12.52_{0.23}$	$0.4252_{0.0041}$	$20.056_{0.078}$	$0.893_{0.016}$
320	$555.0_{1.0}$	$9.71_{0.28}$	$0.3271_{0.0037}$	$20.68_{0.11}$	$0.913_{0.029}$
310	$565.5_{1.4}$	$7.43_{0.32}$	$0.2473_{0.0044}$	$21.25_{0.18}$	$0.931_{0.052}$
300	$576.4_{1.8}$	$5.60_{0.33}$	$0.1832_{0.0061}$	$21.82_{0.28}$	$0.947_{0.087}$
290	$588.4_{1.3}$	$4.13_{0.32}$	$0.1327_{0.0084}$	$22.41_{0.38}$	$0.96_{0.14}$
280	$600.2_{1.1}$	$2.98_{0.29}$	$0.093_{0.011}$	$22.98_{0.55}$	$0.97_{0.22}$

Table S12: GCMC-MBAR results for 2,2-dimethylbutane with the iMiPPE force field (optimal ψ value from Table S6). Subscripts correspond to the 95% confidence interval computed with bootstrap re-sampling.

T ^{sat} (K)	$ ho_{ m liq}^{ m sat}$ (kg/m ³)	$ ho_{ m vap}^{ m sat}$ (kg/m ³)	P _{vap} (MPa)	$\Delta H_{ m v}$ (kJ/mol)	$Z_{ m vap}^{ m sat}$
470	$410.4_{5.2}$	86.7 _{8.5}	$2.34_{0.11}$	$12.61_{0.20}$	$0.595_{0.027}$
460	$436.5_{4.9}$	$70.3_{8.7}$	$2.014_{0.071}$	$14.48_{0.34}$	$0.645_{0.049}$
450	$457.9_{3.1}$	$57.7_{7.2}$	$1.724_{0.036}$	$16.04_{0.45}$	$0.689_{0.061}$
440	$476.4_{1.5}$	$47.7_{4.6}$	$1.467_{0.011}$	$17.37_{0.41}$	$0.725_{0.057}$
430	$493.01_{0.95}$	$39.4_{2.1}$	$1.2386_{0.0045}$	$18.53_{0.25}$	$0.757_{0.039}$
420	$508.03_{0.71}$	$32.56_{0.58}$	$1.0375_{0.0094}$	$19.573_{0.098}$	$0.786_{0.020}$
410	$521.74_{0.38}$	$26.79_{0.14}$	$0.862_{0.010}$	$20.513_{0.035}$	$0.81_{0.01}$
400	$534.75_{0.29}$	$21.94_{0.16}$	$0.7088_{0.0094}$	$21.383_{0.026}$	$0.84_{0.01}$
390	$547.49_{0.34}$	$17.86_{0.11}$	$0.5771_{0.0086}$	$22.210_{0.027}$	$0.859_{0.010}$
380	$559.93_{0.37}$	$14.416_{0.067}$	$0.4643_{0.0081}$	$22.998_{0.038}$	$0.878_{0.013}$
370	$571.83_{0.42}$	$11.528_{0.058}$	$0.3687_{0.0077}$	$23.738_{0.053}$	$0.896_{0.017}$
360	$582.92_{0.45}$	$9.115_{0.074}$	$0.2885_{0.0074}$	$24.416_{0.062}$	$0.911_{0.022}$
350	$593.10_{0.52}$	$7.115_{0.099}$	$0.2224_{0.0070}$	$25.030_{0.081}$	$0.925_{0.029}$
340	$602.70_{0.55}$	$5.47_{0.12}$	$0.1685_{0.0067}$	$25.60_{0.11}$	$0.938_{0.041}$
330	$612.20_{0.41}$	$4.14_{0.14}$	$0.1253_{0.0065}$	$26.15_{0.16}$	$0.949_{0.061}$
320	$621.65_{0.33}$	$3.08_{0.13}$	$0.0912_{0.0065}$	$26.69_{0.23}$	$0.959_{0.091}$
310	$631.20_{0.30}$	$2.24_{0.12}$	$0.0649_{0.0068}$	$27.22_{0.34}$	$0.97_{0.14}$

Table S13: GCMC-MBAR results for 2,3-dimethylbutane with the iMiPPE force field (optimal ψ value from Table S6). Subscripts correspond to the 95% confidence interval computed with bootstrap re-sampling.

$T^{\mathrm{sat}}\left(\mathbf{K}\right)$	$ ho_{ m liq}^{ m sat}$ (kg/m ³)	$ ho_{ m vap}^{ m sat}$ (kg/m ³)	$P_{\mathrm{vap}}^{\mathrm{sat}}$ (MPa)	$\Delta H_{\rm v}$ (kJ/mol)	$Z_{ m vap}^{ m sat}$
480	$411.7_{1.1}$	$88.4_{2.2}$	$2.369_{0.027}$	$12.87_{0.14}$	$0.58_{0.01}$
470	$437.1_{1.0}$	$71.6_{2.1}$	$2.037_{0.019}$	$14.80_{0.17}$	$0.627_{0.013}$
460	$459.23_{0.86}$	$58.1_{1.6}$	$1.742_{0.013}$	$16.53_{0.18}$	$0.676_{0.015}$
450	$478.07_{0.79}$	$47.5_{1.1}$	$1.4813_{0.0074}$	$18.00_{0.16}$	$0.718_{0.014}$
440	$494.54_{0.81}$	$39.07_{0.72}$	$1.2513_{0.0041}$	$19.26_{0.13}$	$0.754_{0.012}$
430	$509.51_{0.77}$	$32.20_{0.43}$	$1.0493_{0.0024}$	$20.37_{0.10}$	$0.79_{0.01}$
420	$523.51_{0.64}$	$26.49_{0.25}$	$0.8726_{0.0019}$	$21.382_{0.079}$	$0.81_{0.01}$
410	$536.78_{0.54}$	$21.70_{0.15}$	$0.7189_{0.0020}$	$22.310_{0.063}$	$0.84_{0.01}$
400	$549.39_{0.59}$	$17.68_{0.10}$	$0.5863_{0.0021}$	$23.171_{0.060}$	$0.86_{0.01}$
390	$561.38_{0.73}$	$14.296_{0.082}$	$0.4727_{0.0023}$	$23.971_{0.062}$	$0.88_{0.01}$
380	$572.70_{0.68}$	$11.455_{0.085}$	$0.3764_{0.0025}$	$24.712_{0.056}$	$0.896_{0.011}$
370	$583.42_{0.40}$	$9.083_{0.092}$	$0.2957_{0.0028}$	$25.402_{0.050}$	$0.912_{0.016}$
360	$593.75_{0.21}$	$7.115_{0.095}$	$0.2289_{0.0033}$	$26.054_{0.064}$	$0.926_{0.024}$
350	$603.97_{0.20}$	$5.497_{0.091}$	$0.1742_{0.0037}$	$26.686_{0.091}$	$0.938_{0.034}$
340	$614.11_{0.22}$	$4.179_{0.082}$	$0.1302_{0.0042}$	$27.30_{0.13}$	$0.950_{0.047}$
330	$623.72_{0.26}$	$3.121_{0.069}$	$0.0953_{0.0047}$	$27.87_{0.18}$	$0.959_{0.066}$
320	$632.83_{0.34}$	$2.284_{0.057}$	$0.0682_{0.0050}$	$28.41_{0.25}$	$0.968_{0.092}$

Table S14: GCMC-MBAR results for 2,2,4-trimethylpentane with the iMiPPE force field (optimal ψ value from Table S6). Subscripts correspond to the 95% confidence interval computed with bootstrap re-sampling.

$T^{\mathrm{sat}}(\mathbf{K})$	$\rho_{\rm liq}^{\rm sat}$ (kg/m ³)	$ ho_{ m vap}^{ m sat}$ (kg/m ³)	$P_{\mathrm{vap}}^{\mathrm{sat}}$ (MPa)	$\Delta H_{\rm v}$ (kJ/mol)	$Z_{ m vap}^{ m sat}$
530	$401.6_{2.0}$	$97.3_{2.8}$	$2.113_{0.013}$	$13.65_{0.15}$	$0.563_{0.014}$
520	$428.08_{0.71}$	$79.0_{1.7}$	$1.8383_{0.0085}$	$15.95_{0.17}$	$0.615_{0.012}$
510	$449.27_{0.69}$	$64.82_{0.80}$	$1.5924_{0.0067}$	$17.85_{0.12}$	$0.66_{0.01}$
500	$467.26_{0.83}$	$53.68_{0.34}$	$1.3733_{0.0059}$	$19.449_{0.068}$	$0.70_{0.01}$
490	$484.19_{0.91}$	$44.67_{0.32}$	$1.1784_{0.0050}$	$20.898_{0.058}$	$0.74_{0.01}$
480	$500.20_{0.83}$	$37.25_{0.39}$	$1.0051_{0.0038}$	$22.224_{0.066}$	$0.77_{0.01}$
470	$514.73_{0.48}$	$31.08_{0.39}$	$0.8515_{0.0027}$	$23.414_{0.060}$	$0.80_{0.01}$
460	$527.91_{0.42}$	$25.89_{0.30}$	$0.7160_{0.0022}$	$24.486_{0.050}$	$0.83_{0.01}$
450	$540.02_{0.69}$	$21.49_{0.18}$	$0.5973_{0.0026}$	$25.458_{0.051}$	$0.85_{0.01}$
440	$551.36_{0.72}$	$17.746_{0.095}$	$0.4939_{0.0030}$	$26.355_{0.050}$	$0.87_{0.01}$
430	$562.92_{0.74}$	$14.553_{0.071}$	$0.4046_{0.0031}$	$27.239_{0.050}$	$0.89_{0.01}$
420	$574.83_{0.92}$	$11.836_{0.082}$	$0.3278_{0.0033}$	$28.116_{0.049}$	$0.906_{0.013}$
410	$585.23_{0.62}$	$9.54_{0.11}$	$0.2626_{0.0037}$	$28.885_{0.042}$	$0.922_{0.022}$
400	$594.42_{0.22}$	$7.62_{0.14}$	$0.2078_{0.0042}$	$29.567_{0.098}$	$0.937_{0.036}$
390	$604.54_{0.21}$	$6.02_{0.18}$	$0.1623_{0.0051}$	$30.29_{0.17}$	$0.949_{0.058}$
380	$615.63_{0.16}$	$4.70_{0.20}$	$0.1247_{0.0061}$	$31.04_{0.27}$	$0.959_{0.089}$
370	$625.43_{0.14}$	$3.62_{0.20}$	$0.0942_{0.0072}$	$31.71_{0.40}$	$0.97_{0.13}$

S5.2.2 Alkynes

Table S15: GCMC-MBAR results for ethyne with the iMiPPE force field (optimal ψ value from Table S6). Subscripts correspond to the 95% confidence interval computed with bootstrap re-sampling.

$T^{\mathrm{sat}}(\mathbf{K})$	$ ho_{ m liq}^{ m sat}$ (kg/m ³)	$ ho_{ m vap}^{ m sat}$ (kg/m ³)	$P_{ m vap}^{ m sat}$ (MPa)	$\Delta H_{\rm v}$ (kJ/mol)	$Z_{ m vap}^{ m sat}$
290	$421.8_{1.7}$	$69.4_{1.8}$	$4.071_{0.027}$	$8.835_{0.094}$	$0.634_{0.013}$
280	$451.1_{1.2}$	$50.48_{0.65}$	$3.187_{0.018}$	$10.290_{0.067}$	$0.71_{0.01}$
270	$475.2_{2.5}$	$37.51_{0.33}$	$2.457_{0.013}$	$11.409_{0.072}$	$0.76_{0.01}$
260	$497.6_{1.7}$	$27.84_{0.34}$	$1.8584_{0.0078}$	$12.379_{0.043}$	$0.80_{0.01}$
250	$518.16_{0.83}$	$20.45_{0.22}$	$1.3737_{0.0065}$	$13.231_{0.027}$	$0.84_{0.01}$
240	$537.09_{0.92}$	$14.759_{0.088}$	$0.9884_{0.0067}$	$13.991_{0.021}$	$0.87_{0.01}$
230	$554.32_{0.93}$	$10.40_{0.10}$	$0.6899_{0.0056}$	$14.664_{0.024}$	$0.90_{0.01}$
220	$571.08_{0.74}$	$7.12_{0.12}$	$0.4649_{0.0046}$	$15.298_{0.035}$	$0.929_{0.019}$

Table S16: GCMC-MBAR results for propyne with the iMiPPE force field (optimal ψ value from Table S6). Subscripts correspond to the 95% confidence interval computed with bootstrap re-sampling.

$T^{\mathrm{sat}}(\mathbf{K})$	$ ho_{ m liq}^{ m sat}$ (kg/m ³)	$\rho_{\rm vap}^{\rm sat}$ (kg/m ³)	$P_{\mathrm{vap}}^{\mathrm{sat}}$ (MPa)	$\Delta H_{\rm v}$ (kJ/mol)	$Z_{ m vap}^{ m sat}$
380	$436.3_{5.1}$	$85.3_{1.7}$	$3.923_{0.045}$	$10.64_{0.20}$	$0.58_{0.01}$
370	$468.9_{3.2}$	$64.9_{1.9}$	$3.234_{0.036}$	$12.56_{0.18}$	$0.649_{0.012}$
360	$495.3_{1.2}$	$50.2_{1.4}$	$2.643_{0.025}$	$14.12_{0.13}$	$0.705_{0.014}$
350	$517.6_{1.1}$	$39.26_{0.77}$	$2.137_{0.018}$	$15.39_{0.10}$	$0.750_{0.011}$
340	$537.2_{1.3}$	$30.77_{0.40}$	$1.708_{0.013}$	$16.469_{0.084}$	$0.79_{0.01}$
330	$554.7_{1.7}$	$24.00_{0.28}$	$1.3456_{0.0097}$	$17.416_{0.089}$	$0.82_{0.01}$
320	$570.4_{2.2}$	$18.56_{0.23}$	$1.0444_{0.0070}$	$18.26_{0.10}$	$0.85_{0.01}$
310	$585.8_{2.1}$	$14.18_{0.18}$	$0.7969_{0.0050}$	$19.048_{0.098}$	$0.87_{0.01}$
300	$601.7_{1.6}$	$10.67_{0.12}$	$0.5964_{0.0038}$	$19.823_{0.073}$	$0.90_{0.01}$
290	$616.5_{2.2}$	$7.899_{0.078}$	$0.4365_{0.0038}$	$20.532_{0.077}$	$0.918_{0.012}$

Table S17: GCMC-MBAR results for 1-butyne with the iMiPPE force field (optimal ψ value from Table S6). Subscripts correspond to the 95% confidence interval computed with bootstrap re-sampling.

$T^{\mathrm{sat}}(\mathbf{K})$	$ ho_{ m liq}^{ m sat}$ (kg/m ³)	$ ho_{ m vap}^{ m sat}$ (kg/m ³)	$P_{\mathrm{vap}}^{\mathrm{sat}}$ (MPa)	$\Delta H_{\rm v}$ (kJ/mol)	$Z_{ m vap}^{ m sat}$
410	452.84.0	$70.9_{5.6}$	$2.840_{0.093}$	$13.41_{0.28}$	$0.636_{0.032}$
400	$478.29_{0.92}$	$55.9_{2.7}$	$2.366_{0.066}$	$15.10_{0.20}$	$0.689_{0.016}$
390	$500.1_{1.3}$	$44.5_{1.3}$	$1.955_{0.052}$	$16.52_{0.12}$	$0.73_{0.01}$
380	$520.1_{1.4}$	$35.6_{1.1}$	$1.599_{0.043}$	$17.771_{0.095}$	$0.77_{0.01}$
370	$538.8_{1.1}$	$28.3_{1.2}$	$1.293_{0.033}$	$18.90_{0.10}$	$0.802_{0.015}$
360	$555.7_{1.3}$	$22.5_{1.2}$	$1.032_{0.021}$	$19.92_{0.14}$	$0.831_{0.031}$
350	$571.1_{1.3}$	$17.64_{0.98}$	$0.8126_{0.0098}$	$20.83_{0.15}$	$0.856_{0.041}$
340	$585.1_{1.0}$	$13.72_{0.65}$	$0.6302_{0.0033}$	$21.64_{0.16}$	$0.879_{0.044}$
330	$598.8_{2.7}$	$10.54_{0.36}$	$0.4806_{0.0057}$	$22.41_{0.19}$	$0.899_{0.042}$
320	$613.6_{4.5}$	$7.97_{0.19}$	$0.3595_{0.0080}$	$23.21_{0.25}$	$0.917_{0.039}$
310	$627.0_{2.2}$	$5.92_{0.13}$	$0.2629_{0.0086}$	$23.93_{0.17}$	$0.932_{0.040}$

Table S18: GCMC-MBAR results for 2-butyne with the iMiPPE force field (optimal ψ value from Table S6). Subscripts correspond to the 95% confidence interval computed with bootstrap re-sampling.

$T^{\mathrm{sat}}(K)$	$ ho_{ m liq}^{ m sat}$ (kg/m ³)	$ ho_{ m vap}^{ m sat}$ (kg/m ³)	$P_{\mathrm{vap}}^{\mathrm{sat}}$ (MPa)	$\Delta H_{\rm v}$ (kJ/mol)	$Z_{ m vap}^{ m sat}$
450	$437.2_{4.2}$	$90.5_{3.2}$	$3.554_{0.053}$	$12.28_{0.20}$	$0.568_{0.014}$
440	$470.0_{3.7}$	$71.8_{2.3}$	$3.012_{0.037}$	$14.30_{0.20}$	$0.620_{0.017}$
430	$494.6_{1.6}$	$57.4_{1.2}$	$2.535_{0.029}$	$15.96_{0.15}$	$0.668_{0.014}$
420	$514.58_{0.50}$	$46.27_{0.57}$	$2.118_{0.025}$	$17.336_{0.085}$	$0.71_{0.01}$
410	$532.82_{0.48}$	$37.39_{0.49}$	$1.757_{0.022}$	$18.554_{0.040}$	$0.75_{0.01}$
400	$550.44_{0.50}$	$30.16_{0.62}$	$1.444_{0.017}$	$19.684_{0.065}$	$0.78_{0.01}$
390	$567.00_{0.68}$	$24.23_{0.63}$	$1.175_{0.012}$	$20.72_{0.11}$	$0.809_{0.013}$
380	$582.34_{0.91}$	$19.36_{0.53}$	$0.9452_{0.0067}$	$21.66_{0.13}$	$0.836_{0.017}$
370	$596.57_{0.71}$	$15.35_{0.39}$	$0.7513_{0.0033}$	$22.51_{0.12}$	$0.860_{0.019}$
360	$610.15_{0.68}$	$12.07_{0.25}$	$0.5893_{0.0027}$	$23.32_{0.12}$	$0.882_{0.019}$
350	$623.0_{1.1}$	$9.39_{0.13}$	$0.4552_{0.0037}$	$24.06_{0.12}$	$0.901_{0.018}$
340	$635.13_{0.92}$	$7.213_{0.060}$	$0.3458_{0.0041}$	$24.75_{0.10}$	$0.917_{0.016}$
330	$647.43_{0.75}$	$5.454_{0.041}$	$0.2577_{0.0039}$	$25.410_{0.086}$	$0.931_{0.015}$

Table S19: GCMC-MBAR results for 1-pentyne with the iMiPPE force field (optimal ψ value from Table S6). Subscripts correspond to the 95% confidence interval computed with bootstrap re-sampling.

$T^{\mathrm{sat}}(K)$	$ ho_{ m liq}^{ m sat}$ (kg/m ³)	$ ho_{ m vap}^{ m sat}$ (kg/m ³)	$P_{\mathrm{vap}}^{\mathrm{sat}}$ (MPa)	$\Delta H_{\rm v}$ (kJ/mol)	$Z_{ m vap}^{ m sat}$
450	$445.1_{1.3}$	$77.7_{1.0}$	$2.582_{0.012}$	$14.14_{0.12}$	$0.61_{0.01}$
440	$471.10_{0.57}$	$61.18_{0.83}$	$2.1759_{0.0091}$	$16.143_{0.079}$	$0.66_{0.01}$
430	$493.03_{0.73}$	$48.93_{0.57}$	$1.8221_{0.0082}$	$17.791_{0.054}$	$0.71_{0.01}$
420	$512.1_{1.0}$	$39.44_{0.30}$	$1.5143_{0.0083}$	$19.182_{0.025}$	$0.75_{0.01}$
410	$529.2_{1.4}$	$31.85_{0.22}$	$1.2476_{0.0079}$	$20.400_{0.045}$	$0.78_{0.01}$
400	$545.2_{1.3}$	$25.65_{0.31}$	$1.0180_{0.0064}$	$21.503_{0.073}$	$0.81_{0.01}$
390	$560.39_{0.90}$	$20.55_{0.33}$	$0.8216_{0.0042}$	$22.528_{0.075}$	$0.84_{0.01}$
380	$574.87_{0.92}$	$16.34_{0.27}$	$0.6551_{0.0022}$	$23.483_{0.088}$	$0.865_{0.012}$
370	$588.2_{1.7}$	$12.87_{0.20}$	$0.5155_{0.0014}$	$24.35_{0.13}$	$0.887_{0.014}$
360	$600.8_{2.1}$	$10.03_{0.16}$	$0.4000_{0.0020}$	$25.16_{0.15}$	$0.907_{0.018}$
350	$613.6_{1.5}$	$7.72_{0.15}$	$0.3052_{0.0029}$	$25.96_{0.14}$	$0.925_{0.026}$
340	$626.2_{1.2}$	$5.86_{0.16}$	$0.2288_{0.0041}$	$26.72_{0.17}$	$0.941_{0.042}$

Table S20: GCMC-MBAR results for 2-pentyne with the iMiPPE force field (optimal ψ value from Table S6). Subscripts correspond to the 95% confidence interval computed with bootstrap re-sampling.

$T^{\mathrm{sat}}(K)$	$\rho_{ m liq}^{ m sat}$ (kg/m ³)	$ ho_{ m vap}^{ m sat}$ (kg/m ³)	$P_{\mathrm{vap}}^{\mathrm{sat}}$ (MPa)	$\Delta H_{\rm v}$ (kJ/mol)	$Z_{ m vap}^{ m sat}$
470	$470.2_{2.0}$	$67.8_{1.5}$	$2.443_{0.022}$	$16.285_{0.075}$	$0.628_{0.016}$
460	$493.37_{0.97}$	$54.31_{0.93}$	$2.066_{0.024}$	$18.127_{0.084}$	$0.677_{0.016}$
450	$513.26_{0.50}$	$43.98_{0.45}$	$1.735_{0.025}$	$19.667_{0.065}$	$0.718_{0.013}$
440	$531.38_{0.38}$	$35.74_{0.41}$	$1.447_{0.023}$	$21.022_{0.031}$	$0.75_{0.01}$
430	$548.11_{0.47}$	$29.01_{0.58}$	$1.197_{0.020}$	$22.242_{0.067}$	$0.79_{0.01}$
420	$563.44_{0.72}$	$23.48_{0.64}$	$0.981_{0.015}$	$23.34_{0.12}$	$0.81_{0.01}$
410	$577.72_{0.97}$	$18.92_{0.59}$	$0.796_{0.011}$	$24.35_{0.16}$	$0.840_{0.015}$
400	$591.5_{1.4}$	$15.15_{0.47}$	$0.6386_{0.0070}$	$25.30_{0.20}$	$0.863_{0.018}$
390	$604.8_{1.9}$	$12.03_{0.32}$	$0.5062_{0.0042}$	$26.19_{0.22}$	$0.884_{0.018}$
380	$617.3_{1.8}$	$9.46_{0.18}$	$0.3957_{0.0027}$	$27.01_{0.19}$	$0.902_{0.014}$
370	$629.1_{1.5}$	$7.353_{0.077}$	$0.3048_{0.0022}$	$27.78_{0.14}$	$0.92_{0.01}$
360	$640.7_{1.8}$	$5.637_{0.054}$	$0.2308_{0.0024}$	$28.52_{0.12}$	$0.932_{0.016}$
350	$652.0_{1.7}$	$4.255_{0.079}$	$0.1717_{0.0030}$	$29.229_{0.082}$	$0.944_{0.032}$

Table S21: GCMC-MBAR results for 1-hexyne with the iMiPPE force field (optimal ψ value from Table S6). Subscripts correspond to the 95% confidence interval computed with bootstrap re-sampling.

$T^{\mathrm{sat}}(\mathbf{K})$	$ ho_{ m liq}^{ m sat}$ (kg/m ³)	$\rho_{\rm vap}^{\rm sat}$ (kg/m ³)	$P_{ m vap}^{ m sat}$ (MPa)	$\Delta H_{\rm v}$ (kJ/mol)	$Z_{ m vap}^{ m sat}$
490	$433.3_{7.6}$	$81.5_{3.5}$	$2.435_{0.037}$	$15.09_{0.17}$	$0.602_{0.017}$
480	$461.1_{2.9}$	$65.5_{2.5}$	$2.080_{0.022}$	$17.26_{0.14}$	$0.654_{0.019}$
470	$483.65_{0.76}$	$53.2_{1.3}$	$1.766_{0.014}$	$19.07_{0.11}$	$0.698_{0.013}$
460	$502.56_{0.55}$	$43.45_{0.54}$	$1.489_{0.010}$	$20.586_{0.041}$	$0.74_{0.01}$
450	$519.59_{0.69}$	$35.56_{0.36}$	$1.2468_{0.0083}$	$21.936_{0.038}$	$0.77_{0.01}$
440	$536.0_{1.0}$	$29.06_{0.41}$	$1.0351_{0.0065}$	$23.201_{0.073}$	$0.80_{0.01}$
430	$551.44_{0.96}$	$23.66_{0.47}$	$0.8514_{0.0043}$	$24.36_{0.10}$	$0.827_{0.014}$
420	$565.34_{0.57}$	$19.17_{0.42}$	$0.6934_{0.0031}$	$25.40_{0.11}$	$0.851_{0.019}$
410	$578.56_{0.49}$	$15.43_{0.30}$	$0.5583_{0.0037}$	$26.378_{0.089}$	$0.872_{0.021}$
400	$591.16_{0.88}$	$12.31_{0.18}$	$0.4443_{0.0049}$	$27.296_{0.062}$	$0.892_{0.022}$
390	$602.46_{0.56}$	$9.72_{0.10}$	$0.3488_{0.0056}$	$28.119_{0.069}$	$0.909_{0.022}$
380	$612.80_{0.61}$	$7.587_{0.080}$	$0.2702_{0.0059}$	$28.86_{0.10}$	$0.926_{0.027}$
370	$624.2_{1.5}$	$5.851_{0.083}$	$0.2061_{0.0060}$	$29.65_{0.15}$	$0.940_{0.037}$
360	$637.2_{1.1}$	$4.445_{0.086}$	$0.1543_{0.0064}$	$30.50_{0.19}$	$0.953_{0.053}$

Table S22: GCMC-MBAR results for 2-hexyne with the iMiPPE force field (optimal ψ value from Table S6). Subscripts correspond to the 95% confidence interval computed with bootstrap re-sampling.

$T^{\mathrm{sat}}(\mathbf{K})$	$ ho_{ m liq}^{ m sat}$ (kg/m ³)	$ ho_{ m vap}^{ m sat}$ (kg/m ³)	$P_{ m vap}^{ m sat}$ (MPa)	$\Delta H_{\rm v}$ (kJ/mol)	$Z_{ m vap}^{ m sat}$
500	$467.54_{0.99}$	$66.01_{0.94}$	$2.140_{0.019}$	$17.945_{0.093}$	$0.64_{0.01}$
490	$488.44_{0.86}$	$53.67_{0.62}$	$1.825_{0.016}$	$19.766_{0.070}$	$0.69_{0.01}$
480	$506.42_{0.87}$	$44.07_{0.54}$	$1.547_{0.012}$	$21.286_{0.048}$	$0.72_{0.01}$
470	$523.2_{1.3}$	$36.28_{0.58}$	$1.3025_{0.0090}$	$22.660_{0.039}$	$0.75_{0.01}$
460	$539.7_{1.9}$	$29.82_{0.56}$	$1.0881_{0.0054}$	$23.957_{0.044}$	$0.784_{0.012}$
450	$555.2_{1.7}$	$24.42_{0.46}$	$0.9014_{0.0029}$	$25.157_{0.042}$	$0.810_{0.015}$
440	$569.3_{1.2}$	$19.91_{0.33}$	$0.7397_{0.0032}$	$26.240_{0.053}$	$0.834_{0.016}$
430	$582.7_{1.3}$	$16.13_{0.20}$	$0.6010_{0.0043}$	$27.253_{0.058}$	$0.856_{0.016}$
420	$596.1_{1.2}$	$12.96_{0.11}$	$0.4831_{0.0051}$	$28.236_{0.062}$	$0.876_{0.015}$
410	$608.84_{0.86}$	$10.324_{0.065}$	$0.3835_{0.0054}$	$29.161_{0.058}$	$0.895_{0.014}$
400	$620.4_{1.4}$	$8.136_{0.057}$	$0.3005_{0.0053}$	$30.003_{0.073}$	$0.912_{0.015}$
390	$631.7_{1.6}$	$6.340_{0.060}$	$0.2321_{0.0051}$	$30.807_{0.083}$	$0.928_{0.018}$
380	$642.43_{0.53}$	$4.878_{0.064}$	$0.1766_{0.0049}$	$31.568_{0.066}$	$0.941_{0.026}$
370	$652.13_{0.63}$	$3.702_{0.067}$	$0.1322_{0.0047}$	$32.24_{0.12}$	$0.953_{0.040}$

Table S23: GCMC-MBAR results for 1-heptyne with the iMiPPE force field (optimal ψ value from Table S6). Subscripts correspond to the 95% confidence interval computed with bootstrap re-sampling.

T ^{sat} (K)	$ ho_{ m liq}^{ m sat}$ (kg/m ³)	$ ho_{ m vap}^{ m sat}$ (kg/m ³)	P _{vap} (MPa)	$\Delta H_{\rm v}$ (kJ/mol)	$Z_{ m vap}^{ m sat}$
520	$437.2_{2.6}$	$77.0_{2.2}$	$2.122_{0.017}$	$16.99_{0.12}$	$0.613_{0.013}$
510	$462.1_{1.5}$	$62.4_{1.4}$	$1.822_{0.011}$	$19.188_{0.099}$	$0.662_{0.013}$
500	$483.1_{1.1}$	$51.09_{0.74}$	$1.5560_{0.0076}$	$21.050_{0.060}$	$0.70_{0.01}$
490	$501.4_{1.0}$	$42.07_{0.40}$	$1.3207_{0.0063}$	$22.662_{0.042}$	$0.74_{0.01}$
480	$518.0_{1.1}$	$34.69_{0.32}$	$1.1135_{0.0053}$	$24.100_{0.057}$	$0.77_{0.01}$
470	$533.2_{1.2}$	$28.57_{0.30}$	$0.9318_{0.0044}$	$25.399_{0.069}$	$0.80_{0.01}$
460	$547.3_{1.1}$	$23.46_{0.24}$	$0.7736_{0.0042}$	$26.588_{0.061}$	$0.83_{0.01}$
450	$560.81_{1.0}$	$19.18_{0.16}$	$0.6364_{0.0046}$	$27.703_{0.047}$	$0.853_{0.011}$
440	$573.98_{0.87}$	$15.59_{0.12}$	$0.5185_{0.0052}$	$28.768_{0.035}$	$0.874_{0.015}$
430	$586.56_{0.51}$	$12.58_{0.10}$	$0.4179_{0.0057}$	$29.770_{0.052}$	$0.894_{0.019}$
420	$598.39_{0.36}$	$10.06_{0.10}$	$0.3329_{0.0061}$	$30.703_{0.082}$	$0.911_{0.024}$
410	$609.60_{0.41}$	$7.97_{0.12}$	$0.2618_{0.0064}$	$31.576_{0.098}$	$0.927_{0.030}$
400	$620.43_{0.28}$	$6.24_{0.16}$	$0.2031_{0.0065}$	$32.41_{0.13}$	$0.941_{0.042}$
390	$631.53_{0.29}$	$4.82_{0.19}$	$0.1551_{0.0067}$	$33.24_{0.20}$	$0.953_{0.062}$

Table S24: GCMC-MBAR results for 1-octyne with the iMiPPE force field (optimal ψ value from Table S6). Subscripts correspond to the 95% confidence interval computed with bootstrap re-sampling.

$T^{\mathrm{sat}}(\mathbf{K})$	$ ho_{ m liq}^{ m sat}$ (kg/m ³)	$ ho_{ m vap}^{ m sat}$ (kg/m ³)	$P_{ m vap}^{ m sat}$ (MPa)	$\Delta H_{\rm v}$ (kJ/mol)	$Z_{ m vap}^{ m sat}$
550	$424.4_{3.1}$	$85.7_{2.4}$	$2.025_{0.020}$	$16.856_{0.096}$	$0.570_{0.012}$
540	$449.6_{2.4}$	$68.1_{1.6}$	$1.745_{0.012}$	$19.509_{0.082}$	$0.629_{0.011}$
530	$471.3_{1.4}$	$55.11_{0.94}$	$1.4972_{0.0080}$	$21.746_{0.072}$	$0.68_{0.01}$
520	$490.29_{0.85}$	$45.27_{0.56}$	$1.2786_{0.0057}$	$23.612_{0.065}$	$0.72_{0.01}$
510	$507.10_{0.64}$	$37.43_{0.38}$	$1.0854_{0.0043}$	$25.219_{0.062}$	$0.75_{0.01}$
500	$522.35_{0.60}$	$30.99_{0.30}$	$0.9152_{0.0033}$	$26.653_{0.065}$	$0.78_{0.01}$
490	$536.64_{0.61}$	$25.61_{0.25}$	$0.7660_{0.0026}$	$27.971_{0.072}$	$0.81_{0.01}$
480	$550.42_{0.57}$	$21.08_{0.21}$	$0.6360_{0.0023}$	$29.216_{0.075}$	$0.83_{0.01}$
470	$563.64_{0.48}$	$17.26_{0.16}$	$0.5234_{0.0024}$	$30.392_{0.075}$	$0.85_{0.01}$
460	$576.05_{0.40}$	$14.05_{0.13}$	$0.4265_{0.0026}$	$31.485_{0.074}$	$0.875_{0.012}$
450	$587.80_{0.34}$	$11.35_{0.11}$	$0.3440_{0.0029}$	$32.510_{0.077}$	$0.893_{0.014}$
440	$599.21_{0.42}$	$9.09_{0.11}$	$0.2743_{0.0031}$	$33.488_{0.090}$	$0.909_{0.018}$
430	$610.23_{0.53}$	$7.210_{0.099}$	$0.2160_{0.0034}$	$34.42_{0.11}$	$0.923_{0.023}$
420	$620.82_{0.50}$	$5.656_{0.089}$	$0.1678_{0.0037}$	$35.31_{0.12}$	$0.936_{0.031}$
410	$631.54_{0.36}$	$4.383_{0.076}$	$0.1285_{0.0039}$	$36.19_{0.15}$	$0.948_{0.041}$

Table S25: GCMC-MBAR results for 1-nonyne with the iMiPPE force field (optimal ψ value from Table S6). Subscripts correspond to the 95% confidence interval computed with bootstrap re-sampling.

$T^{\mathrm{sat}}\left(\mathbf{K}\right)$	$ ho_{ m liq}^{ m sat}$ (kg/m ³)	$ ho_{ m vap}^{ m sat}$ (kg/m ³)	$P_{\mathrm{vap}}^{\mathrm{sat}}$ (MPa)	$\Delta H_{\rm v}$ (kJ/mol)	$Z_{ m vap}^{ m sat}$
570	$427.1_{1.4}$	$80.51_{0.73}$	$1.776_{0.010}$	$18.58_{0.12}$	$0.58_{0.01}$
560	$450.90_{0.83}$	$64.43_{0.54}$	$1.5311_{0.0083}$	$21.279_{0.086}$	$0.63_{0.01}$
550	$471.72_{0.65}$	$52.31_{0.42}$	$1.3149_{0.0067}$	$23.583_{0.093}$	$0.68_{0.01}$
540	$489.89_{0.61}$	$43.02_{0.39}$	$1.1239_{0.0056}$	$25.52_{0.11}$	$0.72_{0.01}$
530	$506.26_{0.52}$	$35.61_{0.32}$	$0.9552_{0.0047}$	$27.21_{0.11}$	$0.76_{0.01}$
520	$521.47_{0.54}$	$29.51_{0.25}$	$0.8067_{0.0040}$	$28.739_{0.079}$	$0.79_{0.01}$
510	$535.75_{0.66}$	$24.42_{0.23}$	$0.6762_{0.0031}$	$30.149_{0.058}$	$0.81_{0.01}$
500	$549.10_{0.71}$	$20.14_{0.24}$	$0.5626_{0.0022}$	$31.452_{0.059}$	$0.83_{0.01}$
490	$561.65_{0.67}$	$16.54_{0.23}$	$0.4641_{0.0013}$	$32.666_{0.073}$	$0.856_{0.010}$
480	$573.68_{0.55}$	$13.50_{0.21}$	$0.37923_{0.00095}$	$33.811_{0.085}$	$0.875_{0.014}$
470	$585.26_{0.38}$	$10.94_{0.18}$	$0.3068_{0.0015}$	$34.896_{0.092}$	$0.892_{0.018}$
460	$596.35_{0.30}$	$8.79_{0.16}$	$0.2455_{0.0022}$	$35.92_{0.10}$	$0.907_{0.023}$
450	$607.27_{0.32}$	$7.00_{0.14}$	$0.1942_{0.0030}$	$36.92_{0.13}$	$0.921_{0.031}$
440	$618.21_{0.22}$	$5.52_{0.12}$	$0.1516_{0.0036}$	$37.91_{0.16}$	$0.933_{0.041}$
430	$628.74_{0.19}$	$4.29_{0.11}$	$0.1166_{0.0042}$	$38.85_{0.22}$	$0.944_{0.055}$
420	$638.50_{0.35}$	$3.296_{0.094}$	$0.0885_{0.0047}$	$39.72_{0.29}$	$0.955_{0.074}$

S6 Case study: Cyclohexane optimization

S6.1 Phase equilibria plots

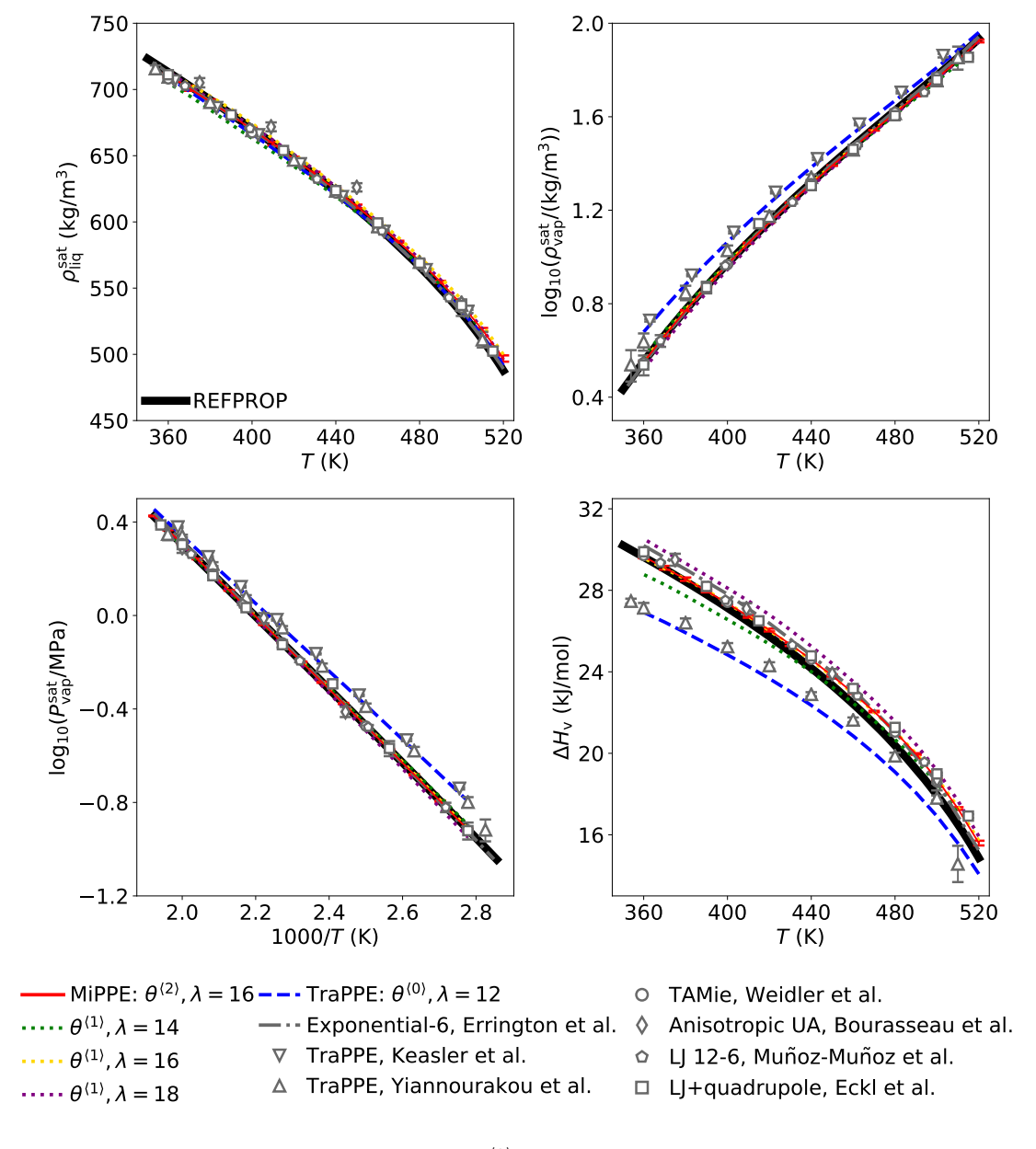


Figure S2: Phase equilibria for MiPPE ($\theta^{(2)}$, $\lambda_{\text{CH}_2} = 16$), zeroth iteration (TraPPE: $\theta^{(0)}$), first iterations ($\theta^{(1)}$, $\lambda_{\text{CH}_2} = 14, 16, 18, 20$), and several literature force fields. See caption of Figure 9 in manuscript for details.

S6.2 Twenty replicates

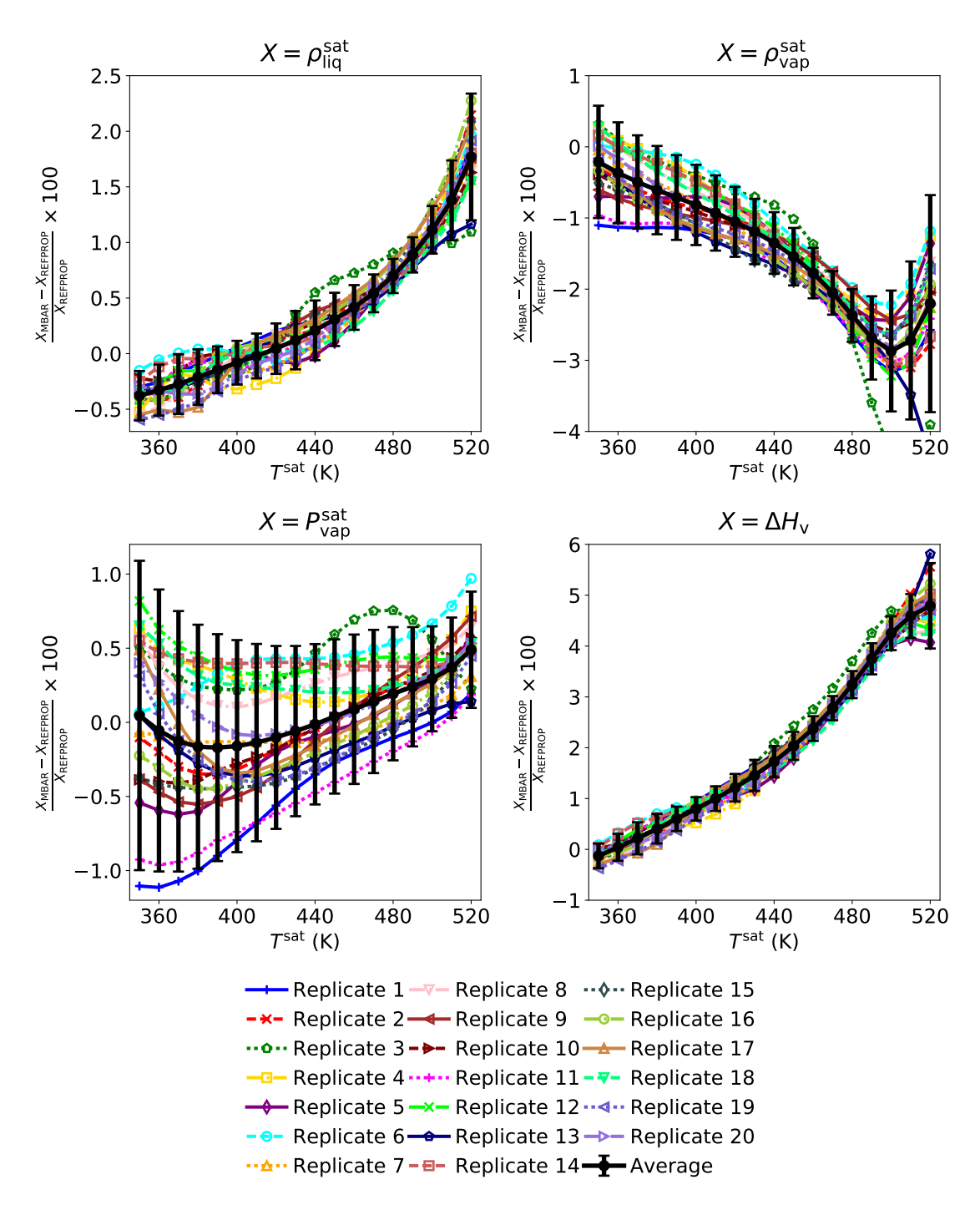


Figure S3: Percent deviations of MiPPE force field relative to REFPROP cyclohexane values for twenty replicates and average.

S6.3 TAMie comparison

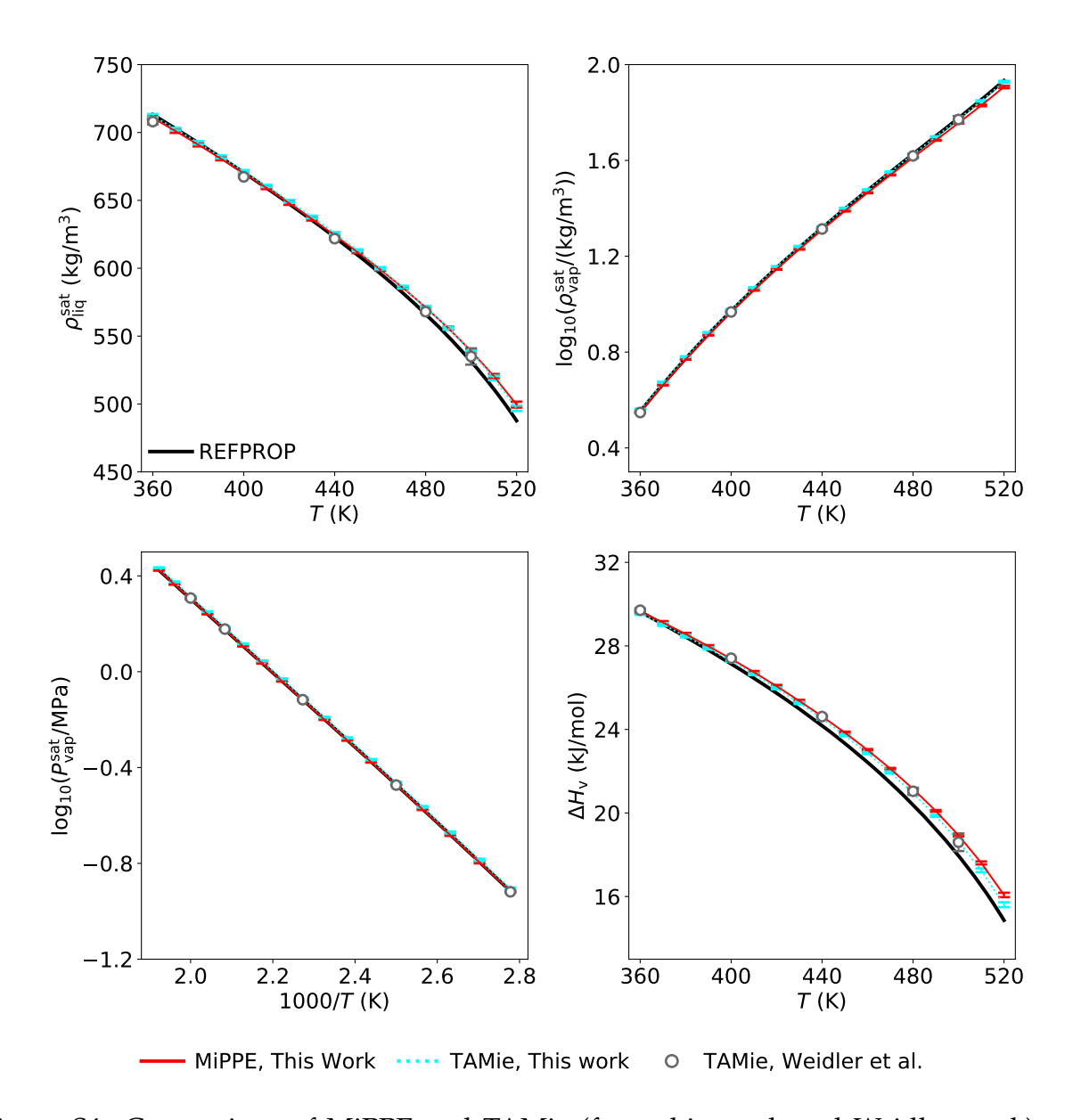


Figure S4: Comparison of MiPPE and TAMie (from this work and Weidler et al.) cyclohexane phase equilibria. All simulations from this work utilized 3.5 nm box length. TAMie simulations used a 1.4 nm cut-off.

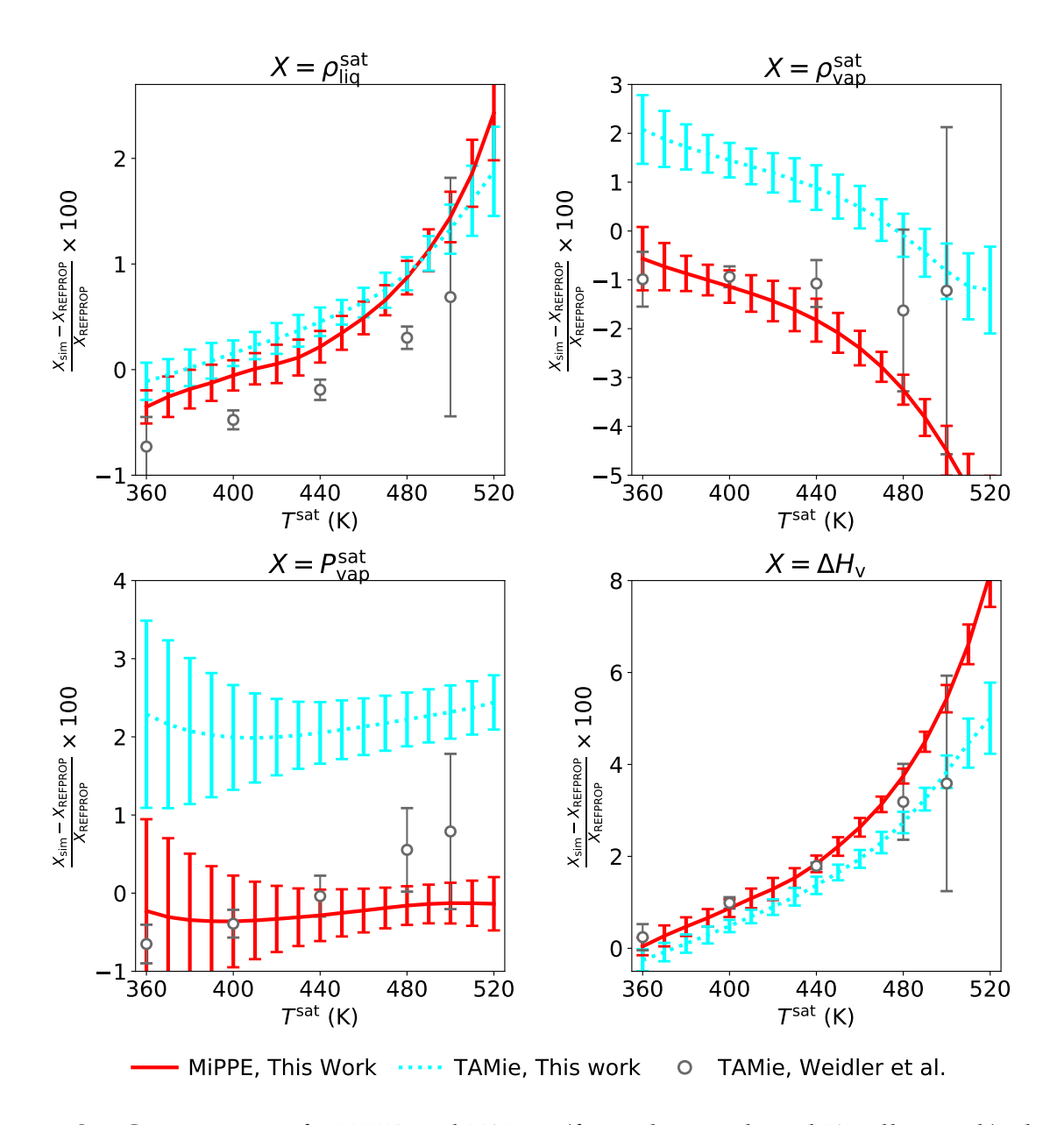


Figure S5: Comparison of MiPPE and TAMie (from this work and Weidler et al.) deviations relative to REFPROP cyclohexane values. All simulations from this work utilized 3.5 nm box length. TAMie simulations used a 1.4 nm cut-off. Note that discrepancies between TAMie results from this work and Weidler et al. are larger than the combined uncertainties (although they are typically between 0.5 and 2%). Such systematic discrepancies in phase equilibria are not completely unexpected when comparing simulation results across different platforms. Efforts to elucidate the source of these small (albeit non-negligible) discrepancies were unsuccessful.

Table S26: GCMC-MBAR results for the TAMie force field with 3.5 nm box length and 1.4 nm cut-off. Subscripts correspond to the 95% confidence interval computed with twenty independent replicate GCMC simulations at each state point.

$T^{\mathrm{sat}}(\mathbf{K})$	$ ho_{ m liq}^{ m sat}$ (kg/m ³)	$\rho_{\mathrm{vap}}^{\mathrm{sat}}$ (kg/m ³)	$P_{ m vap}^{ m sat}$ (MPa)	$\Delta H_{\rm v}$ (kJ/mol)	$Z_{ m vap}^{ m sat}$
360	712.4 _{1.3}	$3.64_{0.03}$	$0.1242_{0.0015}$	$29.560_{0.071}$	$0.959_{0.026}$
370	$702.5_{1.1}$	$4.72_{0.03}$	$0.1640_{0.0017}$	$29.019_{0.058}$	$0.951_{0.022}$
380	$692.4_{1.2}$	$6.04_{0.03}$	$0.2132_{0.0020}$	$28.462_{0.057}$	$0.941_{0.019}$
390	$682.1_{1.1}$	$7.62_{0.03}$	$0.2728_{0.0021}$	$27.880_{0.051}$	$0.930_{0.016}$
400	$671.5_{0.8}$	$9.50_{0.03}$	$0.3445_{0.0023}$	$27.274_{0.036}$	$0.917_{0.013}$
410	$660.7_{0.9}$	$11.74_{0.04}$	$0.4295_{0.0024}$	$26.639_{0.039}$	$0.903_{0.012}$
420	$649.4_{0.9}$	$14.36_{0.06}$	$0.5294_{0.0025}$	$25.969_{0.044}$	$0.888_{0.011}$
430	$637.8_{1.0}$	$17.43_{0.08}$	$0.6457_{0.0027}$	$25.262_{0.048}$	$0.872_{0.010}$
440	$625.8_{0.8}$	$21.01_{0.10}$	$0.7800_{0.0030}$	$24.514_{0.046}$	$0.854_{0.010}$
450	$613.3_{0.7}$	$25.18_{0.11}$	$0.9339_{0.0034}$	$23.717_{0.040}$	$0.834_{0.009}$
460	$600.0_{0.8}$	$30.02_{0.13}$	$1.1092_{0.0039}$	$22.861_{0.043}$	$0.813_{0.009}$
470	$586.1_{1.0}$	$35.66_{0.15}$	$1.3076_{0.0045}$	$21.942_{0.050}$	$0.790_{0.008}$
480	$571.4_{0.9}$	$42.25_{0.19}$	$1.5310_{0.0052}$	$20.948_{0.047}$	$0.764_{0.008}$
490	$555.7_{0.9}$	$50.00_{0.25}$	$1.7813_{0.0059}$	$19.859_{0.047}$	$0.736_{0.009}$
500	$538.4_{1.2}$	$59.24_{0.34}$	$2.0608_{0.0069}$	$18.645_{0.064}$	$0.704_{0.009}$
510	$519.2_{1.7}$	$70.50_{0.48}$	$2.3718_{0.0079}$	$17.255_{0.088}$	$0.668_{0.010}$
520	$496.9_{2.1}$	$84.74_{0.76}$	$2.7175_{0.0092}$	$15.61_{0.12}$	$0.624_{0.012}$

S6.4 Minimum number of effective snapshots

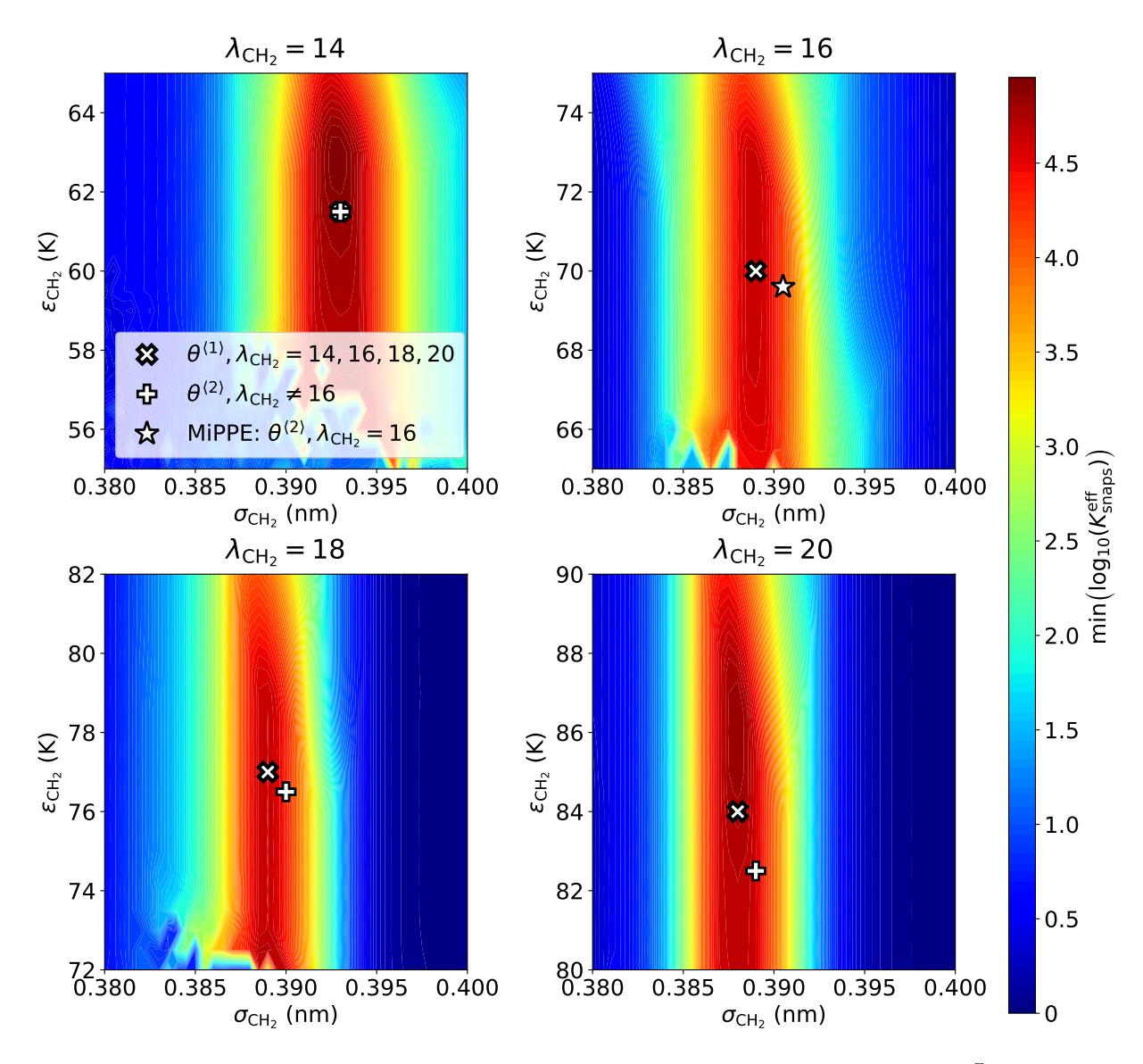


Figure S6: Second iteration minimum number of effective snapshots $(\min(K_{\mathrm{snaps}}^{\mathrm{eff}}))$ with respect to $\epsilon_{\mathrm{CH_2}}$ and $\sigma_{\mathrm{CH_2}}$ for cyclohexane. Optimization has converged as $\min(K_{\mathrm{snaps}}^{\mathrm{eff}}) \gg 50$ for the optimal $\epsilon_{\mathrm{CH_2}}$, $\sigma_{\mathrm{CH_2}}$, $\lambda_{\mathrm{CH_2}}$ parameter set. Top-left, top-right, bottom-left, and bottom-right panels correspond $\lambda_{\mathrm{CH_2}} = 14$, $\lambda_{\mathrm{CH_2}} = 16$, $\lambda_{\mathrm{CH_2}} = 18$, and $\lambda_{\mathrm{CH_2}} = 12$, respectively. White star represents the optimal parameter set, i.e., the lowest value of S, for a given $\lambda_{\mathrm{CH_2}}$.

S6.5 Finite-size effects

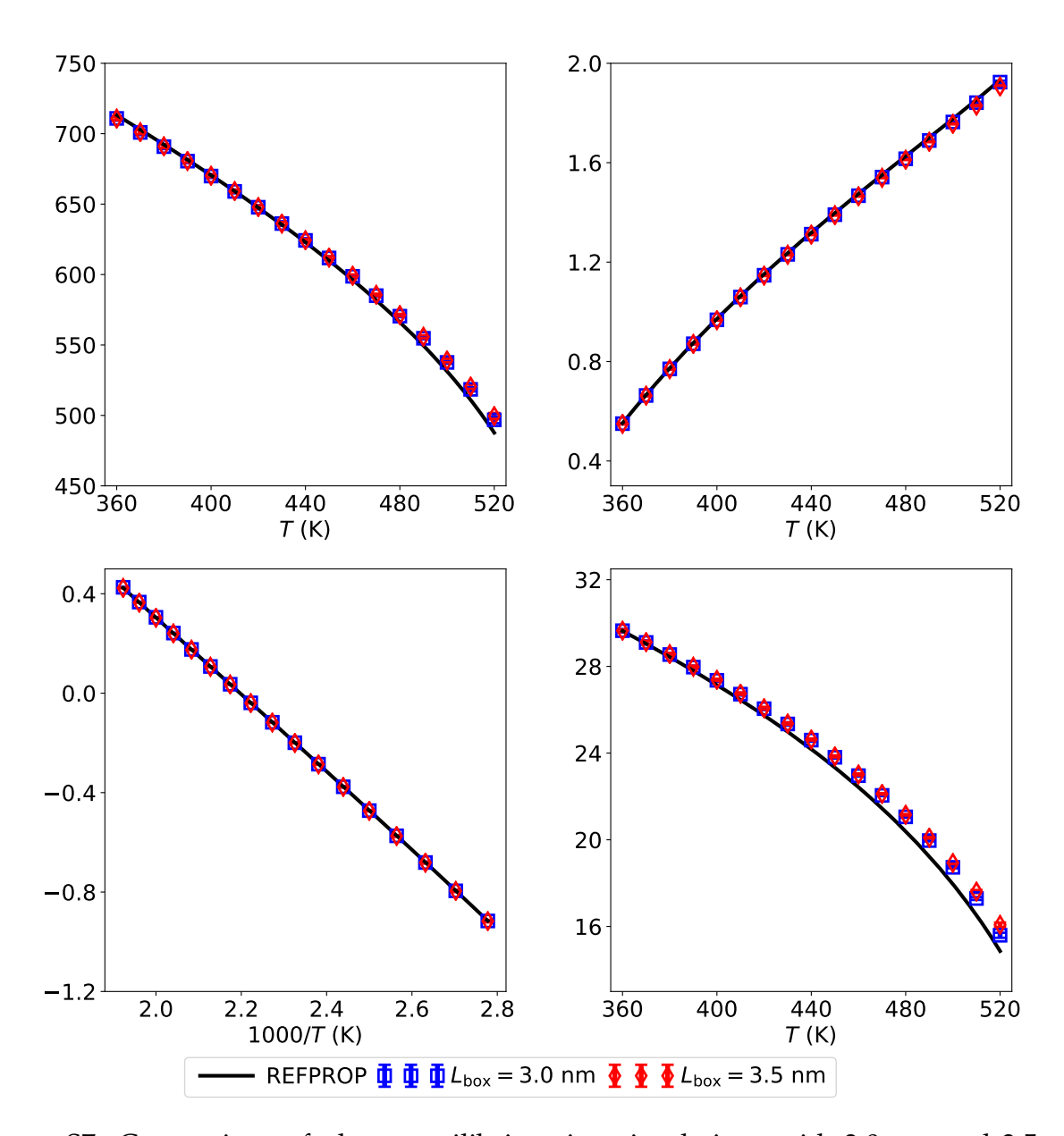


Figure S7: Comparison of phase equilibria using simulations with 3.0 nm and 3.5 nm box lengths for cyclohexane with MiPPE force field. Estimated values and uncertainties are obtained from 20 independent replicate simulations. See Figure S8 for quantitative assessment of finite-size effects.

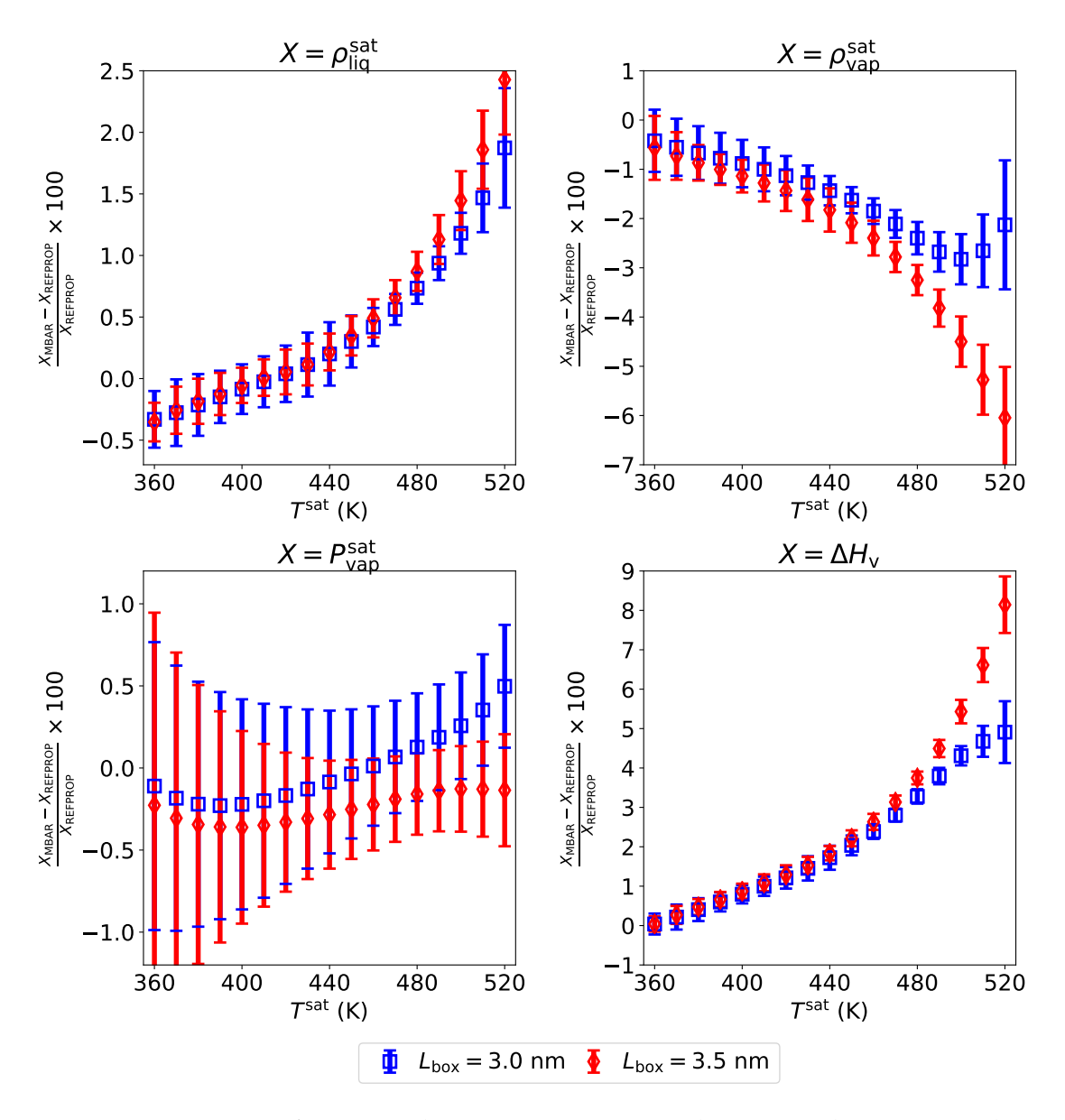


Figure S8: Comparison of percent deviations using simulations with 3.0 nm and 3.5 nm box lengths for cyclohexane with MiPPE force field. Agreement is typically within the combined uncertainties for low to moderate temperatures. Finite-size effects are most prevalent in $\rho_{\rm vap}^{\rm sat}$ and $\Delta H_{\rm v}$ near the critical temperature ($T^{\rm sat}>480$ K). Estimated values and uncertainties are obtained from 20 independent replicate simulations.

Table S27: GCMC-MBAR results for the MiPPE force field with 3.5 nm box length to test finite-size effects. Subscripts correspond to the 95% confidence interval computed with twenty independent replicate GCMC simulations at each state point.

$T^{\mathrm{sat}}(K)$	$ ho_{ m liq}^{ m sat}$ (kg/m ³)	$ ho_{ m vap}^{ m sat}$ (kg/m ³)	$P_{ m vap}^{ m sat}$ (MPa)	$\Delta H_{\rm v}$ (kJ/mol)	$Z_{ m vap}^{ m sat}$
360	$710.7_{1.2}$	$3.545_{0.025}$	$0.1211_{0.0015}$	$29.648_{0.061}$	$0.961_{0.014}$
370	$701.0_{1.4}$	$4.600_{0.024}$	$0.1601_{0.0017}$	$29.122_{0.071}$	$0.952_{0.011}$
380	$691.0_{1.4}$	$5.882_{0.023}$	$0.2081_{0.0019}$	$28.567_{0.062}$	$0.9424_{0.0093}$
390	$680.7_{1.2}$	$7.424_{0.025}$	$0.2665_{0.0020}$	$27.984_{0.057}$	$0.9315_{0.0077}$
400	$670.1_{1.0}$	$9.261_{0.033}$	$0.3365_{0.0021}$	$27.379_{0.056}$	$0.9195_{0.0067}$
410	$659.2_{1.0}$	$11.434_{0.046}$	$0.4196_{0.0022}$	$26.743_{0.060}$	$0.9061_{0.0061}$
420	$647.9_{1.3}$	$13.987_{0.063}$	$0.5173_{0.0023}$	$26.070_{0.066}$	$0.8913_{0.0057}$
430	$636.2_{1.2}$	$16.970_{0.081}$	$0.6309_{0.0025}$	$25.364_{0.057}$	$0.8752_{0.0054}$
440	$624.3_{1.0}$	$20.444_{0.098}$	$0.7621_{0.0027}$	$24.627_{0.047}$	$0.8576_{0.0051}$
450	$612.1_{1.0}$	$24.48_{0.11}$	$0.9125_{0.0029}$	$23.849_{0.050}$	$0.8385_{0.0046}$
460	$599.17_{0.99}$	$29.16_{0.11}$	$1.0837_{0.0032}$	$23.015_{0.049}$	$0.8178_{0.0040}$
470	$585.58_{0.89}$	$34.59_{0.12}$	$1.2774_{0.0036}$	$22.120_{0.039}$	$0.7953_{0.0035}$
480	$571.22_{0.96}$	$40.91_{0.14}$	$1.4953_{0.0040}$	$21.154_{0.035}$	$0.7707_{0.0033}$
490	$555.8_{1.2}$	$48.31_{0.20}$	$1.7394_{0.0046}$	$20.099_{0.045}$	$0.7438_{0.0037}$
500	$539.0_{1.4}$	$57.04_{0.33}$	$2.0115_{0.0056}$	$18.930_{0.057}$	$0.7139_{0.0045}$
510	$520.5_{1.7}$	$67.54_{0.54}$	$2.3139_{0.0072}$	$17.610_{0.076}$	$0.6799_{0.0058}$
520	$499.5_{2.3}$	$80.59_{0.95}$	$2.6492_{0.0097}$	$16.07_{0.11}$	$0.6399_{0.0079}$

S6.6 Tabulated phase equilibria for iterations

Table S28: GCMC-MBAR results for the MiPPE force field (second iteration, $\theta^{(2)}$ $\lambda_{\text{CH}_2} = 16$). Subscripts correspond to the 95% confidence interval computed with twenty independent replicate GCMC simulations at each state point.

$T^{\mathrm{sat}}(\mathbf{K})$	$ ho_{ m liq}^{ m sat}$ (kg/m ³)	$ ho_{ m vap}^{ m sat}$ (kg/m ³)	$P_{\mathrm{vap}}^{\mathrm{sat}}$ (MPa)	$\Delta H_{\rm v}$ (kJ/mol)	$Z_{ m vap}^{ m sat}$
360	$710.9_{1.7}$	$3.552_{0.027}$	$0.1213_{0.0012}$	$29.648_{0.084}$	$0.960_{0.012}$
370	$700.9_{2.0}$	$4.611_{0.032}$	$0.1604_{0.0015}$	$29.106_{0.098}$	$0.952_{0.011}$
380	$690.8_{1.8}$	$5.898_{0.039}$	$0.2085_{0.0018}$	$28.548_{0.088}$	$0.942_{0.010}$
390	$680.5_{1.5}$	$7.446_{0.048}$	$0.2670_{0.0022}$	$27.967_{0.071}$	$0.9306_{0.0097}$
400	$669.9_{1.4}$	$9.291_{0.056}$	$0.3372_{0.0026}$	$27.359_{0.067}$	$0.9183_{0.0090}$
410	$659.0_{1.4}$	$11.474_{0.065}$	$0.4205_{0.0030}$	$26.720_{0.069}$	$0.9048_{0.0083}$
420	$647.8_{1.6}$	$14.040_{0.075}$	$0.5185_{0.0034}$	$26.050_{0.074}$	$0.8899_{0.0075}$
430	$636.3_{1.8}$	$17.043_{0.085}$	$0.6325_{0.0039}$	$25.346_{0.082}$	$0.8736_{0.0069}$
440	$624.3_{1.8}$	$20.543_{0.096}$	$0.7642_{0.0044}$	$24.600_{0.080}$	$0.8558_{0.0064}$
450	$611.8_{1.6}$	$24.61_{0.11}$	$0.9152_{0.0051}$	$23.807_{0.069}$	$0.8363_{0.0059}$
460	$598.7_{1.3}$	$29.35_{0.11}$	$1.0871_{0.0058}$	$22.958_{0.058}$	$0.8151_{0.0054}$
470	$584.9_{1.1}$	$34.85_{0.12}$	$1.2816_{0.0066}$	$22.044_{0.055}$	$0.7920_{0.0049}$
480	$570.25_{0.93}$	$41.29_{0.17}$	$1.5006_{0.0072}$	$21.051_{0.058}$	$0.7665_{0.0048}$
490	$554.49_{0.93}$	$48.88_{0.31}$	$1.7460_{0.0075}$	$19.956_{0.063}$	$0.7379_{0.0057}$
500	$537.3_{1.2}$	$58.02_{0.54}$	$2.0200_{0.0076}$	$18.718_{0.064}$	$0.7049_{0.0071}$
510	$518.0_{2.0}$	$69.36_{0.85}$	$2.3254_{0.0084}$	$17.276_{0.076}$	$0.6654_{0.0085}$
520	$496.3_{3.0}$	$83.9_{1.4}$	$2.666_{0.011}$	$15.58_{0.13}$	$0.619_{0.011}$

Table S29: GCMC-MBAR results for the TraPPE force field (zeroth iteration, $\theta^{(0)}$). Subscripts correspond to the 95% confidence interval computed with bootstrap re-sampling.

$T^{\mathrm{sat}}(K)$	$ ho_{ m liq}^{ m sat}$ (kg/m ³)	$ ho_{ m vap}^{ m sat}$ (kg/m ³)	$P_{\mathrm{vap}}^{\mathrm{sat}}$ (MPa)	$\Delta H_{\rm v}$ (kJ/mol)	$Z_{ m vap}^{ m sat}$
360	$709.02_{0.33}$	$4.775_{0.062}$	$0.161_{0.016}$	$26.916_{0.050}$	$0.946_{0.096}$
370	$698.93_{0.39}$	$6.067_{0.072}$	$0.208_{0.012}$	$26.440_{0.042}$	$0.937_{0.055}$
380	$688.03_{0.44}$	$7.610_{0.088}$	$0.26_{0.01}$	$25.919_{0.036}$	$0.927_{0.026}$
390	$677.14_{0.49}$	$9.43_{0.11}$	$0.33_{0.01}$	$25.382_{0.033}$	$0.916_{0.015}$
400	$666.43_{0.55}$	$11.57_{0.12}$	$0.41_{0.01}$	$24.835_{0.030}$	$0.904_{0.023}$
410	$655.56_{0.39}$	$14.07_{0.13}$	$0.507_{0.017}$	$24.266_{0.023}$	$0.890_{0.032}$
420	$644.33_{0.48}$	$16.97_{0.13}$	$0.616_{0.025}$	$23.665_{0.027}$	$0.875_{0.036}$
430	$632.76_{0.54}$	$20.32_{0.12}$	$0.741_{0.031}$	$23.030_{0.030}$	$0.858_{0.037}$
440	$620.79_{0.67}$	$24.18_{0.26}$	$0.883_{0.039}$	$22.356_{0.051}$	$0.840_{0.038}$
450	$608.2_{1.2}$	$28.64_{0.96}$	$1.045_{0.052}$	$21.63_{0.10}$	$0.821_{0.049}$
460	$595.0_{2.9}$	$33.8_{2.4}$	$1.227_{0.098}$	$20.85_{0.20}$	$0.799_{0.085}$
470	$581.0_{4.6}$	$39.7_{3.8}$	$1.43_{0.17}$	$20.01_{0.30}$	$0.78_{0.12}$
480	$566.2_{4.8}$	$46.7_{4.6}$	$1.66_{0.24}$	$19.08_{0.33}$	$0.75_{0.13}$
490	$550.4_{4.5}$	$54.8_{4.7}$	$1.91_{0.29}$	$18.06_{0.38}$	$0.72_{0.13}$
500	$533.2_{5.4}$	$64.6_{3.8}$	$2.19_{0.38}$	$16.913_{0.088}$	$0.69_{0.13}$
510	$513.8_{5.3}$	$76.6_{5.4}$	$2.50_{0.37}$	$15.59_{0.33}$	$0.65_{0.11}$
520	$491.6_{3.8}$	$91.4_{7.6}$	$2.85_{0.28}$	$14.08_{0.34}$	$0.607_{0.078}$

Table S30: GCMC-MBAR results for the first iteration $(\theta^{\langle 1 \rangle})$ $\lambda_{\rm CH_2}=14$ force field. Subscripts correspond to the 95% confidence interval computed with bootstrap re-sampling.

$T^{\mathrm{sat}}(K)$	$ ho_{ m liq}^{ m sat}$ (kg/m ³)	$ ho_{ m vap}^{ m sat}$ (kg/m ³)	$P_{\mathrm{vap}}^{\mathrm{sat}}$ (MPa)	$\Delta H_{\rm v}$ (kJ/mol)	$Z_{ m vap}^{ m sat}$
360	$704.93_{0.26}$	$3.743_{0.073}$	$0.127_{0.044}$	$28.78_{0.10}$	$0.96_{0.33}$
370	$695.36_{0.63}$	$4.822_{0.057}$	$0.167_{0.048}$	$28.28_{0.11}$	$0.95_{0.27}$
380	$684.68_{0.79}$	$6.125_{0.057}$	$0.216_{0.049}$	$27.73_{0.11}$	$0.94_{0.21}$
390	$673.71_{0.68}$	$7.680_{0.084}$	$0.274_{0.048}$	$27.144_{0.099}$	$0.93_{0.16}$
400	$663.17_{0.45}$	$9.52_{0.13}$	$0.345_{0.044}$	$26.568_{0.086}$	$0.92_{0.12}$
410	$652.73_{0.24}$	$11.68_{0.17}$	$0.427_{0.039}$	$25.980_{0.062}$	$0.903_{0.084}$
420	$641.98_{0.82}$	$14.21_{0.23}$	$0.524_{0.033}$	$25.360_{0.039}$	$0.889_{0.058}$
430	$630.8_{1.2}$	$17.15_{0.30}$	$0.636_{0.032}$	$24.703_{0.036}$	$0.873_{0.046}$
440	$619.3_{1.1}$	$20.57_{0.39}$	$0.765_{0.041}$	$24.005_{0.044}$	$0.856_{0.049}$
450	$607.24_{0.80}$	$24.53_{0.54}$	$0.912_{0.062}$	$23.261_{0.063}$	$0.837_{0.060}$
460	$594.62_{0.73}$	$29.11_{0.77}$	$1.080_{0.093}$	$22.463_{0.085}$	$0.816_{0.074}$
470	$581.33_{0.87}$	$34.4_{1.1}$	$1.27_{0.14}$	$21.60_{0.11}$	$0.793_{0.091}$
480	$567.3_{1.1}$	$40.6_{1.6}$	$1.48_{0.21}$	$20.68_{0.13}$	$0.77_{0.11}$
490	$552.4_{1.5}$	$47.9_{2.1}$	$1.72_{0.30}$	$19.66_{0.14}$	$0.74_{0.13}$
500	$536.3_{2.5}$	$56.5_{2.6}$	$1.98_{0.41}$	$18.52_{0.14}$	$0.71_{0.15}$
510	$518.2_{4.3}$	$67.2_{2.8}$	$2.27_{0.54}$	$17.20_{0.16}$	$0.67_{0.16}$

Table S31: GCMC-MBAR results for the first iteration $(\theta^{\langle 1 \rangle})$ $\lambda_{\rm CH_2}=16$ force field. Subscripts correspond to the 95% confidence interval computed with bootstrap re-sampling.

T ^{sat} (K)	$ ho_{ m liq}^{ m sat}$ (kg/m ³)	$ ho_{ m vap}^{ m sat}$ (kg/m ³)	$P_{ m vap}^{ m sat}$ (MPa)	$\Delta H_{\rm v}$ (kJ/mol)	$Z_{ m vap}^{ m sat}$
360	$713.64_{0.38}$	$3.583_{0.049}$	$0.122_{0.039}$	$29.59_{0.13}$	$0.96_{0.31}$
370	$704.1_{1.2}$	$4.647_{0.057}$	$0.162_{0.036}$	$29.065_{0.088}$	$0.95_{0.21}$
380	$695.0_{2.4}$	$5.943_{0.071}$	$0.210_{0.032}$	$28.551_{0.098}$	$0.94_{0.14}$
390	$685.2_{2.3}$	$7.505_{0.090}$	$0.269_{0.027}$	$27.993_{0.084}$	$0.931_{0.094}$
400	$674.3_{1.1}$	$9.37_{0.11}$	$0.340_{0.024}$	$27.376_{0.037}$	$0.918_{0.066}$
410	$662.91_{0.76}$	$11.57_{0.12}$	$0.424_{0.026}$	$26.717_{0.040}$	$0.905_{0.056}$
420	$651.2_{1.0}$	$14.16_{0.14}$	$0.523_{0.032}$	$26.027_{0.065}$	$0.890_{0.055}$
430	$639.4_{1.1}$	$17.19_{0.18}$	$0.638_{0.040}$	$25.310_{0.078}$	$0.873_{0.056}$
440	$627.31_{0.89}$	$20.71_{0.22}$	$0.770_{0.050}$	$24.565_{0.072}$	$0.856_{0.056}$
450	$614.82_{0.58}$	$24.79_{0.24}$	$0.922_{0.059}$	$23.777_{0.051}$	$0.837_{0.055}$
460	$601.71_{0.56}$	$29.53_{0.25}$	$1.095_{0.067}$	$22.935_{0.053}$	$0.816_{0.050}$
470	$587.98_{0.65}$	$35.03_{0.48}$	$1.291_{0.067}$	$22.033_{0.094}$	$0.794_{0.042}$
480	$573.59_{0.74}$	$41.45_{0.99}$	$1.511_{0.063}$	$21.06_{0.15}$	$0.768_{0.037}$
490	$558.19_{0.80}$	$49.0_{1.7}$	$1.757_{0.086}$	$19.99_{0.20}$	$0.740_{0.045}$
500	$541.27_{0.93}$	$58.2_{2.6}$	$2.03_{0.16}$	$18.78_{0.24}$	$0.707_{0.064}$
510	$522.1_{1.7}$	$69.5_{3.4}$	$2.34_{0.28}$	$17.36_{0.25}$	$0.668_{0.087}$
520	$499.8_{2.6}$	$83.7_{3.9}$	$2.68_{0.43}$	$15.71_{0.22}$	$0.62_{0.10}$

Table S32: GCMC-MBAR results for the first iteration $(\theta^{\langle 1 \rangle})$ $\lambda_{\rm CH_2}=18$ force field. Subscripts correspond to the 95% confidence interval computed with bootstrap re-sampling.

$T^{\mathrm{sat}}(K)$	$ ho_{ m liq}^{ m sat}$ (kg/m ³)	$ ho_{ m vap}^{ m sat}$ (kg/m ³)	$P_{\mathrm{vap}}^{\mathrm{sat}}$ (MPa)	$\Delta H_{\rm v}$ (kJ/mol)	$Z_{ m vap}^{ m sat}$
360	$713.60_{0.89}$	$3.294_{0.099}$	$0.113_{0.020}$	$30.527_{0.066}$	$0.96_{0.17}$
370	$702.86_{0.81}$	$4.306_{0.092}$	$0.150_{0.015}$	$29.921_{0.044}$	$0.95_{0.10}$
380	$692.51_{0.62}$	$5.545_{0.081}$	$0.196_{0.013}$	$29.327_{0.039}$	$0.943_{0.063}$
390	$682.23_{0.53}$	$7.043_{0.088}$	$0.253_{0.011}$	$28.725_{0.043}$	$0.932_{0.043}$
400	$671.99_{0.38}$	$8.84_{0.13}$	$0.32_{0.01}$	$28.110_{0.043}$	$0.920_{0.030}$
410	$661.74_{0.33}$	$10.98_{0.17}$	$0.403_{0.013}$	$27.478_{0.038}$	$0.906_{0.033}$
420	$650.92_{0.46}$	$13.51_{0.21}$	$0.499_{0.024}$	$26.801_{0.037}$	$0.891_{0.046}$
430	$639.09_{0.44}$	$16.48_{0.24}$	$0.613_{0.039}$	$26.056_{0.039}$	$0.875_{0.057}$
440	$626.49_{0.39}$	$19.96_{0.27}$	$0.744_{0.055}$	$25.253_{0.042}$	$0.857_{0.065}$
450	$613.53_{0.38}$	$24.02_{0.35}$	$0.894_{0.073}$	$24.409_{0.048}$	$0.837_{0.069}$
460	$600.27_{0.57}$	$28.75_{0.70}$	$1.066_{0.096}$	$23.525_{0.086}$	$0.816_{0.076}$
470	$586.50_{0.90}$	$34.3_{1.6}$	$1.26_{0.14}$	$22.58_{0.16}$	$0.793_{0.095}$
480	$571.9_{1.5}$	$40.7_{2.6}$	$1.48_{0.23}$	$21.56_{0.21}$	$0.77_{0.13}$
490	$556.3_{2.5}$	$48.4_{3.2}$	$1.73_{0.35}$	$20.44_{0.25}$	$0.74_{0.16}$
500	$538.9_{3.0}$	$57.7_{3.1}$	$2.01_{0.46}$	$19.16_{0.25}$	$0.71_{0.16}$
510	$519.1_{2.0}$	$69.1_{2.7}$	$2.32_{0.54}$	$17.67_{0.18}$	$0.67_{0.16}$
520	$495.9_{1.6}$	$83.5_{2.4}$	$2.67_{0.62}$	$15.93_{0.12}$	$0.62_{0.15}$

Table S33: GCMC-MBAR results for the first iteration $(\theta^{\langle 1 \rangle})$ $\lambda_{\rm CH_2}=20$ force field. Subscripts correspond to the 95% confidence interval computed with bootstrap re-sampling.

T ^{sat} (K)	$ ho_{ m liq}^{ m sat}$ (kg/m ³)	$ ho_{ m vap}^{ m sat}$ (kg/m ³)	$P_{\mathrm{vap}}^{\mathrm{sat}}$ (MPa)	$\Delta H_{\rm v}$ (kJ/mol)	$Z_{ m vap}^{ m sat}$
360	$721.21_{0.17}$	$2.885_{0.047}$	$0.099_{0.059}$	$31.72_{0.18}$	$0.96_{0.57}$
370	$711.38_{0.48}$	$3.812_{0.043}$	$0.133_{0.056}$	$31.13_{0.11}$	$0.96_{0.40}$
380	$701.58_{0.81}$	$4.955_{0.041}$	$0.176_{0.054}$	$30.545_{0.066}$	$0.95_{0.29}$
390	$691.47_{0.70}$	$6.351_{0.048}$	$0.229_{0.054}$	$29.931_{0.055}$	$0.94_{0.22}$
400	$680.14_{0.36}$	$8.033_{0.065}$	$0.293_{0.055}$	$29.243_{0.046}$	$0.92_{0.17}$
410	$668.26_{0.63}$	$10.039_{0.086}$	$0.370_{0.057}$	$28.510_{0.057}$	$0.91_{0.14}$
420	$656.5_{1.6}$	$12.41_{0.11}$	$0.462_{0.061}$	$27.77_{0.10}$	$0.90_{0.12}$
430	$644.5_{2.3}$	$15.21_{0.13}$	$0.570_{0.065}$	$27.00_{0.14}$	$0.88_{0.10}$
440	$631.8_{1.8}$	$18.50_{0.16}$	$0.695_{0.068}$	$26.17_{0.12}$	$0.864_{0.085}$
450	$618.8_{1.1}$	$22.34_{0.20}$	$0.840_{0.072}$	$25.308_{0.082}$	$0.845_{0.072}$
460	$605.44_{0.73}$	$26.84_{0.33}$	$1.005_{0.072}$	$24.399_{0.086}$	$0.824_{0.060}$
470	$591.81_{0.70}$	$32.11_{0.65}$	$1.194_{0.069}$	$23.44_{0.13}$	$0.801_{0.049}$
480	$577.60_{0.68}$	$38.3_{1.2}$	$1.408_{0.074}$	$22.41_{0.19}$	$0.775_{0.048}$
490	$562.27_{0.91}$	$45.7_{2.1}$	$1.65_{0.12}$	$21.28_{0.23}$	$0.746_{0.064}$
500	$545.2_{2.6}$	$54.6_{2.9}$	$1.92_{0.23}$	$20.00_{0.19}$	$0.713_{0.092}$
510	$526.1_{5.6}$	$65.5_{3.4}$	$2.23_{0.38}$	$18.526_{0.093}$	$0.68_{0.12}$
520	$504.1_{9.3}$	$79.2_{3.3}$	$2.57_{0.57}$	$16.81_{0.22}$	$0.63_{0.14}$

S7 Compressibility factor

S7.1 Validation of GCMC-MBAR

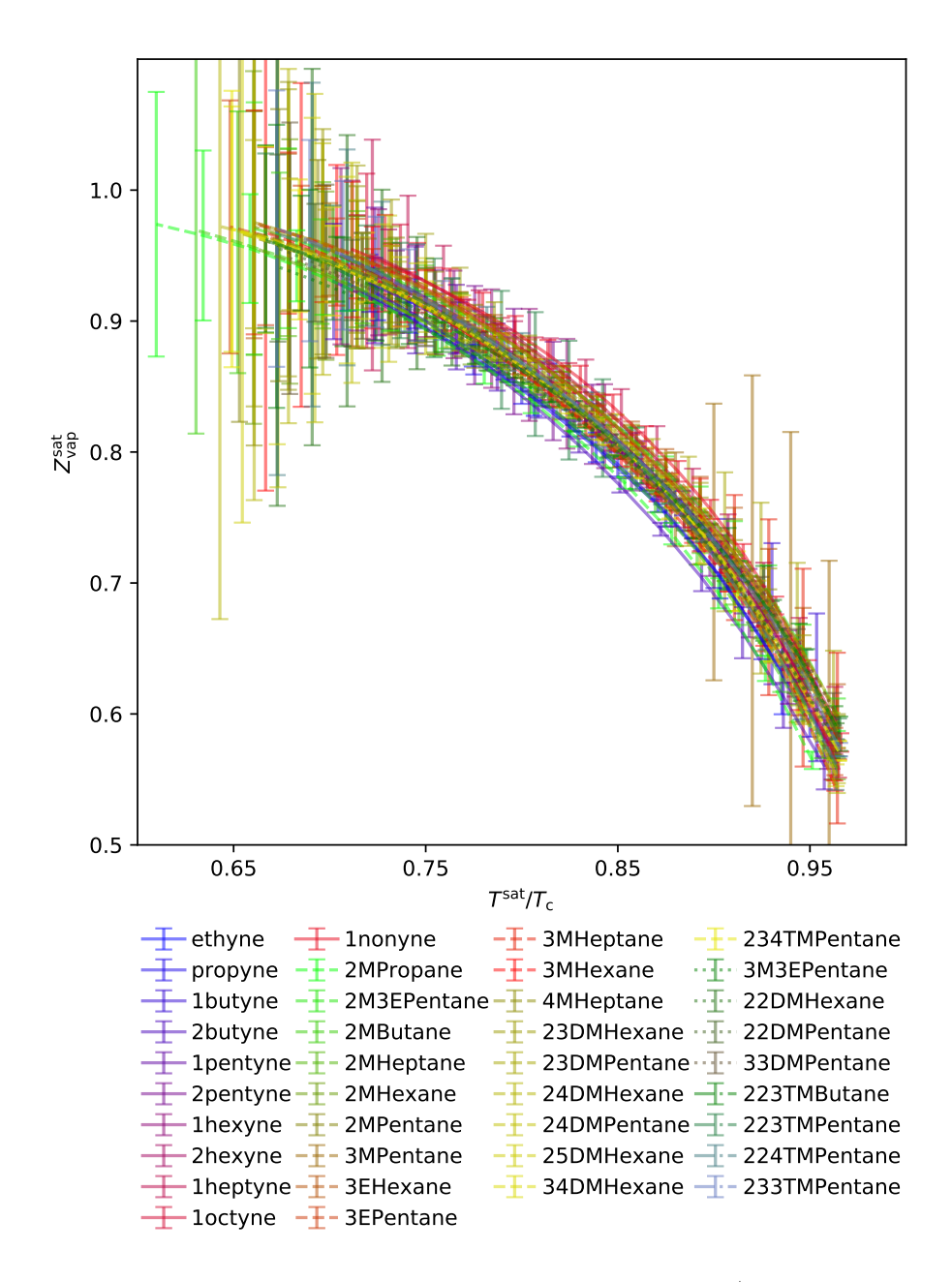


Figure S9: Compressibility factor in saturated vapor phase $(Z_{\mathrm{vap}}^{\mathrm{sat}})$ for all compounds simulated in Mick et al. and Soroush Barhaghi et al. Note that symmetric (normal) 95% confidence intervals are ill-suited when $Z_{\mathrm{vap}}^{\mathrm{sat}} \approx$ 1, as this assumption can result in $Z_{\mathrm{vap}}^{\mathrm{sat}} > 1$.

S7.2 Case study: Cyclohexane optimization

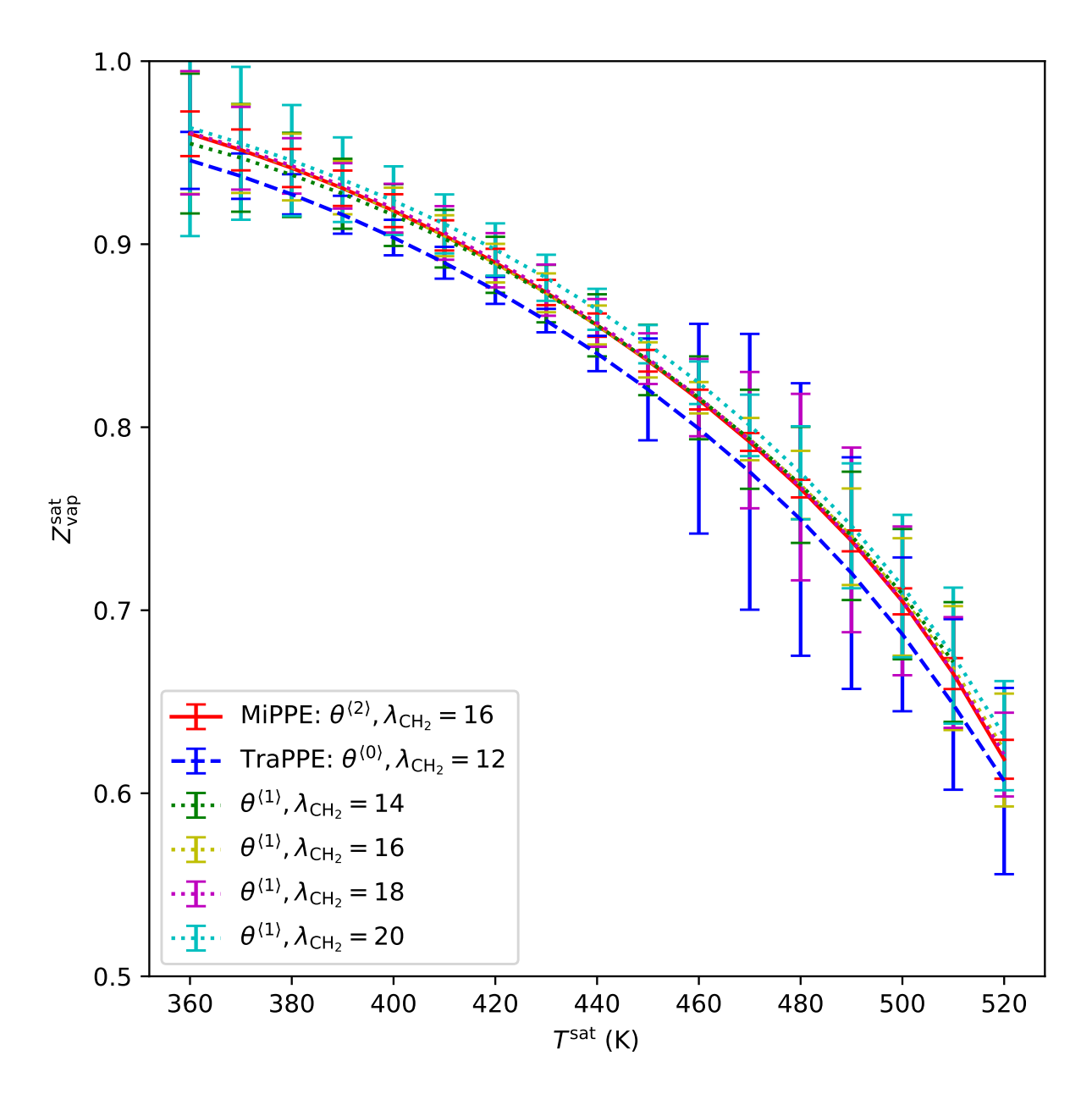


Figure S10: Compressibility factor in saturated vapor phase $(Z_{\rm vap}^{\rm sat})$ for iterations of cyclohexane optimization. Note that symmetric (normal) 95% confidence intervals are ill-suited when $Z_{\rm vap}^{\rm sat} \approx 1$, as this assumption can result in $Z_{\rm vap}^{\rm sat} > 1$.

S7.3 TAMie validation

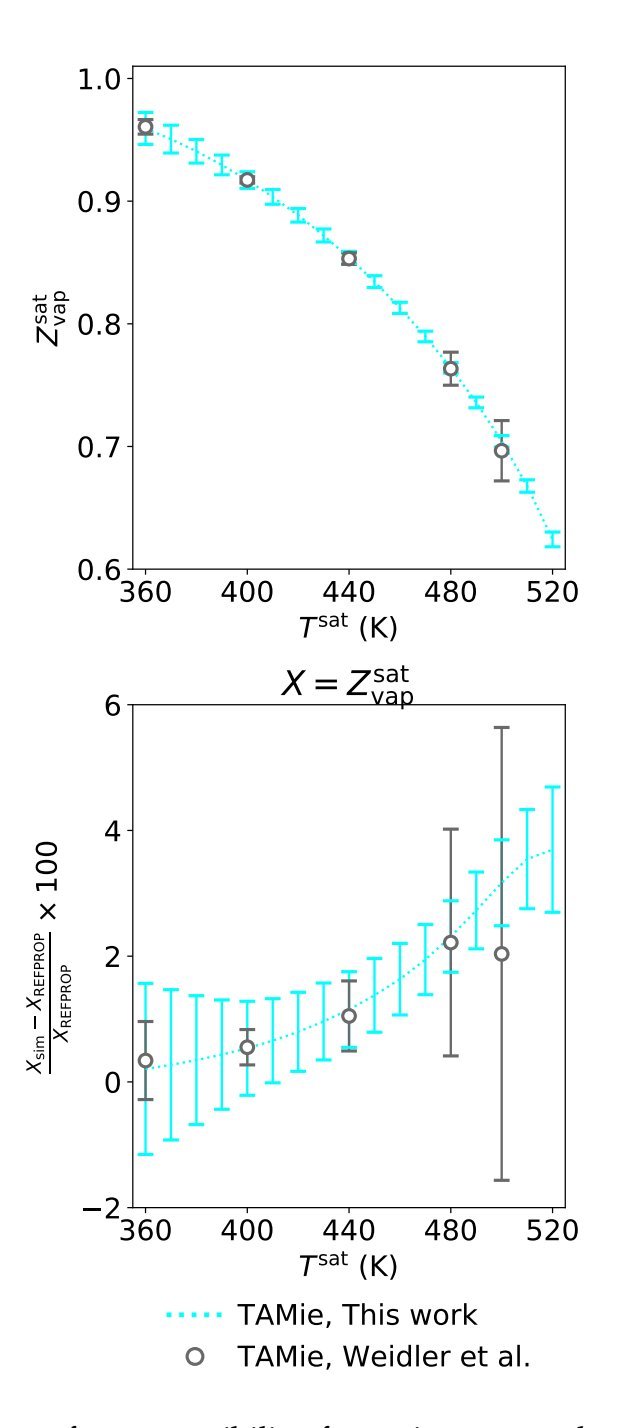


Figure S11: Comparison of compressibility factor in saturated vapor phase $(Z_{\rm vap}^{\rm sat})$ for TAMie (from this work and Weidler et al.). Simulations from this work utilized 3.5 nm box length with a 1.4 nm cut-off. Error bars apply standard propagation of error that assumes independence of $\rho_{\rm vap}^{\rm sat}$ and $P_{\rm vap}^{\rm sat}$.

S8 Tabulated phase equilibria for validation of GCMC-MBAR

S8.1 Branched alkanes

Table S34: GCMC-MBAR results for 2-methylpropane with the MiPPE-SL force field. Subscripts correspond to the 95% confidence interval computed with bootstrap re-sampling.

$T^{\mathrm{sat}}(\mathbf{K})$	$ ho_{ m liq}^{ m sat}$ (kg/m ³)	$ ho_{ m vap}^{ m sat}$ (kg/m ³)	$P_{\mathrm{vap}}^{\mathrm{sat}}$ (MPa)	$\Delta H_{\rm v}$ (kJ/mol)	$Z_{ m vap}^{ m sat}$
390	$388.8_{8.4}$	$87.1_{1.6}$	$2.742_{0.026}$	$9.76_{0.34}$	$0.56_{0.01}$
380	$416.6_{4.6}$	$66.4_{1.2}$	$2.292_{0.026}$	$11.69_{0.17}$	$0.63_{0.01}$
370	$439.7_{1.3}$	$51.95_{0.77}$	$1.903_{0.025}$	$13.219_{0.077}$	$0.692_{0.011}$
360	$459.18_{0.47}$	$41.22_{0.53}$	$1.566_{0.023}$	$14.442_{0.060}$	$0.74_{0.01}$
350	$476.39_{0.48}$	$32.82_{0.53}$	$1.276_{0.019}$	$15.485_{0.049}$	$0.78_{0.01}$
340	$492.09_{0.59}$	$26.09_{0.54}$	$1.028_{0.015}$	$16.404_{0.052}$	$0.81_{0.01}$
330	$506.65_{0.67}$	$20.62_{0.48}$	$0.817_{0.011}$	$17.227_{0.055}$	$0.84_{0.01}$
320	$520.48_{0.53}$	$16.16_{0.39}$	$0.6403_{0.0069}$	$17.980_{0.058}$	$0.865_{0.013}$
310	$533.93_{0.54}$	$12.53_{0.27}$	$0.4935_{0.0043}$	$18.686_{0.062}$	$0.889_{0.015}$
300	$546.58_{0.63}$	$9.57_{0.17}$	$0.3733_{0.0032}$	$19.332_{0.062}$	$0.909_{0.016}$
290	$558.46_{0.48}$	$7.19_{0.12}$	$0.2765_{0.0030}$	$19.925_{0.061}$	$0.927_{0.019}$
280	$570.30_{0.67}$	$5.300_{0.094}$	$0.2000_{0.0032}$	$20.498_{0.077}$	$0.942_{0.027}$
270	$582.5_{1.0}$	$3.815_{0.083}$	$0.1408_{0.0037}$	$21.07_{0.11}$	$0.955_{0.042}$
260	$593.47_{0.60}$	$2.672_{0.071}$	$0.0959_{0.0043}$	$21.57_{0.14}$	$0.965_{0.065}$
250	$603.0_{1.0}$	$1.815_{0.057}$	$0.0632_{0.0048}$	$22.01_{0.22}$	$0.97_{0.10}$

Table S35: GCMC-MBAR results for 2-methylbutane with the MiPPE-SL force field. Subscripts correspond to the 95% confidence interval computed with bootstrap re-sampling.

$T^{\mathrm{sat}}(K)$	$ ho_{ m liq}^{ m sat}$ (kg/m ³)	$ ho_{ m vap}^{ m sat}$ (kg/m ³)	$P_{ m vap}^{ m sat}$ (MPa)	$\Delta H_{\rm v}$ (kJ/mol)	$Z_{ m vap}^{ m sat}$
440	$399.8_{3.5}$	$86.6_{2.1}$	$2.528_{0.020}$	$11.558_{0.090}$	$0.58_{0.01}$
430	$426.9_{2.6}$	$68.9_{1.7}$	$2.149_{0.011}$	$13.44_{0.11}$	$0.629_{0.012}$
420	$449.4_{1.4}$	$55.1_{1.2}$	$1.8149_{0.0059}$	$15.07_{0.11}$	$0.680_{0.012}$
410	$468.58_{0.70}$	$44.49_{0.66}$	$1.5225_{0.0039}$	$16.438_{0.094}$	$0.724_{0.010}$
400	$485.59_{0.52}$	$36.12_{0.31}$	$1.2671_{0.0037}$	$17.615_{0.066}$	$0.76_{0.01}$
390	$501.08_{0.68}$	$29.33_{0.15}$	$1.0450_{0.0036}$	$18.654_{0.048}$	$0.79_{0.01}$
380	$515.41_{0.89}$	$23.73_{0.12}$	$0.8532_{0.0034}$	$19.590_{0.055}$	$0.82_{0.01}$
370	$528.88_{0.98}$	$19.09_{0.11}$	$0.6887_{0.0031}$	$20.447_{0.064}$	$0.85_{0.01}$
360	$541.7_{1.0}$	$15.230_{0.098}$	$0.5489_{0.0029}$	$21.238_{0.067}$	$0.87_{0.01}$
350	$553.9_{1.1}$	$12.03_{0.10}$	$0.4315_{0.0028}$	$21.976_{0.071}$	$0.889_{0.010}$
340	$565.8_{1.3}$	$9.40_{0.11}$	$0.3341_{0.0029}$	$22.678_{0.085}$	$0.907_{0.016}$
330	$577.7_{1.7}$	$7.24_{0.12}$	$0.2541_{0.0033}$	$23.35_{0.12}$	$0.923_{0.025}$
320	$588.9_{1.7}$	$5.48_{0.14}$	$0.1896_{0.0039}$	$23.98_{0.16}$	$0.938_{0.040}$
310	$598.9_{1.2}$	$4.08_{0.14}$	$0.1385_{0.0047}$	$24.53_{0.20}$	$0.950_{0.064}$
300	$608.6_{1.2}$	$2.98_{0.14}$	$0.0988_{0.0055}$	$25.06_{0.28}$	$0.960_{0.10}$
290	$618.9_{1.3}$	$2.12_{0.13}$	$0.0686_{0.0064}$	$25.61_{0.41}$	$0.97_{0.16}$

Table S36: GCMC-MBAR results for 2-methylpentane with the MiPPE-SL force field. Subscripts correspond to the 95% confidence interval computed with bootstrap re-sampling.

$T^{\mathrm{sat}}(K)$	$ ho_{ m liq}^{ m sat}$ (kg/m ³)	$ ho_{ m vap}^{ m sat}$ (kg/m ³)	$P_{\mathrm{vap}}^{\mathrm{sat}}$ (MPa)	$\Delta H_{\rm v}$ (kJ/mol)	$Z_{ m vap}^{ m sat}$
470	$422.20_{0.56}$	$76.7_{1.5}$	$2.068_{0.017}$	$14.14_{0.11}$	$0.59_{0.01}$
460	$444.71_{0.79}$	$61.2_{1.2}$	$1.761_{0.013}$	$16.06_{0.12}$	$0.65_{0.01}$
450	$464.38_{0.87}$	$49.31_{0.88}$	$1.4918_{0.0096}$	$17.71_{0.11}$	$0.70_{0.01}$
440	$481.69_{0.77}$	$40.17_{0.64}$	$1.2557_{0.0068}$	$19.106_{0.090}$	$0.74_{0.01}$
430	$497.34_{0.70}$	$32.86_{0.47}$	$1.0491_{0.0045}$	$20.318_{0.074}$	$0.77_{0.01}$
420	$511.89_{0.78}$	$26.86_{0.36}$	$0.8690_{0.0027}$	$21.408_{0.068}$	$0.80_{0.01}$
410	$525.69_{0.84}$	$21.87_{0.29}$	$0.7130_{0.0017}$	$22.412_{0.069}$	$0.824_{0.011}$
400	$538.82_{0.88}$	$17.70_{0.25}$	$0.5788_{0.0020}$	$23.344_{0.069}$	$0.848_{0.014}$
390	$551.23_{0.87}$	$14.21_{0.22}$	$0.4645_{0.0031}$	$24.207_{0.075}$	$0.869_{0.018}$
380	$562.89_{0.80}$	$11.30_{0.19}$	$0.3681_{0.0042}$	$25.004_{0.096}$	$0.888_{0.024}$
370	$573.96_{0.88}$	$8.90_{0.16}$	$0.2878_{0.0051}$	$25.75_{0.14}$	$0.906_{0.032}$
360	$584.8_{1.1}$	$6.92_{0.14}$	$0.2215_{0.0059}$	$26.46_{0.18}$	$0.922_{0.042}$
350	$595.6_{1.2}$	$5.31_{0.12}$	$0.1677_{0.0065}$	$27.15_{0.22}$	$0.935_{0.056}$
340	$606.3_{1.2}$	$4.01_{0.10}$	$0.1245_{0.0070}$	$27.83_{0.27}$	$0.947_{0.076}$
330	$616.4_{1.0}$	$2.969_{0.085}$	$0.0906_{0.0074}$	$28.45_{0.32}$	$0.96_{0.10}$
320	$625.82_{0.57}$	$2.156_{0.068}$	$0.0644_{0.0078}$	$29.04_{0.40}$	$0.97_{0.14}$

Table S37: GCMC-MBAR results for 2-methylhexane with the MiPPE-SL force field. Subscripts correspond to the 95% confidence interval computed with bootstrap re-sampling.

T ^{sat} (K)	$ ho_{ m liq}^{ m sat}$ (kg/m ³)	$ ho_{ m vap}^{ m sat}$ (kg/m ³)	$P_{ m vap}^{ m sat}$ (MPa)	$\Delta H_{\rm v}$ (kJ/mol)	$Z_{ m vap}^{ m sat}$
510	$406.8_{3.4}$	$88.4_{2.0}$	$2.092_{0.011}$	$14.14_{0.12}$	$0.56_{0.01}$
500	$431.2_{2.2}$	$70.0_{1.6}$	$1.7989_{0.0052}$	$16.506_{0.085}$	$0.620_{0.013}$
490	$452.1_{1.2}$	$56.5_{1.0}$	$1.5403_{0.0041}$	$18.472_{0.088}$	$0.671_{0.013}$
480	$470.38_{0.73}$	$46.30_{0.50}$	$1.3120_{0.0056}$	$20.092_{0.065}$	$0.712_{0.010}$
470	$486.88_{0.50}$	$38.21_{0.17}$	$1.1104_{0.0062}$	$21.497_{0.034}$	$0.75_{0.01}$
460	$502.20_{0.37}$	$31.56_{0.16}$	$0.9327_{0.0058}$	$22.762_{0.022}$	$0.77_{0.01}$
450	$516.52_{0.39}$	$26.01_{0.17}$	$0.7772_{0.0050}$	$23.921_{0.024}$	$0.80_{0.01}$
440	$530.01_{0.34}$	$21.34_{0.15}$	$0.6417_{0.0043}$	$24.994_{0.024}$	$0.82_{0.01}$
430	$542.86_{0.37}$	$17.41_{0.14}$	$0.5245_{0.0039}$	$25.998_{0.031}$	$0.84_{0.01}$
420	$554.93_{0.46}$	$14.10_{0.13}$	$0.4241_{0.0037}$	$26.928_{0.041}$	$0.86_{0.01}$
410	$566.22_{0.43}$	$11.32_{0.14}$	$0.3390_{0.0036}$	$27.789_{0.046}$	$0.881_{0.014}$
400	$577.21_{0.43}$	$8.99_{0.14}$	$0.2674_{0.0037}$	$28.610_{0.060}$	$0.896_{0.020}$
390	$588.02_{0.38}$	$7.06_{0.15}$	$0.2080_{0.0039}$	$29.403_{0.089}$	$0.910_{0.030}$
380	$598.35_{0.22}$	$5.47_{0.16}$	$0.1593_{0.0044}$	$30.15_{0.14}$	$0.923_{0.044}$
370	$608.04_{0.19}$	$4.18_{0.16}$	$0.1200_{0.0050}$	$30.85_{0.20}$	$0.935_{0.064}$
360	$617.49_{0.27}$	$3.14_{0.16}$	$0.0888_{0.0057}$	$31.52_{0.28}$	$0.945_{0.093}$
350	$627.22_{0.26}$	$2.32_{0.15}$	$0.0644_{0.0065}$	$32.20_{0.39}$	$0.96_{0.13}$

Table S38: GCMC-MBAR results for 2-methylheptane with the MiPPE-SL force field. Subscripts correspond to the 95% confidence interval computed with bootstrap re-sampling.

$T^{\mathrm{sat}}(\mathbf{K})$	$ ho_{ m liq}^{ m sat}$ (kg/m ³)	$ ho_{ m vap}^{ m sat}$ (kg/m ³)	$P_{\mathrm{vap}}^{\mathrm{sat}}$ (MPa)	$\Delta H_{\rm v}$ (kJ/mol)	$Z_{ m vap}^{ m sat}$
540	$401.3_{3.7}$	88.7 _{2.6}	$1.947_{0.032}$	$15.17_{0.13}$	$0.56_{0.01}$
530	$426.3_{2.7}$	$71.5_{2.6}$	$1.683_{0.023}$	$17.60_{0.12}$	$0.610_{0.015}$
520	$448.1_{1.4}$	$58.0_{2.1}$	$1.447_{0.015}$	$19.75_{0.16}$	$0.660_{0.020}$
510	$467.12_{0.68}$	$47.5_{1.5}$	$1.2389_{0.0097}$	$21.59_{0.16}$	$0.702_{0.019}$
500	$483.89_{0.51}$	$39.23_{0.90}$	$1.0545_{0.0068}$	$23.17_{0.13}$	$0.738_{0.016}$
490	$499.04_{0.51}$	$32.49_{0.54}$	$0.8917_{0.0055}$	$24.571_{0.096}$	$0.770_{0.012}$
480	$513.07_{0.62}$	$26.88_{0.35}$	$0.7488_{0.0048}$	$25.842_{0.079}$	$0.80_{0.01}$
470	$526.33_{0.63}$	$22.18_{0.26}$	$0.6238_{0.0042}$	$27.019_{0.072}$	$0.82_{0.01}$
460	$538.86_{0.70}$	$18.22_{0.22}$	$0.5151_{0.0038}$	$28.112_{0.079}$	$0.844_{0.010}$
450	$550.62_{0.83}$	$14.88_{0.19}$	$0.4215_{0.0036}$	$29.125_{0.091}$	$0.865_{0.013}$
440	$561.64_{0.82}$	$12.07_{0.16}$	$0.3414_{0.0037}$	$30.06_{0.10}$	$0.883_{0.017}$
430	$572.07_{0.80}$	$9.71_{0.14}$	$0.2735_{0.0040}$	$30.94_{0.11}$	$0.900_{0.022}$
420	$582.24_{0.77}$	$7.74_{0.11}$	$0.2165_{0.0043}$	$31.78_{0.13}$	$0.915_{0.028}$
410	$592.62_{0.67}$	$6.108_{0.092}$	$0.1691_{0.0045}$	$32.62_{0.14}$	$0.927_{0.035}$
400	$603.09_{0.65}$	$4.758_{0.074}$	$0.1302_{0.0047}$	$33.44_{0.16}$	$0.940_{0.044}$
390	$612.67_{0.70}$	$3.655_{0.061}$	$0.0986_{0.0049}$	$34.20_{0.19}$	$0.950_{0.056}$
380	$621.39_{0.62}$	$2.766_{0.052}$	$0.0734_{0.0049}$	$34.89_{0.24}$	$0.960_{0.071}$
370	$630.41_{0.64}$	$2.057_{0.045}$	$0.0536_{0.0049}$	$35.58_{0.31}$	$0.967_{0.093}$

Table S39: GCMC-MBAR results for 3-methylpentane with the MiPPE-SL force field. Subscripts correspond to the 95% confidence interval computed with bootstrap re-sampling.

T ^{sat} (K)	$ ho_{ m liq}^{ m sat}$ (kg/m ³)	$ ho_{ m vap}^{ m sat}$ (kg/m ³)	$P_{\mathrm{vap}}^{\mathrm{sat}}$ (MPa)	$\Delta H_{\rm v}$ (kJ/mol)	$Z_{ m vap}^{ m sat}$
480	$415.8_{1.5}$	84 ₂₄	$2.31_{0.24}$	$13.7_{1.3}$	$0.60_{0.12}$
470	$440.0_{2.3}$	67_{24}	$1.99_{0.14}$	$15.6_{1.7}$	$0.65_{0.17}$
460	$459.8_{2.5}$	55_{18}	$1.698_{0.059}$	$17.2_{1.6}$	$0.69_{0.16}$
450	$477.1_{1.9}$	$45.4_{7.6}$	$1.443_{0.012}$	$18.52_{0.94}$	$0.73_{0.11}$
440	$493.2_{1.2}$	$37.5_{1.5}$	$1.217_{0.014}$	$19.74_{0.27}$	$0.764_{0.036}$
430	$508.9_{1.4}$	$30.95_{0.38}$	$1.019_{0.015}$	$20.87_{0.11}$	$0.794_{0.013}$
420	$523.6_{1.1}$	$25.42_{0.36}$	$0.845_{0.014}$	$21.917_{0.094}$	$0.821_{0.016}$
410	$536.8_{1.4}$	$20.78_{0.32}$	$0.695_{0.014}$	$22.85_{0.12}$	$0.845_{0.020}$
400	$548.9_{1.7}$	$16.89_{0.24}$	$0.565_{0.013}$	$23.69_{0.15}$	$0.867_{0.021}$
390	$560.5_{1.5}$	$13.63_{0.21}$	$0.455_{0.012}$	$24.49_{0.13}$	$0.887_{0.018}$
380	$571.8_{1.2}$	$10.88_{0.20}$	$0.361_{0.010}$	$25.250_{0.099}$	$0.905_{0.016}$
370	$582.3_{1.1}$	$8.59_{0.18}$	$0.2829_{0.0089}$	$25.950_{0.093}$	$0.922_{0.018}$
360	$593.0_{1.1}$	$6.70_{0.16}$	$0.2185_{0.0077}$	$26.64_{0.12}$	$0.939_{0.024}$
350	$603.8_{1.0}$	$5.15_{0.14}$	$0.1661_{0.0067}$	$27.33_{0.14}$	$0.955_{0.035}$

Table S40: GCMC-MBAR results for 3-methylhexane with the MiPPE-SL force field. Subscripts correspond to the 95% confidence interval computed with bootstrap re-sampling.

T ^{sat} (K)	$ ho_{ m liq}^{ m sat}$ (kg/m ³)	$\rho_{\mathrm{vap}}^{\mathrm{sat}}$ (kg/m ³)	$P_{ m vap}^{ m sat}$ (MPa)	$\Delta H_{\rm v}$ (kJ/mol)	$Z_{ m vap}^{ m sat}$
520	398.4 _{4.6}	98.1 _{1.2}	$2.307_{0.018}$	$13.25_{0.29}$	$0.55_{0.01}$
510	$426.2_{3.4}$	$77.3_{1.3}$	$1.996_{0.015}$	$15.86_{0.21}$	$0.61_{0.01}$
500	$449.0_{1.8}$	$62.6_{1.1}$	$1.720_{0.012}$	$17.92_{0.14}$	$0.66_{0.01}$
490	$467.85_{0.87}$	$51.64_{0.76}$	$1.474_{0.011}$	$19.56_{0.10}$	$0.70_{0.01}$
480	$484.12_{0.71}$	$42.82_{0.51}$	$1.2562_{0.0093}$	$20.963_{0.074}$	$0.74_{0.01}$
470	$498.93_{0.76}$	$35.54_{0.44}$	$1.0638_{0.0075}$	$22.215_{0.069}$	$0.77_{0.01}$
460	$512.9_{1.0}$	$29.46_{0.42}$	$0.8944_{0.0056}$	$23.366_{0.088}$	$0.80_{0.01}$
450	$526.2_{1.3}$	$24.34_{0.36}$	$0.7463_{0.0040}$	$24.442_{0.093}$	$0.82_{0.01}$
440	$539.09_{0.79}$	$20.03_{0.26}$	$0.6171_{0.0029}$	$25.454_{0.048}$	$0.84_{0.01}$
430	$551.25_{0.90}$	$16.38_{0.15}$	$0.5055_{0.0025}$	$26.397_{0.089}$	$0.86_{0.01}$
420	$563.0_{1.6}$	$13.302_{0.087}$	$0.4097_{0.0025}$	$27.29_{0.16}$	$0.88_{0.01}$
410	$574.5_{1.4}$	$10.70_{0.12}$	$0.3283_{0.0024}$	$28.15_{0.18}$	$0.90_{0.01}$
400	$585.3_{1.3}$	$8.53_{0.18}$	$0.2598_{0.0021}$	$28.96_{0.19}$	$0.918_{0.019}$
390	$595.7_{2.4}$	$6.72_{0.26}$	$0.2028_{0.0021}$	$29.72_{0.30}$	$0.933_{0.039}$
380	$605.9_{2.8}$	$5.23_{0.33}$	$0.1560_{0.0032}$	$30.45_{0.41}$	$0.947_{0.073}$
370	$615.4_{1.3}$	$4.01_{0.38}$	$0.1181_{0.0053}$	$31.13_{0.47}$	$0.96_{0.12}$
360	$624.92_{0.55}$	$3.04_{0.40}$	$0.0878_{0.0081}$	$31.78_{0.63}$	$0.97_{0.20}$

Table S41: GCMC-MBAR results for 3-methylheptane with the MiPPE-SL force field. Subscripts correspond to the 95% confidence interval computed with bootstrap re-sampling.

$T^{\mathrm{sat}}(K)$	$ ho_{ m liq}^{ m sat}$ (kg/m ³)	$ ho_{ m vap}^{ m sat}$ (kg/m ³)	$P_{\mathrm{vap}}^{\mathrm{sat}}$ (MPa)	$\Delta H_{\rm v}$ (kJ/mol)	$Z_{ m vap}^{ m sat}$
540	$417.2_{1.2}$	83 ₁₂	$1.890_{0.063}$	$16.23_{0.82}$	$0.582_{0.065}$
530	$440.3_{1.2}$	$66.7_{9.0}$	$1.634_{0.033}$	$18.58_{0.89}$	$0.635_{0.076}$
520	$460.5_{1.2}$	$54.5_{5.6}$	$1.407_{0.012}$	$20.58_{0.75}$	$0.681_{0.067}$
510	$478.1_{1.2}$	$45.1_{2.8}$	$1.2045_{0.0059}$	$22.26_{0.50}$	$0.719_{0.048}$
500	$494.01_{0.92}$	$37.5_{1.1}$	$1.0252_{0.0098}$	$23.73_{0.26}$	$0.752_{0.028}$
490	$508.73_{0.65}$	$31.13_{0.27}$	$0.867_{0.011}$	$25.068_{0.10}$	$0.781_{0.013}$
480	$522.52_{0.51}$	$25.80_{0.29}$	$0.728_{0.010}$	$26.295_{0.066}$	$0.81_{0.01}$
470	$535.46_{0.54}$	$21.31_{0.32}$	$0.6061_{0.0088}$	$27.431_{0.087}$	$0.83_{0.01}$
460	$547.59_{0.69}$	$17.52_{0.28}$	$0.5005_{0.0075}$	$28.484_{0.098}$	$0.85_{0.01}$
450	$559.13_{0.85}$	$14.31_{0.24}$	$0.4094_{0.0063}$	$29.47_{0.11}$	$0.87_{0.01}$
440	$570.31_{0.88}$	$11.61_{0.22}$	$0.3315_{0.0051}$	$30.41_{0.11}$	$0.89_{0.01}$
430	$581.03_{0.75}$	$9.34_{0.20}$	$0.2656_{0.0041}$	$31.30_{0.11}$	$0.91_{0.01}$
420	$591.11_{0.65}$	$7.44_{0.18}$	$0.2102_{0.0031}$	$32.12_{0.12}$	$0.924_{0.015}$
410	$600.65_{0.78}$	$5.87_{0.16}$	$0.1642_{0.0025}$	$32.89_{0.15}$	$0.937_{0.022}$
400	$610.1_{1.1}$	$4.58_{0.14}$	$0.1265_{0.0021}$	$33.65_{0.20}$	$0.949_{0.032}$
390	$620.1_{1.3}$	$3.52_{0.12}$	$0.0959_{0.0022}$	$34.43_{0.24}$	$0.959_{0.044}$
380	$630.35_{0.84}$	$2.67_{0.10}$	$0.0714_{0.0025}$	$35.23_{0.26}$	$0.967_{0.062}$
370	$640.62_{0.56}$	$1.986_{0.080}$	$0.0522_{0.0029}$	$36.01_{0.30}$	$0.975_{0.085}$

Table S42: GCMC-MBAR results for 3-ethylpentane with the MiPPE-SL force field. Subscripts correspond to the 95% confidence interval computed with bootstrap re-sampling.

$T^{\mathrm{sat}}\left(\mathbf{K}\right)$	$ ho_{ m liq}^{ m sat}$ (kg/m ³)	$ ho_{ m vap}^{ m sat}$ (kg/m ³)	$P_{\mathrm{vap}}^{\mathrm{sat}}$ (MPa)	$\Delta H_{\rm v}$ (kJ/mol)	$Z_{ m vap}^{ m sat}$
520	$405.9_{2.5}$	$92.5_{3.7}$	$2.279_{0.020}$	$13.93_{0.27}$	$0.571_{0.018}$
510	$433.2_{1.4}$	$75.3_{2.9}$	$1.975_{0.011}$	$16.14_{0.27}$	$0.620_{0.021}$
500	$456.01_{0.97}$	$61.6_{1.8}$	$1.7031_{0.0070}$	$18.08_{0.24}$	$0.667_{0.019}$
490	$474.95_{0.93}$	$50.83_{0.86}$	$1.4607_{0.0069}$	$19.70_{0.17}$	$0.707_{0.013}$
480	$491.46_{0.83}$	$42.20_{0.30}$	$1.2454_{0.0072}$	$21.10_{0.11}$	$0.74_{0.01}$
470	$506.63_{0.68}$	$35.08_{0.18}$	$1.0550_{0.0067}$	$22.354_{0.060}$	$0.77_{0.01}$
460	$521.02_{0.50}$	$29.12_{0.22}$	$0.8870_{0.0058}$	$23.514_{0.046}$	$0.80_{0.01}$
450	$534.61_{0.44}$	$24.08_{0.23}$	$0.7398_{0.0048}$	$24.589_{0.057}$	$0.82_{0.01}$
440	$547.23_{0.42}$	$19.82_{0.21}$	$0.6115_{0.0037}$	$25.575_{0.058}$	$0.85_{0.01}$
430	$559.10_{0.45}$	$16.21_{0.17}$	$0.5007_{0.0028}$	$26.491_{0.043}$	$0.87_{0.01}$
420	$570.66_{0.61}$	$13.16_{0.11}$	$0.4058_{0.0023}$	$27.365_{0.031}$	$0.88_{0.01}$
410	$582.02_{0.53}$	$10.587_{0.082}$	$0.3251_{0.0022}$	$28.205_{0.034}$	$0.90_{0.01}$
400	$592.79_{0.41}$	$8.438_{0.086}$	$0.2572_{0.0023}$	$28.992_{0.054}$	$0.918_{0.015}$
390	$602.92_{0.51}$	$6.653_{0.098}$	$0.2007_{0.0026}$	$29.724_{0.089}$	$0.932_{0.023}$
380	$612.81_{0.53}$	$5.18_{0.10}$	$0.1544_{0.0030}$	$30.43_{0.12}$	$0.945_{0.033}$
370	$622.47_{0.37}$	$3.982_{0.097}$	$0.1168_{0.0035}$	$31.10_{0.15}$	$0.956_{0.048}$
360	$631.88_{0.27}$	$3.012_{0.090}$	$0.0868_{0.0040}$	$31.75_{0.21}$	$0.965_{0.068}$
350	$641.27_{0.30}$	$2.238_{0.081}$	$0.0632_{0.0044}$	$32.39_{0.29}$	$0.972_{0.097}$

Table S43: GCMC-MBAR results for 3-ethylhexane with the MiPPE-SL force field. Subscripts correspond to the 95% confidence interval computed with bootstrap re-sampling.

$T^{\mathrm{sat}}(\mathbf{K})$	$ ho_{ m liq}^{ m sat}$ (kg/m ³)	$ ho_{ m vap}^{ m sat}$ (kg/m ³)	$P_{ m vap}^{ m sat}$ (MPa)	$\Delta H_{\rm v}$ (kJ/mol)	$Z_{ m vap}^{ m sat}$
540	$425.4_{1.8}$	$79.4_{4.9}$	$1.866_{0.043}$	$16.85_{0.40}$	$0.598_{0.025}$
530	$449.1_{1.4}$	$64.7_{4.4}$	$1.614_{0.029}$	$19.05_{0.45}$	$0.647_{0.034}$
520	$468.9_{1.0}$	$53.1_{3.2}$	$1.390_{0.017}$	$20.94_{0.42}$	$0.691_{0.035}$
510	$486.13_{0.88}$	$44.0_{2.0}$	$1.1907_{0.0092}$	$22.56_{0.34}$	$0.728_{0.029}$
500	$501.71_{0.68}$	$36.6_{1.1}$	$1.0141_{0.0047}$	$23.99_{0.23}$	$0.760_{0.021}$
490	$516.13_{0.49}$	$30.49_{0.54}$	$0.8581_{0.0029}$	$25.28_{0.14}$	$0.789_{0.013}$
480	$529.64_{0.54}$	$25.32_{0.27}$	$0.7207_{0.0024}$	$26.475_{0.089}$	$0.81_{0.01}$
470	$542.43_{0.64}$	$20.95_{0.17}$	$0.6006_{0.0021}$	$27.583_{0.069}$	$0.84_{0.01}$
460	$554.62_{0.65}$	$17.25_{0.13}$	$0.4962_{0.0019}$	$28.624_{0.065}$	$0.86_{0.01}$
450	$566.22_{0.66}$	$14.11_{0.11}$	$0.4063_{0.0017}$	$29.600_{0.066}$	$0.88_{0.01}$
440	$577.33_{0.67}$	$11.466_{0.088}$	$0.3292_{0.0016}$	$30.521_{0.065}$	$0.90_{0.01}$
430	$588.23_{0.68}$	$9.237_{0.067}$	$0.2638_{0.0016}$	$31.409_{0.064}$	$0.91_{0.01}$
420	$598.94_{0.67}$	$7.369_{0.055}$	$0.2088_{0.0018}$	$32.268_{0.063}$	$0.927_{0.013}$
410	$609.11_{0.53}$	$5.815_{0.055}$	$0.1630_{0.0019}$	$33.074_{0.060}$	$0.939_{0.019}$
400	$618.75_{0.46}$	$4.534_{0.059}$	$0.1255_{0.0022}$	$33.831_{0.070}$	$0.950_{0.028}$
390	$628.18_{0.46}$	$3.487_{0.060}$	$0.0950_{0.0025}$	$34.56_{0.10}$	$0.960_{0.041}$
380	$637.85_{0.36}$	$2.641_{0.057}$	$0.0707_{0.0028}$	$35.31_{0.15}$	$0.968_{0.060}$
370	$647.74_{0.30}$	$1.965_{0.051}$	$0.0515_{0.0031}$	$36.05_{0.23}$	$0.974_{0.087}$

Table S44: GCMC-MBAR results for 4-methylheptane with the MiPPE-SL force field. Subscripts correspond to the 95% confidence interval computed with bootstrap re-sampling.

$T^{\mathrm{sat}}\left(\mathbf{K}\right)$	$ ho_{ m liq}^{ m sat}$ (kg/m ³)	$ ho_{ m vap}^{ m sat}$ (kg/m ³)	$P_{\mathrm{vap}}^{\mathrm{sat}}$ (MPa)	$\Delta H_{\rm v}$ (kJ/mol)	$Z_{ m vap}^{ m sat}$
540	$418.9_{1.9}$	$80.1_{1.6}$	$1.858_{0.017}$	$16.62_{0.17}$	$0.59_{0.01}$
530	$442.2_{1.4}$	$65.0_{1.3}$	$1.606_{0.015}$	$18.87_{0.15}$	$0.640_{0.010}$
520	$462.3_{1.1}$	$53.3_{1.1}$	$1.382_{0.013}$	$20.81_{0.15}$	$0.685_{0.011}$
510	$479.9_{1.1}$	$44.10_{0.88}$	$1.183_{0.010}$	$22.48_{0.16}$	$0.722_{0.010}$
500	$495.8_{1.0}$	$36.63_{0.73}$	$1.0060_{0.0083}$	$23.95_{0.16}$	$0.755_{0.011}$
490	$510.3_{1.0}$	$30.43_{0.61}$	$0.8501_{0.0062}$	$25.28_{0.16}$	$0.783_{0.011}$
480	$523.91_{0.96}$	$25.22_{0.47}$	$0.7132_{0.0044}$	$26.49_{0.15}$	$0.809_{0.011}$
470	$536.77_{0.78}$	$20.83_{0.32}$	$0.5936_{0.0029}$	$27.62_{0.11}$	$0.83_{0.01}$
460	$548.98_{0.49}$	$17.12_{0.19}$	$0.4897_{0.0020}$	$28.679_{0.071}$	$0.85_{0.01}$
450	$560.48_{0.39}$	$13.982_{0.094}$	$0.4002_{0.0014}$	$29.660_{0.044}$	$0.87_{0.01}$
440	$571.22_{0.45}$	$11.338_{0.062}$	$0.3238_{0.0012}$	$30.567_{0.048}$	$0.89_{0.01}$
430	$581.42_{0.48}$	$9.118_{0.092}$	$0.2591_{0.0013}$	$31.419_{0.060}$	$0.908_{0.012}$
420	$591.67_{0.57}$	$7.26_{0.12}$	$0.2049_{0.0018}$	$32.257_{0.078}$	$0.923_{0.023}$
410	$602.13_{0.53}$	$5.72_{0.14}$	$0.1598_{0.0025}$	$33.10_{0.12}$	$0.936_{0.037}$
400	$612.18_{0.47}$	$4.45_{0.14}$	$0.1228_{0.0033}$	$33.90_{0.18}$	$0.947_{0.056}$
390	$621.73_{0.54}$	$3.42_{0.14}$	$0.0928_{0.0042}$	$34.65_{0.25}$	$0.957_{0.082}$
380	$631.63_{0.45}$	$2.58_{0.12}$	$0.0690_{0.0050}$	$35.41_{0.37}$	$0.97_{0.12}$
370	$641.49_{0.32}$	$1.92_{0.11}$	$0.0502_{0.0057}$	$36.15_{0.52}$	$0.97_{0.17}$

Table S45: GCMC-MBAR results for 2,3-dimethylbutane with the MiPPE-SL force field. Subscripts correspond to the 95% confidence interval computed with bootstrap resampling.

T ^{sat} (K)	a sat $(1/a/m^3)$	$a^{\text{sat}} \left(\frac{1}{2} \left(\frac{\pi}{3} \right) \right)$	Dsat (MD ₂)	Λ <i>H</i> (l/I /mol)	7 sat
$T^{\mathrm{sat}}\left(\mathbf{K}\right)$	$ ho_{ m liq}^{ m sat}$ (kg/m ³)	$\rho_{\rm vap}^{\rm sat}$ (kg/m ³)	$P_{\mathrm{vap}}^{\mathrm{sat}}$ (MPa)	$\Delta H_{\rm v}$ (kJ/mol)	$Z_{ m vap}^{ m sat}$
480	$ 411.7_{1.1} $	$88.4_{2.2}$	$2.369_{0.027}$	$12.87_{0.14}$	$0.58_{0.01}$
470	$437.1_{1.0}$	$71.6_{2.1}$	$2.037_{0.019}$	$14.80_{0.17}$	$0.627_{0.013}$
460	$459.23_{0.86}$	$58.1_{1.6}$	$1.742_{0.013}$	$16.53_{0.18}$	$0.676_{0.015}$
450	$478.07_{0.79}$	$47.5_{1.1}$	$1.4813_{0.0074}$	$18.00_{0.16}$	$0.718_{0.014}$
440	$494.54_{0.81}$	$39.07_{0.72}$	$1.2513_{0.0041}$	$19.26_{0.13}$	$0.754_{0.012}$
430	$509.51_{0.77}$	$32.20_{0.43}$	$1.0493_{0.0024}$	$20.37_{0.10}$	$0.79_{0.01}$
420	$523.51_{0.64}$	$26.49_{0.25}$	$0.8726_{0.0019}$	$21.382_{0.079}$	$0.81_{0.01}$
410	$536.78_{0.54}$	$21.70_{0.15}$	$0.7189_{0.0020}$	$22.310_{0.063}$	$0.84_{0.01}$
400	$549.39_{0.59}$	$17.68_{0.10}$	$0.5863_{0.0021}$	$23.171_{0.060}$	$0.86_{0.01}$
390	$561.38_{0.73}$	$14.296_{0.082}$	$0.4727_{0.0023}$	$23.971_{0.062}$	$0.88_{0.01}$
380	$572.70_{0.68}$	$11.455_{0.085}$	$0.3764_{0.0025}$	$24.712_{0.056}$	$0.896_{0.011}$
370	$583.42_{0.40}$	$9.083_{0.092}$	$0.2957_{0.0028}$	$25.402_{0.050}$	$0.912_{0.016}$
360	$593.75_{0.21}$	$7.115_{0.095}$	$0.2289_{0.0033}$	$26.054_{0.064}$	$0.926_{0.024}$
350	$603.97_{0.20}$	$5.497_{0.091}$	$0.1742_{0.0037}$	$26.686_{0.091}$	$0.938_{0.034}$
340	$614.11_{0.22}$	$4.179_{0.082}$	$0.1302_{0.0042}$	$27.30_{0.13}$	$0.950_{0.047}$
330	$623.72_{0.26}$	$3.121_{0.069}$	$0.0953_{0.0047}$	$27.87_{0.18}$	$0.959_{0.066}$
320	$632.83_{0.34}$	$2.284_{0.057}$	$0.0682_{0.0050}$	$28.41_{0.25}$	$0.968_{0.092}$

Table S46: GCMC-MBAR results for 2,3-dimethylhexane with the MiPPE-SL force field. Subscripts correspond to the 95% confidence interval computed with bootstrap resampling.

$T^{\mathrm{sat}}(\mathbf{K})$	$\rho_{ m liq}^{ m sat}$ (kg/m ³)	$ ho_{ m vap}^{ m sat}$ (kg/m ³)	$P_{\mathrm{vap}}^{\mathrm{sat}}$ (MPa)	$\Delta H_{\rm v}$ (kJ/mol)	$Z_{ m vap}^{ m sat}$
540	$422.2_{1.1}$	$84.5_{3.7}$	$1.948_{0.048}$	$15.98_{0.12}$	$0.586_{0.012}$
530	$445.87_{0.82}$	$68.6_{3.6}$	$1.689_{0.036}$	$18.23_{0.22}$	$0.638_{0.022}$
520	$466.30_{0.66}$	$56.3_{3.0}$	$1.458_{0.024}$	$20.17_{0.26}$	$0.684_{0.027}$
510	$484.13_{0.59}$	$46.7_{2.1}$	$1.253_{0.015}$	$21.81_{0.23}$	$0.722_{0.026}$
500	$499.99_{0.52}$	$39.0_{1.4}$	$1.0703_{0.0092}$	$23.24_{0.18}$	$0.755_{0.022}$
490	$514.34_{0.48}$	$32.51_{0.80}$	$0.9084_{0.0054}$	$24.51_{0.13}$	$0.783_{0.016}$
480	$527.67_{0.54}$	$27.08_{0.47}$	$0.7657_{0.0032}$	$25.677_{0.096}$	$0.809_{0.012}$
470	$540.41_{0.64}$	$22.49_{0.30}$	$0.6406_{0.0019}$	$26.765_{0.082}$	$0.833_{0.010}$
460	$552.77_{0.76}$	$18.58_{0.23}$	$0.5313_{0.0015}$	$27.797_{0.085}$	$0.854_{0.011}$
450	$564.84_{0.87}$	$15.26_{0.22}$	$0.4366_{0.0018}$	$28.78_{0.11}$	$0.874_{0.015}$
440	$576.56_{0.95}$	$12.43_{0.23}$	$0.3553_{0.0025}$	$29.73_{0.14}$	$0.892_{0.022}$
430	$587.55_{0.97}$	$10.05_{0.23}$	$0.2860_{0.0034}$	$30.60_{0.18}$	$0.909_{0.032}$
420	$597.72_{0.83}$	$8.05_{0.21}$	$0.2274_{0.0044}$	$31.40_{0.21}$	$0.924_{0.043}$
410	$607.46_{0.53}$	$6.39_{0.18}$	$0.1787_{0.0053}$	$32.16_{0.22}$	$0.937_{0.055}$
400	$617.12_{0.48}$	$5.01_{0.14}$	$0.1384_{0.0061}$	$32.90_{0.24}$	$0.949_{0.070}$
390	$626.72_{0.62}$	$3.88_{0.10}$	$0.1056_{0.0067}$	$33.64_{0.28}$	$0.959_{0.087}$
380	$636.43_{0.54}$	$2.959_{0.070}$	$0.0792_{0.0071}$	$34.36_{0.35}$	$0.97_{0.11}$
370	$646.47_{0.59}$	$2.219_{0.049}$	$0.0583_{0.0072}$	$35.10_{0.46}$	$0.98_{0.14}$

Table S47: GCMC-MBAR results for 2,3-dimethylpentane with the MiPPE-SL force field. Subscripts correspond to the 95% confidence interval computed with bootstrap re-sampling.

T ^{sat} (K)	$ ho_{ m liq}^{ m sat}$ (kg/m ³)	$ ho_{ m vap}^{ m sat}$ (kg/m ³)	P _{vap} (MPa)	$\Delta H_{ m v}$ (kJ/mol)	$Z_{ m vap}^{ m sat}$
510	$427.9_{1.6}$	81 ₁₀	$2.082_{0.091}$	$15.20_{0.53}$	$0.606_{0.042}$
500	$451.7_{1.0}$	$66.3_{9.6}$	$1.800_{0.057}$	$17.17_{0.70}$	$0.654_{0.061}$
490	$471.41_{0.86}$	$54.7_{7.1}$	$1.549_{0.028}$	$18.83_{0.70}$	$0.696_{0.065}$
480	488.48 _{0.89}	$45.5_{4.0}$	$1.3245_{0.0092}$	$20.25_{0.54}$	$0.731_{0.053}$
470	$503.90_{0.73}$	$37.9_{1.7}$	$1.1257_{0.0050}$	$21.50_{0.32}$	$0.762_{0.034}$
460	$518.28_{0.52}$	$31.50_{0.62}$	$0.9501_{0.0072}$	$22.64_{0.14}$	$0.790_{0.020}$
450	$532.03_{0.63}$	$26.12_{0.25}$	$0.7956_{0.0080}$	$23.709_{0.054}$	$0.816_{0.013}$
440	$545.26_{0.62}$	$21.57_{0.18}$	$0.6606_{0.0080}$	$24.711_{0.037}$	$0.839_{0.011}$
430	$557.77_{0.54}$	$17.70_{0.16}$	$0.5435_{0.0075}$	$25.646_{0.038}$	$0.860_{0.010}$
420	$569.33_{0.53}$	$14.43_{0.15}$	$0.4426_{0.0070}$	$26.504_{0.037}$	$0.880_{0.011}$
410	$580.03_{0.59}$	$11.68_{0.14}$	$0.3565_{0.0063}$	$27.290_{0.040}$	$0.897_{0.012}$
400	$590.33_{0.66}$	$9.36_{0.13}$	$0.2837_{0.0057}$	$28.032_{0.047}$	$0.913_{0.014}$
390	$600.50_{0.61}$	$7.43_{0.11}$	$0.2229_{0.0052}$	$28.747_{0.057}$	$0.927_{0.019}$
380	$610.33_{0.59}$	$5.831_{0.094}$	$0.1726_{0.0048}$	$29.424_{0.079}$	$0.939_{0.025}$
370	$620.01_{0.64}$	$4.512_{0.077}$	$0.1315_{0.0046}$	$30.08_{0.11}$	$0.950_{0.036}$
360	$630.25_{0.55}$	$3.438_{0.066}$	$0.0984_{0.0045}$	$30.75_{0.14}$	$0.959_{0.050}$
350	$640.58_{0.49}$	$2.572_{0.058}$	$0.0722_{0.0046}$	$31.42_{0.20}$	$0.966_{0.072}$

Table S48: GCMC-MBAR results for 2,4-dimethylhexane with the MiPPE-SL force field. Subscripts correspond to the 95% confidence interval computed with bootstrap resampling.

$T^{\mathrm{sat}}\left(\mathbf{K}\right)$	$\rho_{ m liq}^{ m sat}$ (kg/m ³)	$\rho_{\rm vap}^{\rm sat}$ (kg/m ³)	$P_{ m vap}^{ m sat}$ (MPa)	$\Delta H_{\rm v}$ (kJ/mol)	$Z_{ m vap}^{ m sat}$
540	$406.0_{3.8}$	97.8 _{2.1}	$2.090_{0.036}$	$14.21_{0.22}$	$0.54_{0.01}$
530	$430.3_{3.2}$	$78.1_{2.3}$	$1.810_{0.028}$	$16.71_{0.16}$	$0.60_{0.01}$
520	$452.1_{1.9}$	$63.1_{2.2}$	$1.562_{0.019}$	$18.90_{0.15}$	$0.654_{0.016}$
510	$470.9_{1.1}$	$51.8_{1.9}$	$1.342_{0.013}$	$20.72_{0.19}$	$0.698_{0.020}$
500	$487.5_{1.1}$	$42.9_{1.4}$	$1.1472_{0.0080}$	$22.26_{0.19}$	$0.734_{0.020}$
490	$502.5_{1.2}$	$35.72_{0.85}$	$0.9745_{0.0054}$	$23.60_{0.16}$	$0.765_{0.017}$
480	$516.3_{1.4}$	$29.69_{0.47}$	$0.8222_{0.0043}$	$24.83_{0.13}$	$0.793_{0.012}$
470	$529.5_{1.6}$	$24.62_{0.27}$	$0.6886_{0.0037}$	$25.96_{0.11}$	$0.82_{0.01}$
460	$542.1_{1.7}$	$20.34_{0.18}$	$0.5720_{0.0031}$	$27.026_{0.098}$	$0.84_{0.01}$
450	$554.3_{1.8}$	$16.71_{0.13}$	$0.4708_{0.0026}$	$28.031_{0.098}$	$0.86_{0.01}$
440	$566.1_{1.8}$	$13.63_{0.10}$	$0.3836_{0.0024}$	$28.98_{0.10}$	$0.88_{0.01}$
430	$577.4_{1.6}$	$11.03_{0.11}$	$0.3092_{0.0023}$	$29.89_{0.11}$	$0.895_{0.010}$
420	$588.1_{1.4}$	$8.85_{0.15}$	$0.2463_{0.0022}$	$30.73_{0.13}$	$0.910_{0.019}$
410	$598.1_{1.1}$	$7.02_{0.19}$	$0.1937_{0.0024}$	$31.51_{0.17}$	$0.924_{0.033}$
400	$607.97_{0.72}$	$5.51_{0.22}$	$0.1503_{0.0031}$	$32.27_{0.22}$	$0.937_{0.056}$
390	$617.69_{0.31}$	$4.27_{0.23}$	$0.1148_{0.0042}$	$33.01_{0.29}$	$0.947_{0.088}$
380	$627.04_{0.22}$	$3.26_{0.22}$	$0.0862_{0.0055}$	$33.71_{0.42}$	$0.96_{0.14}$
370	$635.81_{0.19}$	$2.45_{0.20}$	$0.0636_{0.0068}$	$34.36_{0.62}$	$0.97_{0.20}$
360	$644.04_{0.32}$	$1.80_{0.18}$	$0.0460_{0.0080}$	$34.97_{0.91}$	$0.97_{0.30}$

Table S49: GCMC-MBAR results for 2,4-dimethylpentane with the MiPPE-SL force field. Subscripts correspond to the 95% confidence interval computed with bootstrap re-sampling.

$T^{\mathrm{sat}}\left(\mathbf{K}\right)$	$ ho_{ m liq}^{ m sat}$ (kg/m ³)	$ ho_{ m vap}^{ m sat}$ (kg/m ³)	$P_{ m vap}^{ m sat}$ (MPa)	$\Delta H_{\rm v}$ (kJ/mol)	$Z_{ m vap}^{ m sat}$
500	$420.0_{1.7}$	$81.9_{2.0}$	$2.003_{0.018}$	$14.77_{0.12}$	$0.590_{0.011}$
490	$443.0_{1.0}$	$65.6_{1.4}$	$1.722_{0.014}$	$16.87_{0.12}$	$0.646_{0.011}$
480	$462.83_{0.68}$	$53.40_{0.95}$	$1.473_{0.011}$	$18.632_{0.099}$	$0.69_{0.01}$
470	$480.50_{0.59}$	$43.96_{0.74}$	$1.2527_{0.0088}$	$20.125_{0.093}$	$0.73_{0.01}$
460	$496.63_{0.64}$	$36.33_{0.64}$	$1.0583_{0.0067}$	$21.44_{0.10}$	$0.763_{0.010}$
450	$511.50_{0.67}$	$30.02_{0.54}$	$0.8873_{0.0049}$	$22.62_{0.10}$	$0.792_{0.012}$
440	$525.28_{0.65}$	$24.73_{0.40}$	$0.7377_{0.0038}$	$23.700_{0.095}$	$0.817_{0.012}$
430	$538.33_{0.62}$	$20.28_{0.26}$	$0.6076_{0.0032}$	$24.704_{0.085}$	$0.840_{0.011}$
420	$550.86_{0.66}$	$16.52_{0.19}$	$0.4955_{0.0029}$	$25.650_{0.080}$	$0.86_{0.01}$
410	$562.59_{0.67}$	$13.35_{0.21}$	$0.3996_{0.0024}$	$26.522_{0.078}$	$0.880_{0.014}$
400	$573.32_{0.65}$	$10.70_{0.23}$	$0.3184_{0.0024}$	$27.312_{0.092}$	$0.897_{0.023}$
390	$583.50_{0.57}$	$8.49_{0.25}$	$0.2504_{0.0031}$	$28.05_{0.13}$	$0.911_{0.037}$
380	$593.48_{0.38}$	$6.66_{0.25}$	$0.1942_{0.0044}$	$28.75_{0.18}$	$0.925_{0.056}$
370	$603.16_{0.41}$	$5.15_{0.26}$	$0.1483_{0.0059}$	$29.42_{0.26}$	$0.937_{0.084}$
360	$613.02_{0.44}$	$3.93_{0.28}$	$0.1113_{0.0076}$	$30.09_{0.36}$	$0.95_{0.13}$
350	$623.28_{0.28}$	$2.94_{0.28}$	$0.0819_{0.0093}$	$30.77_{0.52}$	$0.96_{0.18}$

Table S50: GCMC-MBAR results for 2,5-dimethylhexane with the MiPPE-SL force field. Subscripts correspond to the 95% confidence interval computed with bootstrap resampling.

$T^{\mathrm{sat}}(\mathbf{K})$	$\rho_{ m liq}^{ m sat}$ (kg/m ³)	$ ho_{ m vap}^{ m sat}$ (kg/m ³)	$P_{\mathrm{vap}}^{\mathrm{sat}}$ (MPa)	$\Delta H_{\rm v}$ (kJ/mol)	$Z_{ m vap}^{ m sat}$
530	405.4 _{2.2}	$92.0_{1.7}$	$1.963_{0.011}$	$14.59_{0.15}$	$0.55_{0.01}$
520	$429.1_{1.3}$	$73.2_{1.3}$	$1.6929_{0.0078}$	$17.04_{0.13}$	$0.61_{0.01}$
510	$450.43_{0.78}$	$59.06_{0.93}$	$1.4547_{0.0055}$	$19.17_{0.12}$	$0.66_{0.01}$
500	$469.12_{0.68}$	$48.33_{0.60}$	$1.2442_{0.0042}$	$20.967_{0.088}$	$0.71_{0.01}$
490	$485.77_{0.64}$	$39.90_{0.39}$	$1.0581_{0.0034}$	$22.495_{0.063}$	$0.74_{0.01}$
480	$500.89_{0.55}$	$33.04_{0.27}$	$0.8939_{0.0028}$	$23.843_{0.049}$	$0.77_{0.01}$
470	$514.91_{0.60}$	$27.35_{0.18}$	$0.7498_{0.0025}$	$25.066_{0.046}$	$0.80_{0.01}$
460	$528.20_{0.87}$	$22.57_{0.11}$	$0.6237_{0.0025}$	$26.198_{0.050}$	$0.83_{0.01}$
450	$540.9_{1.0}$	$18.541_{0.071}$	$0.5141_{0.0025}$	$27.259_{0.054}$	$0.85_{0.01}$
440	$553.03_{0.89}$	$15.132_{0.065}$	$0.4196_{0.0026}$	$28.254_{0.049}$	$0.87_{0.01}$
430	$564.47_{0.80}$	$12.255_{0.087}$	$0.3388_{0.0028}$	$29.185_{0.043}$	$0.883_{0.012}$
420	$575.38_{0.95}$	$9.83_{0.12}$	$0.2703_{0.0031}$	$30.060_{0.042}$	$0.899_{0.019}$
410	$586.0_{1.0}$	$7.81_{0.15}$	$0.2130_{0.0036}$	$30.900_{0.064}$	$0.914_{0.030}$
400	$596.47_{0.83}$	$6.13_{0.17}$	$0.1654_{0.0044}$	$31.71_{0.12}$	$0.927_{0.047}$
390	$606.50_{0.59}$	$4.75_{0.18}$	$0.1266_{0.0053}$	$32.48_{0.20}$	$0.939_{0.071}$
380	$615.90_{0.53}$	$3.63_{0.18}$	$0.0953_{0.0064}$	$33.20_{0.30}$	$0.95_{0.11}$
370	$624.82_{0.36}$	$2.73_{0.18}$	$0.0704_{0.0075}$	$33.87_{0.44}$	$0.96_{0.15}$
360	$633.58_{0.39}$	$2.01_{0.16}$	$0.0510_{0.0085}$	$34.52_{0.65}$	$0.97_{0.22}$

Table S51: GCMC-MBAR results for 3,4-dimethylhexane with the MiPPE-SL force field. Subscripts correspond to the 95% confidence interval computed with bootstrap resampling.

$T^{\mathrm{sat}}(\mathbf{K})$	$\rho_{\rm liq}^{\rm sat}$ (kg/m ³)	$ ho_{ m vap}^{ m sat}$ (kg/m ³)	$P_{\mathrm{vap}}^{\mathrm{sat}}$ (MPa)	$\Delta H_{\rm v}$ (kJ/mol)	$Z_{ m vap}^{ m sat}$
550	416.97 _{0.84}	$91.7_{2.1}$	$2.100_{0.024}$	$15.29_{0.11}$	$0.57_{0.01}$
540	$441.75_{0.84}$	$75.2_{2.0}$	$1.828_{0.018}$	$17.53_{0.13}$	$0.619_{0.011}$
530	$462.97_{0.65}$	$61.9_{1.6}$	$1.584_{0.012}$	$19.50_{0.14}$	$0.664_{0.014}$
520	$481.27_{0.52}$	$51.4_{1.2}$	$1.3670_{0.0076}$	$21.20_{0.13}$	$0.703_{0.014}$
510	$497.59_{0.51}$	$42.88_{0.80}$	$1.1732_{0.0044}$	$22.68_{0.12}$	$0.737_{0.012}$
500	$512.45_{0.50}$	$35.87_{0.49}$	$1.0010_{0.0025}$	$23.994_{0.090}$	$0.77_{0.01}$
490	$526.21_{0.55}$	$30.00_{0.31}$	$0.8485_{0.0015}$	$25.192_{0.073}$	$0.79_{0.01}$
480	$539.20_{0.79}$	$25.02_{0.22}$	$0.7142_{0.0014}$	$26.302_{0.072}$	$0.82_{0.01}$
470	$551.6_{1.1}$	$20.79_{0.18}$	$0.5963_{0.0017}$	$27.341_{0.083}$	$0.84_{0.01}$
460	$563.5_{1.3}$	$17.18_{0.15}$	$0.4936_{0.0023}$	$28.319_{0.097}$	$0.858_{0.011}$
450	$574.7_{1.3}$	$14.10_{0.14}$	$0.4050_{0.0028}$	$29.24_{0.11}$	$0.877_{0.014}$
440	$585.4_{1.2}$	$11.49_{0.12}$	$0.3287_{0.0033}$	$30.09_{0.11}$	$0.893_{0.018}$
430	$595.6_{1.1}$	$9.29_{0.11}$	$0.2642_{0.0037}$	$30.90_{0.11}$	$0.909_{0.022}$
420	$605.36_{0.91}$	$7.437_{0.097}$	$0.2097_{0.0040}$	$31.66_{0.11}$	$0.922_{0.027}$
410	$614.74_{0.65}$	$5.893_{0.085}$	$0.1644_{0.0042}$	$32.38_{0.12}$	$0.935_{0.033}$
400	$624.02_{0.41}$	$4.615_{0.075}$	$0.1271_{0.0044}$	$33.08_{0.14}$	$0.946_{0.041}$
390	$633.41_{0.31}$	$3.566_{0.067}$	$0.0967_{0.0045}$	$33.78_{0.17}$	$0.955_{0.053}$
380	$642.95_{0.22}$	$2.715_{0.059}$	$0.0724_{0.0045}$	$34.48_{0.22}$	$0.964_{0.070}$
370	$652.67_{0.19}$	$2.032_{0.051}$	$0.0531_{0.0046}$	$35.18_{0.29}$	$0.970_{0.094}$

Table S52: GCMC-MBAR results for 2,3,4-trimethylpentane with the MiPPE-SL force field. Subscripts correspond to the 95% confidence interval computed with bootstrap re-sampling.

$T^{\mathrm{sat}}(\mathbf{K})$	$\rho_{ m liq}^{ m sat}$ (kg/m ³)	$\rho_{\rm vap}^{\rm sat}$ (kg/m ³)	$P_{ m vap}^{ m sat}$ (MPa)	$\Delta H_{\rm v}$ (kJ/mol)	$Z_{ m vap}^{ m sat}$
550	$415.7_{1.4}$	$96.1_{3.2}$	$2.199_{0.049}$	$14.71_{0.16}$	$0.57_{0.01}$
540	$442.1_{1.2}$	$79.3_{3.4}$	$1.920_{0.039}$	$16.92_{0.21}$	$0.616_{0.015}$
530	$464.77_{0.78}$	$65.5_{3.0}$	$1.669_{0.029}$	$18.91_{0.25}$	$0.661_{0.021}$
520	$483.71_{0.55}$	$54.4_{2.4}$	$1.444_{0.021}$	$20.61_{0.24}$	$0.701_{0.023}$
510	$499.94_{0.54}$	$45.5_{1.7}$	$1.243_{0.015}$	$22.07_{0.20}$	$0.736_{0.021}$
500	$514.37_{0.58}$	$38.2_{1.1}$	$1.064_{0.011}$	$23.34_{0.15}$	$0.766_{0.017}$
490	$527.58_{0.61}$	$32.03_{0.69}$	$0.9054_{0.0087}$	$24.49_{0.10}$	$0.793_{0.013}$
480	$540.01_{0.71}$	$26.83_{0.52}$	$0.7652_{0.0066}$	$25.541_{0.081}$	$0.816_{0.011}$
470	$552.10_{0.82}$	$22.39_{0.43}$	$0.6419_{0.0048}$	$26.539_{0.074}$	$0.838_{0.011}$
460	$564.06_{0.86}$	$18.59_{0.35}$	$0.5341_{0.0032}$	$27.497_{0.070}$	$0.858_{0.013}$
450	$575.70_{0.84}$	$15.35_{0.26}$	$0.4403_{0.0020}$	$28.409_{0.064}$	$0.876_{0.014}$
440	$586.68_{0.81}$	$12.58_{0.18}$	$0.3594_{0.0017}$	$29.258_{0.061}$	$0.892_{0.013}$
430	$596.87_{0.75}$	$10.22_{0.11}$	$0.2903_{0.0018}$	$30.041_{0.060}$	$0.907_{0.013}$
420	$606.38_{0.61}$	$8.235_{0.070}$	$0.2318_{0.0019}$	$30.766_{0.064}$	$0.921_{0.013}$
410	$615.73_{0.46}$	$6.567_{0.082}$	$0.1828_{0.0020}$	$31.466_{0.074}$	$0.933_{0.018}$
400	$625.40_{0.41}$	$5.18_{0.11}$	$0.1422_{0.0022}$	$32.176_{0.095}$	$0.944_{0.029}$
390	$634.86_{0.32}$	$4.03_{0.13}$	$0.1090_{0.0025}$	$32.86_{0.14}$	$0.953_{0.046}$
380	$643.49_{0.23}$	$3.09_{0.13}$	$0.0822_{0.0031}$	$33.48_{0.20}$	$0.962_{0.071}$
370	$652.26_{0.34}$	$2.33_{0.13}$	$0.0609_{0.0038}$	$34.10_{0.29}$	$0.97_{0.11}$

Table S53: GCMC-MBAR results for 2-methyl-3-ethylpentane with the MiPPE-SL force field. Subscripts correspond to the 95% confidence interval computed with bootstrap resampling.

$T^{\mathrm{sat}}(\mathbf{K})$	$ ho_{ m liq}^{ m sat}$ (kg/m ³)	$ ho_{ m vap}^{ m sat}$ (kg/m ³)	$P_{\mathrm{vap}}^{\mathrm{sat}}$ (MPa)	$\Delta H_{\rm v}$ (kJ/mol)	$Z_{ m vap}^{ m sat}$
540	$433.4_{2.7}$	$82.6_{3.0}$	$1.946_{0.032}$	$16.49_{0.24}$	$0.599_{0.012}$
530	$455.6_{2.0}$	$67.4_{2.8}$	$1.688_{0.024}$	$18.61_{0.30}$	$0.649_{0.019}$
520	$474.7_{1.3}$	$55.6_{2.2}$	$1.458_{0.016}$	$20.42_{0.29}$	$0.692_{0.021}$
510	$491.79_{0.85}$	$46.4_{1.5}$	$1.253_{0.011}$	$21.98_{0.23}$	$0.728_{0.019}$
500	$507.34_{0.64}$	$38.79_{0.93}$	$1.0711_{0.0081}$	$23.35_{0.17}$	$0.759_{0.015}$
490	$521.73_{0.53}$	$32.44_{0.55}$	$0.9094_{0.0062}$	$24.59_{0.11}$	$0.786_{0.011}$
480	$535.29_{0.40}$	$27.07_{0.36}$	$0.7666_{0.0049}$	$25.746_{0.076}$	$0.81_{0.01}$
470	$548.25_{0.30}$	$22.50_{0.28}$	$0.6411_{0.0038}$	$26.827_{0.056}$	$0.83_{0.01}$
460	$560.62_{0.34}$	$18.60_{0.23}$	$0.5316_{0.0028}$	$27.843_{0.047}$	$0.85_{0.01}$
450	$572.31_{0.35}$	$15.28_{0.20}$	$0.4368_{0.0020}$	$28.791_{0.049}$	$0.87_{0.01}$
440	$583.21_{0.31}$	$12.46_{0.17}$	$0.3554_{0.0014}$	$29.667_{0.055}$	$0.891_{0.012}$
430	$593.38_{0.30}$	$10.08_{0.14}$	$0.2861_{0.0014}$	$30.476_{0.064}$	$0.907_{0.015}$
420	$602.98_{0.33}$	$8.09_{0.13}$	$0.2277_{0.0018}$	$31.230_{0.085}$	$0.921_{0.020}$
410	$612.40_{0.54}$	$6.42_{0.11}$	$0.1789_{0.0022}$	$31.96_{0.12}$	$0.933_{0.026}$
400	$622.18_{0.63}$	$5.04_{0.10}$	$0.1387_{0.0027}$	$32.69_{0.15}$	$0.944_{0.036}$
390	$632.26_{0.45}$	$3.907_{0.092}$	$0.1058_{0.0031}$	$33.42_{0.18}$	$0.954_{0.049}$
380	$641.81_{0.31}$	$2.981_{0.084}$	$0.0794_{0.0036}$	$34.12_{0.22}$	$0.963_{0.069}$
370	$650.71_{0.52}$	$2.238_{0.074}$	$0.0585_{0.0039}$	$34.76_{0.31}$	$0.971_{0.096}$

Table S54: GCMC-MBAR results for 3-methyl-3-ethylpentane with the MiPPE-SL force field. Subscripts correspond to the 95% confidence interval computed with bootstrap resampling.

$T^{\mathrm{sat}}(\mathbf{K})$	$ ho_{ m liq}^{ m sat}$ (kg/m ³)	$ ho_{ m vap}^{ m sat}$ (kg/m ³)	$P_{ m vap}^{ m sat}$ (MPa)	$\Delta H_{\rm v}$ (kJ/mol)	$Z_{ m vap}^{ m sat}$
560	$429.6_{1.9}$	$93.3_{3.0}$	$2.224_{0.025}$	$15.51_{0.15}$	$0.585_{0.013}$
550	$453.4_{1.3}$	$76.7_{2.3}$	$1.949_{0.017}$	$17.72_{0.13}$	$0.635_{0.015}$
540	$473.9_{1.5}$	$64.1_{1.4}$	$1.702_{0.012}$	$19.55_{0.10}$	$0.676_{0.012}$
530	$491.5_{1.3}$	$54.07_{0.82}$	$1.4787_{0.0089}$	$21.089_{0.076}$	$0.71_{0.01}$
520	$506.85_{0.72}$	$45.77_{0.59}$	$1.2780_{0.0068}$	$22.420_{0.057}$	$0.74_{0.01}$
510	$520.59_{0.37}$	$38.74_{0.54}$	$1.0984_{0.0049}$	$23.608_{0.064}$	$0.76_{0.01}$
500	$533.49_{0.41}$	$32.75_{0.51}$	$0.9383_{0.0034}$	$24.705_{0.078}$	$0.787_{0.011}$
490	$545.92_{0.68}$	$27.61_{0.41}$	$0.7960_{0.0027}$	$25.736_{0.080}$	$0.808_{0.012}$
480	$557.91_{0.83}$	$23.19_{0.27}$	$0.6704_{0.0029}$	$26.707_{0.072}$	$0.827_{0.012}$
470	$569.50_{0.65}$	$19.38_{0.14}$	$0.5599_{0.0033}$	$27.623_{0.058}$	$0.84_{0.01}$
460	$580.74_{0.49}$	$16.096_{0.094}$	$0.4634_{0.0033}$	$28.496_{0.048}$	$0.86_{0.01}$
450	$591.73_{0.55}$	$13.27_{0.13}$	$0.3799_{0.0029}$	$29.336_{0.044}$	$0.87_{0.01}$
440	$602.39_{0.47}$	$10.84_{0.16}$	$0.3082_{0.0025}$	$30.140_{0.046}$	$0.888_{0.011}$
430	$612.22_{0.39}$	$8.78_{0.18}$	$0.2472_{0.0021}$	$30.879_{0.073}$	$0.900_{0.017}$
420	$621.24_{0.63}$	$7.03_{0.20}$	$0.1959_{0.0020}$	$31.56_{0.12}$	$0.911_{0.026}$
410	$630.11_{0.71}$	$5.57_{0.23}$	$0.1533_{0.0023}$	$32.21_{0.17}$	$0.922_{0.041}$
400	$639.21_{0.40}$	$4.36_{0.28}$	$0.1182_{0.0032}$	$32.87_{0.24}$	$0.932_{0.068}$
390	$648.92_{0.26}$	$3.36_{0.32}$	$0.0898_{0.0047}$	$33.56_{0.35}$	$0.94_{0.11}$

Table S55: GCMC-MBAR results for 2,2-dimethylbutane with the MiPPE-SL force field. Subscripts correspond to the 95% confidence interval computed with bootstrap resampling.

$T^{\mathrm{sat}}(\mathbf{K})$	$ ho_{ m liq}^{ m sat}$ (kg/m ³)	$ ho_{ m vap}^{ m sat}$ (kg/m ³)	$P_{ m vap}^{ m sat}$ (MPa)	$\Delta H_{\rm v}$ (kJ/mol)	$Z_{ m vap}^{ m sat}$
470	$412.4_{5.2}$	$85.4_{8.5}$	$2.32_{0.11}$	$12.77_{0.20}$	$0.598_{0.027}$
460	$438.1_{4.9}$	$69.3_{8.7}$	$1.996_{0.071}$	$14.62_{0.34}$	$0.649_{0.049}$
450	$459.2_{3.1}$	$56.9_{7.2}$	$1.709_{0.036}$	$16.16_{0.45}$	$0.691_{0.061}$
440	$477.5_{1.5}$	$47.1_{4.6}$	$1.453_{0.011}$	$17.47_{0.41}$	$0.727_{0.057}$
430	$494.03_{0.95}$	$39.0_{2.1}$	$1.2267_{0.0045}$	$18.63_{0.25}$	$0.759_{0.039}$
420	$508.92_{0.71}$	$32.17_{0.58}$	$1.0273_{0.0094}$	$19.664_{0.098}$	$0.788_{0.020}$
410	$522.56_{0.38}$	$26.47_{0.14}$	$0.853_{0.010}$	$20.599_{0.035}$	$0.81_{0.01}$
400	$535.52_{0.29}$	$21.68_{0.16}$	$0.7014_{0.0094}$	$21.466_{0.026}$	$0.84_{0.01}$
390	$548.22_{0.34}$	$17.64_{0.11}$	$0.5708_{0.0086}$	$22.291_{0.027}$	$0.860_{0.010}$
380	$560.63_{0.37}$	$14.238_{0.067}$	$0.4591_{0.0081}$	$23.076_{0.038}$	$0.879_{0.013}$
370	$572.47_{0.42}$	$11.382_{0.058}$	$0.3644_{0.0077}$	$23.813_{0.053}$	$0.897_{0.017}$
360	$583.49_{0.45}$	$8.997_{0.074}$	$0.2850_{0.0074}$	$24.488_{0.062}$	$0.912_{0.022}$
350	$593.61_{0.52}$	$7.021_{0.099}$	$0.2196_{0.0070}$	$25.098_{0.081}$	$0.926_{0.029}$
340	$603.19_{0.55}$	$5.40_{0.12}$	$0.1662_{0.0067}$	$25.66_{0.11}$	$0.939_{0.041}$
330	$612.67_{0.41}$	$4.09_{0.14}$	$0.1236_{0.0065}$	$26.22_{0.16}$	$0.950_{0.061}$
320	$622.10_{0.33}$	$3.03_{0.13}$	$0.0899_{0.0065}$	$26.75_{0.23}$	$0.959_{0.091}$
310	$631.64_{0.30}$	$2.21_{0.12}$	$0.0640_{0.0068}$	$27.29_{0.34}$	$0.97_{0.14}$

Table S56: GCMC-MBAR results for 2,2-dimethylhexane with the MiPPE-SL force field. Subscripts correspond to the 95% confidence interval computed with bootstrap resampling.

$T^{\mathrm{sat}}(\mathbf{K})$	$ ho_{ m liq}^{ m sat}$ (kg/m ³)	$ ho_{ m vap}^{ m sat}$ (kg/m ³)	$P_{ m vap}^{ m sat}$ (MPa)	$\Delta H_{\rm v}$ (kJ/mol)	$Z_{ m vap}^{ m sat}$
530	$405.4_{1.1}$	$88.4_{2.4}$	$1.979_{0.012}$	$14.84_{0.19}$	$0.580_{0.013}$
520	$431.48_{0.93}$	$72.7_{1.8}$	$1.7154_{0.0075}$	$16.99_{0.19}$	$0.623_{0.013}$
510	$453.8_{1.0}$	$59.8_{1.2}$	$1.4785_{0.0047}$	$18.93_{0.16}$	$0.666_{0.012}$
500	$472.8_{1.0}$	$49.35_{0.64}$	$1.2675_{0.0038}$	$20.62_{0.13}$	$0.71_{0.01}$
490	$489.55_{0.82}$	$40.92_{0.33}$	$1.0801_{0.0034}$	$22.090_{0.076}$	$0.74_{0.01}$
480	$504.38_{0.54}$	$33.96_{0.19}$	$0.9145_{0.0030}$	$23.386_{0.037}$	$0.77_{0.01}$
470	$517.67_{0.43}$	$28.16_{0.15}$	$0.7689_{0.0025}$	$24.539_{0.032}$	$0.80_{0.01}$
460	$530.06_{0.45}$	$23.29_{0.13}$	$0.6417_{0.0022}$	$25.596_{0.035}$	$0.82_{0.01}$
450	$542.23_{0.55}$	$19.19_{0.13}$	$0.5309_{0.0021}$	$26.601_{0.035}$	$0.84_{0.01}$
440	$554.29_{0.63}$	$15.71_{0.16}$	$0.4353_{0.0023}$	$27.566_{0.050}$	$0.865_{0.012}$
430	$565.90_{0.55}$	$12.78_{0.20}$	$0.3531_{0.0029}$	$28.479_{0.074}$	$0.883_{0.020}$
420	$577.12_{0.44}$	$10.30_{0.25}$	$0.2833_{0.0040}$	$29.35_{0.10}$	$0.899_{0.033}$
410	$588.18_{0.45}$	$8.23_{0.27}$	$0.2243_{0.0053}$	$30.19_{0.16}$	$0.914_{0.050}$
400	$598.75_{0.43}$	$6.49_{0.27}$	$0.1753_{0.0068}$	$30.99_{0.23}$	$0.927_{0.073}$
390	$608.66_{0.49}$	$5.06_{0.26}$	$0.1349_{0.0082}$	$31.74_{0.32}$	$0.94_{0.10}$
380	$618.76_{0.62}$	$3.89_{0.23}$	$0.1021_{0.0096}$	$32.48_{0.43}$	$0.95_{0.14}$
370	$629.14_{0.47}$	$2.94_{0.20}$	$0.076_{0.011}$	$33.23_{0.60}$	$0.96_{0.20}$

Table S57: GCMC-MBAR results for 2,2-dimethylpentane with the MiPPE-SL force field. Subscripts correspond to the 95% confidence interval computed with bootstrap re-sampling.

$T^{\mathrm{sat}}(\mathbf{K})$	$ ho_{ m liq}^{ m sat}$ (kg/m ³)	$\rho_{\rm vap}^{\rm sat}$ (kg/m ³)	$P_{ m vap}^{ m sat}$ (MPa)	$\Delta H_{\rm v}$ (kJ/mol)	$Z_{ m vap}^{ m sat}$
500	$411.2_{4.8}$	88.4 _{3.0}	$2.127_{0.025}$	$13.748_{0.081}$	$0.580_{0.013}$
490	$436.8_{4.1}$	$71.5_{2.2}$	$1.835_{0.014}$	$15.833_{0.068}$	$0.631_{0.015}$
480	$457.9_{2.5}$	$58.3_{1.4}$	$1.5750_{0.0068}$	$17.601_{0.049}$	$0.678_{0.014}$
470	$476.0_{1.4}$	$48.10_{0.81}$	$1.3443_{0.0036}$	$19.097_{0.040}$	$0.717_{0.012}$
460	$492.22_{0.92}$	$39.84_{0.47}$	$1.1402_{0.0035}$	$20.399_{0.036}$	$0.75_{0.01}$
450	$506.85_{0.87}$	$33.01_{0.29}$	$0.9600_{0.0041}$	$21.553_{0.034}$	$0.78_{0.01}$
440	$520.4_{1.0}$	$27.29_{0.18}$	$0.8020_{0.0047}$	$22.600_{0.037}$	$0.80_{0.01}$
430	$533.27_{0.96}$	$22.47_{0.10}$	$0.6642_{0.0050}$	$23.572_{0.034}$	$0.83_{0.01}$
420	$545.67_{0.39}$	$18.398_{0.066}$	$0.5448_{0.0050}$	$24.481_{0.029}$	$0.85_{0.01}$
410	$557.49_{0.37}$	$14.958_{0.060}$	$0.4422_{0.0048}$	$25.331_{0.052}$	$0.87_{0.01}$
400	$568.93_{0.50}$	$12.058_{0.076}$	$0.3547_{0.0047}$	$26.137_{0.064}$	$0.886_{0.013}$
390	$580.08_{0.47}$	$9.622_{0.094}$	$0.2810_{0.0046}$	$26.908_{0.069}$	$0.902_{0.018}$
380	$590.67_{0.42}$	$7.59_{0.11}$	$0.2195_{0.0045}$	$27.631_{0.075}$	$0.917_{0.023}$
370	$601.07_{0.39}$	$5.91_{0.14}$	$0.1689_{0.0043}$	$28.333_{0.091}$	$0.931_{0.031}$
360	$611.44_{0.41}$	$4.53_{0.18}$	$0.1279_{0.0041}$	$29.02_{0.13}$	$0.945_{0.045}$
350	$620.82_{0.40}$	$3.42_{0.21}$	$0.0950_{0.0040}$	$29.64_{0.19}$	$0.956_{0.071}$

Table S58: GCMC-MBAR results for 2,2-dimethylpropane with the MiPPE-SL force field. Subscripts correspond to the 95% confidence interval computed with bootstrap re-sampling.

T ^{sat} (K)	$\rho_{ m liq}^{ m sat}$ (kg/m ³)	$ ho_{ m vap}^{ m sat}$ (kg/m ³)	P _{vap} (MPa)	$\Delta H_{\rm v}$ (kJ/mol)	$Z_{ m vap}^{ m sat}$
410	$409.5_{2.6}$	78.8 _{2.6}	$2.218_{0.029}$	$11.33_{0.11}$	$0.596_{0.013}$
400	$433.9_{2.3}$	$61.3_{1.8}$	$1.869_{0.018}$	$13.140_{0.083}$	$0.661_{0.014}$
390	$454.8_{1.5}$	$48.8_{1.1}$	$1.565_{0.010}$	$14.591_{0.051}$	$0.713_{0.013}$
380	$472.4_{1.1}$	$39.38_{0.72}$	$1.3004_{0.0056}$	$15.750_{0.045}$	$0.754_{0.011}$
370	$487.88_{0.98}$	$31.87_{0.48}$	$1.0704_{0.0035}$	$16.732_{0.045}$	$0.788_{0.011}$
360	$502.34_{0.89}$	$25.71_{0.33}$	$0.8720_{0.0036}$	$17.617_{0.044}$	$0.817_{0.012}$
350	$516.37_{0.86}$	$20.61_{0.21}$	$0.7019_{0.0043}$	$18.443_{0.046}$	$0.844_{0.011}$
340	$529.79_{0.93}$	$16.38_{0.18}$	$0.5574_{0.0045}$	$19.210_{0.057}$	$0.868_{0.011}$
330	$542.27_{0.96}$	$12.88_{0.23}$	$0.4363_{0.0041}$	$19.910_{0.078}$	$0.891_{0.016}$
320	$553.7_{1.0}$	$10.00_{0.28}$	$0.3360_{0.0037}$	$20.54_{0.11}$	$0.911_{0.029}$
310	$564.4_{1.4}$	$7.66_{0.32}$	$0.2543_{0.0044}$	$21.12_{0.18}$	$0.930_{0.052}$
300	$575.3_{1.8}$	$5.77_{0.33}$	$0.1887_{0.0061}$	$21.68_{0.28}$	$0.946_{0.087}$
290	$587.1_{1.3}$	$4.27_{0.32}$	$0.1368_{0.0084}$	$22.27_{0.38}$	$0.96_{0.14}$
280	$599.1_{1.1}$	$3.08_{0.29}$	$0.096_{0.011}$	$22.85_{0.55}$	$0.97_{0.22}$

Table S59: GCMC-MBAR results for 3,3-dimethylpentane with the MiPPE-SL force field. Subscripts correspond to the 95% confidence interval computed with bootstrap re-sampling.

$T^{\mathrm{sat}}(\mathbf{K})$	$ ho_{ m liq}^{ m sat}$ (kg/m ³)	$ ho_{ m vap}^{ m sat}$ (kg/m ³)	$P_{ m vap}^{ m sat}$ (MPa)	$\Delta H_{\rm v}$ (kJ/mol)	$Z_{ m vap}^{ m sat}$
510	$433.8_{1.4}$	$83.3_{2.1}$	$2.128_{0.013}$	$14.92_{0.15}$	$0.604_{0.012}$
500	$456.2_{1.8}$	$68.2_{1.6}$	$1.8431_{0.0076}$	$16.79_{0.16}$	$0.651_{0.013}$
490	$475.3_{1.5}$	$56.40_{0.99}$	$1.5893_{0.0041}$	$18.38_{0.12}$	$0.693_{0.012}$
480	$492.10_{0.90}$	$47.00_{0.51}$	$1.3630_{0.0031}$	$19.752_{0.070}$	$0.73_{0.01}$
470	$507.53_{0.52}$	$39.28_{0.29}$	$1.1617_{0.0029}$	$20.968_{0.041}$	$0.76_{0.01}$
460	$521.91_{0.42}$	$32.81_{0.22}$	$0.9831_{0.0027}$	$22.072_{0.042}$	$0.78_{0.01}$
450	$535.23_{0.39}$	$27.34_{0.16}$	$0.8258_{0.0025}$	$23.077_{0.038}$	$0.81_{0.01}$
440	$547.46_{0.40}$	$22.676_{0.096}$	$0.6879_{0.0023}$	$23.990_{0.031}$	$0.83_{0.01}$
430	$559.01_{0.43}$	$18.706_{0.065}$	$0.5678_{0.0022}$	$24.839_{0.027}$	$0.85_{0.01}$
420	$570.36_{0.53}$	$15.325_{0.054}$	$0.4642_{0.0020}$	$25.651_{0.032}$	$0.87_{0.01}$
410	$581.43_{0.85}$	$12.456_{0.067}$	$0.3754_{0.0020}$	$26.425_{0.058}$	$0.89_{0.01}$
400	$591.91_{0.96}$	$10.03_{0.10}$	$0.3000_{0.0021}$	$27.146_{0.083}$	$0.901_{0.013}$
390	$601.87_{0.71}$	$8.00_{0.14}$	$0.2368_{0.0024}$	$27.82_{0.10}$	$0.915_{0.024}$
380	$611.41_{0.54}$	$6.30_{0.17}$	$0.1842_{0.0031}$	$28.46_{0.14}$	$0.927_{0.040}$
370	$620.56_{0.38}$	$4.90_{0.19}$	$0.1411_{0.0040}$	$29.06_{0.21}$	$0.938_{0.066}$
360	$629.62_{0.19}$	$3.76_{0.19}$	$0.1063_{0.0052}$	$29.64_{0.30}$	$0.95_{0.10}$

Table S60: GCMC-MBAR results for 2,2,3-trimethylbutane with the MiPPE-SL force field. Subscripts correspond to the 95% confidence interval computed with bootstrap re-sampling.

$T^{\mathrm{sat}}(\mathbf{K})$	$ ho_{ m liq}^{ m sat}$ (kg/m ³)	$ ho_{ m vap}^{ m sat}$ (kg/m ³)	$P_{ m vap}^{ m sat}$ (MPa)	$\Delta H_{\rm v}$ (kJ/mol)	$Z_{ m vap}^{ m sat}$
520	$427.6_{2.7}$	90.4 _{3.4}	$2.310_{0.041}$	$14.20_{0.20}$	$0.592_{0.014}$
510	$451.1_{1.5}$	$73.9_{3.6}$	$2.014_{0.030}$	$16.22_{0.27}$	$0.644_{0.025}$
500	$471.00_{0.92}$	$61.5_{2.9}$	$1.748_{0.020}$	$17.84_{0.29}$	$0.684_{0.029}$
490	$488.37_{0.82}$	$51.6_{1.9}$	$1.509_{0.014}$	$19.22_{0.23}$	$0.719_{0.023}$
480	$503.84_{0.76}$	$43.39_{0.99}$	$1.295_{0.011}$	$20.44_{0.15}$	$0.749_{0.015}$
470	$518.11_{0.61}$	$36.42_{0.54}$	$1.1046_{0.0087}$	$21.544_{0.083}$	$0.78_{0.01}$
460	$531.60_{0.50}$	$30.51_{0.45}$	$0.9358_{0.0068}$	$22.566_{0.064}$	$0.80_{0.01}$
450	$544.35_{0.55}$	$25.49_{0.41}$	$0.7870_{0.0049}$	$23.512_{0.070}$	$0.83_{0.01}$
440	$556.68_{0.54}$	$21.21_{0.32}$	$0.6564_{0.0032}$	$24.402_{0.069}$	$0.85_{0.01}$
430	$568.85_{0.50}$	$17.55_{0.23}$	$0.5424_{0.0020}$	$25.255_{0.062}$	$0.87_{0.01}$
420	$580.37_{0.55}$	$14.42_{0.15}$	$0.4436_{0.0014}$	$26.050_{0.058}$	$0.88_{0.01}$
410	$590.79_{0.86}$	$11.748_{0.088}$	$0.3590_{0.0014}$	$26.769_{0.064}$	$0.90_{0.01}$
400	$600.6_{1.0}$	$9.476_{0.069}$	$0.2870_{0.0014}$	$27.440_{0.077}$	$0.91_{0.01}$
390	$610.62_{0.83}$	$7.560_{0.096}$	$0.2267_{0.0013}$	$28.107_{0.086}$	$0.927_{0.013}$
380	$621.8_{1.5}$	$5.96_{0.14}$	$0.1765_{0.0014}$	$28.82_{0.16}$	$0.940_{0.025}$
370	$633.5_{2.1}$	$4.63_{0.17}$	$0.1353_{0.0019}$	$29.56_{0.26}$	$0.952_{0.044}$
360	$643.07_{0.71}$	$3.54_{0.20}$	$0.1019_{0.0029}$	$30.16_{0.26}$	$0.963_{0.071}$

Table S61: GCMC-MBAR results for 2,2,3-trimethylpentane with the MiPPE-SL force field. Subscripts correspond to the 95% confidence interval computed with bootstrap re-sampling.

$T^{\mathrm{sat}}(\mathbf{K})$	$ ho_{ m liq}^{ m sat}$ (kg/m ³)	$ ho_{ m vap}^{ m sat}$ (kg/m ³)	P _{vap} (MPa)	ΔH_{v} (kJ/mol)	$Z_{ m vap}^{ m sat}$
550	$424.5_{1.7}$	$94.6_{5.8}$	$2.204_{0.085}$	$14.90_{0.26}$	$0.582_{0.014}$
540	$446.63_{0.90}$	$77.5_{4.4}$	$1.931_{0.070}$	$17.04_{0.27}$	$0.634_{0.015}$
530	$466.95_{0.61}$	$64.6_{2.9}$	$1.685_{0.058}$	$18.86_{0.22}$	$0.676_{0.010}$
520	$485.81_{0.76}$	$54.4_{1.9}$	$1.463_{0.050}$	$20.45_{0.13}$	$0.71_{0.01}$
510	$502.62_{0.63}$	$45.9_{1.6}$	$1.263_{0.044}$	$21.840_{0.082}$	$0.74_{0.01}$
500	$517.03_{0.59}$	$38.7_{1.7}$	$1.084_{0.037}$	$23.05_{0.11}$	$0.77_{0.01}$
490	$529.98_{0.76}$	$32.6_{1.9}$	$0.925_{0.029}$	$24.14_{0.18}$	$0.795_{0.024}$
480	$542.7_{1.0}$	$27.4_{1.8}$	$0.784_{0.021}$	$25.18_{0.25}$	$0.818_{0.037}$
470	$555.2_{1.2}$	$23.0_{1.6}$	$0.659_{0.013}$	$26.17_{0.29}$	$0.840_{0.045}$
460	$566.7_{1.3}$	$19.1_{1.2}$	$0.5500_{0.0068}$	$27.09_{0.30}$	$0.860_{0.047}$
450	$577.6_{1.2}$	$15.82_{0.81}$	$0.4550_{0.0027}$	$27.94_{0.29}$	$0.878_{0.045}$
440	$588.5_{3.8}$	$13.0_{1.5}$	$0.4_{1.3}$	$28.8_{7.3}$	$0.9_{2.0}$
430	$599.6_{2.4}$	$10.61_{0.31}$	$0.3023_{0.0035}$	$29.58_{0.30}$	$0.910_{0.038}$
420	$610.1_{2.1}$	$8.58_{0.19}$	$0.2423_{0.0044}$	$30.34_{0.26}$	$0.923_{0.036}$
410	$619.5_{1.4}$	$6.88_{0.12}$	$0.1918_{0.0049}$	$31.02_{0.22}$	$0.935_{0.038}$
400	$628.4_{1.5}$	$5.447_{0.098}$	$0.1498_{0.0051}$	$31.66_{0.24}$	$0.945_{0.044}$
380	$645.33_{0.68}$	$3.285_{0.097}$	$0.0874_{0.0051}$	$32.86_{0.25}$	$0.961_{0.067}$

Table S62: GCMC-MBAR results for 2,2,4-trimethylpentane with the MiPPE-SL force field. Subscripts correspond to the 95% confidence interval computed with bootstrap re-sampling.

$T^{\mathrm{sat}}(\mathbf{K})$	$ ho_{ m liq}^{ m sat}$ (kg/m ³)	$ ho_{ m vap}^{ m sat}$ (kg/m ³)	$P_{\mathrm{vap}}^{\mathrm{sat}}$ (MPa)	$\Delta H_{\rm v}$ (kJ/mol)	$Z_{ m vap}^{ m sat}$
530	$400.9_{2.2}$	$97.9_{4.8}$	$2.120_{0.038}$	$13.58_{0.32}$	$0.561_{0.019}$
520	$427.5_{1.3}$	$79.4_{3.2}$	$1.844_{0.028}$	$15.89_{0.27}$	$0.614_{0.018}$
510	$448.78_{0.77}$	$65.1_{1.8}$	$1.597_{0.021}$	$17.79_{0.18}$	$0.661_{0.012}$
500	$466.83_{0.75}$	$53.9_{1.1}$	$1.378_{0.018}$	$19.40_{0.13}$	$0.70_{0.01}$
490	$483.78_{0.81}$	$44.87_{0.89}$	$1.182_{0.015}$	$20.85_{0.12}$	$0.74_{0.01}$
480	$499.84_{0.70}$	$37.41_{0.89}$	$1.009_{0.012}$	$22.18_{0.12}$	$0.772_{0.012}$
470	$514.41_{0.57}$	$31.21_{0.86}$	$0.8545_{0.0083}$	$23.38_{0.13}$	$0.800_{0.016}$
460	$527.62_{0.53}$	$26.00_{0.75}$	$0.7187_{0.0053}$	$24.45_{0.13}$	$0.826_{0.020}$
450	$539.75_{0.68}$	$21.58_{0.59}$	$0.5995_{0.0030}$	$25.42_{0.12}$	$0.848_{0.022}$
440	$551.12_{0.66}$	$17.82_{0.43}$	$0.4958_{0.0022}$	$26.32_{0.12}$	$0.869_{0.022}$
430	$562.67_{0.50}$	$14.62_{0.31}$	$0.4062_{0.0027}$	$27.21_{0.13}$	$0.888_{0.023}$
420	$574.59_{0.49}$	$11.89_{0.25}$	$0.3292_{0.0035}$	$28.09_{0.13}$	$0.906_{0.027}$
410	$585.04_{0.41}$	$9.58_{0.25}$	$0.2637_{0.0042}$	$28.86_{0.15}$	$0.922_{0.037}$
400	$594.23_{0.30}$	$7.66_{0.27}$	$0.2087_{0.0051}$	$29.54_{0.20}$	$0.936_{0.055}$
390	$604.33_{0.26}$	$6.05_{0.29}$	$0.1630_{0.0063}$	$30.26_{0.28}$	$0.949_{0.082}$
380	$615.43_{0.23}$	$4.72_{0.30}$	$0.1252_{0.0077}$	$31.01_{0.41}$	$0.96_{0.12}$
370	$625.27_{0.23}$	$3.63_{0.29}$	$0.0946_{0.0092}$	$31.68_{0.58}$	$0.97_{0.18}$

Table S63: GCMC-MBAR results for 2,3,3-trimethylpentane with the MiPPE-SL force field. Subscripts correspond to the 95% confidence interval computed with bootstrap re-sampling.

$T^{\mathrm{sat}}(\mathbf{K})$	$ ho_{ m liq}^{ m sat}$ (kg/m ³)	$ ho_{ m vap}^{ m sat}$ (kg/m ³)	$P_{\mathrm{vap}}^{\mathrm{sat}}$ (MPa)	$\Delta H_{\rm v}$ (kJ/mol)	$Z_{ m vap}^{ m sat}$
560	$426.5_{9.5}$	$98.7_{1.6}$	$2.304_{0.024}$	$14.76_{0.51}$	$0.57_{0.01}$
550	$452.4_{5.9}$	$80.7_{1.4}$	$2.023_{0.020}$	$17.10_{0.29}$	$0.63_{0.01}$
540	$473.3_{2.0}$	$67.2_{1.1}$	$1.769_{0.018}$	$18.98_{0.12}$	$0.67_{0.01}$
530	$490.60_{0.59}$	$56.53_{0.74}$	$1.540_{0.016}$	$20.523_{0.065}$	$0.71_{0.01}$
520	$505.89_{0.92}$	$47.80_{0.63}$	$1.335_{0.014}$	$21.863_{0.043}$	$0.74_{0.01}$
510	$520.2_{1.1}$	$40.46_{0.65}$	$1.151_{0.012}$	$23.086_{0.038}$	$0.77_{0.01}$
500	$534.1_{1.0}$	$34.21_{0.66}$	$0.9866_{0.0088}$	$24.232_{0.057}$	$0.79_{0.01}$
490	$546.97_{0.93}$	$28.87_{0.60}$	$0.8402_{0.0063}$	$25.283_{0.071}$	$0.816_{0.012}$
480	$558.82_{0.80}$	$24.29_{0.47}$	$0.7108_{0.0044}$	$26.241_{0.071}$	$0.837_{0.013}$
470	$570.25_{0.87}$	$20.36_{0.30}$	$0.5967_{0.0036}$	$27.143_{0.070}$	$0.857_{0.013}$
460	$581.5_{1.1}$	$16.96_{0.17}$	$0.4969_{0.0037}$	$28.007_{0.066}$	$0.875_{0.013}$
450	$592.0_{1.0}$	$14.04_{0.13}$	$0.4101_{0.0041}$	$28.816_{0.071}$	$0.892_{0.016}$
440	$602.0_{1.1}$	$11.53_{0.15}$	$0.3353_{0.0046}$	$29.578_{0.085}$	$0.908_{0.022}$
430	$612.3_{1.6}$	$9.39_{0.16}$	$0.2714_{0.0052}$	$30.34_{0.10}$	$0.924_{0.031}$
420	$622.8_{1.6}$	$7.58_{0.16}$	$0.2171_{0.0058}$	$31.10_{0.13}$	$0.937_{0.042}$
410	$632.87_{0.75}$	$6.05_{0.16}$	$0.1716_{0.0064}$	$31.82_{0.20}$	$0.950_{0.057}$
400	$642.39_{0.29}$	$4.78_{0.17}$	$0.1338_{0.0070}$	$32.50_{0.28}$	$0.961_{0.077}$
390	$651.59_{0.31}$	$3.73_{0.18}$	$0.1028_{0.0075}$	$33.14_{0.37}$	$0.97_{0.11}$

S8.2 Alkynes

Table S64: GCMC-MBAR results for ethyne with the MiPPE force field. Subscripts correspond to the 95% confidence interval computed with bootstrap re-sampling.

$T^{\mathrm{sat}}(\mathbf{K})$	$ ho_{ m liq}^{ m sat}$ (kg/m ³)	$ ho_{ m vap}^{ m sat}$ (kg/m ³)	$P_{ m vap}^{ m sat}$ (MPa)	$\Delta H_{\rm v}$ (kJ/mol)	$Z_{ m vap}^{ m sat}$
290	$421.3_{3.5}$	$69.7_{3.3}$	$4.083_{0.020}$	$8.80_{0.21}$	$0.632_{0.033}$
280	$450.7_{1.9}$	$50.69_{0.91}$	$3.196_{0.026}$	$10.27_{0.12}$	$0.705_{0.017}$
270	$474.9_{3.0}$	$37.66_{0.39}$	$2.465_{0.024}$	$11.390_{0.086}$	$0.76_{0.01}$
260	$497.3_{1.1}$	$27.95_{0.53}$	$1.865_{0.017}$	$12.361_{0.034}$	$0.804_{0.011}$
250	$517.91_{0.59}$	$20.53_{0.34}$	$1.378_{0.012}$	$13.214_{0.042}$	$0.841_{0.013}$
240	$536.87_{0.67}$	$14.82_{0.12}$	$0.992_{0.010}$	$13.975_{0.028}$	$0.87_{0.01}$
230	$554.12_{0.54}$	$10.447_{0.095}$	$0.6925_{0.0089}$	$14.649_{0.037}$	$0.903_{0.012}$
220	$570.90_{0.53}$	$7.155_{0.097}$	$0.4667_{0.0082}$	$15.283_{0.049}$	$0.929_{0.021}$

Table S65: GCMC-MBAR results for propyne with the MiPPE force field. Subscripts correspond to the 95% confidence interval computed with bootstrap re-sampling.

$T^{\mathrm{sat}}(\mathbf{K})$	$ ho_{ m liq}^{ m sat}$ (kg/m 3)	$ ho_{ m vap}^{ m sat}$ (kg/m ³)	$P_{\mathrm{vap}}^{\mathrm{sat}}$ (MPa)	$\Delta H_{\rm v}$ (kJ/mol)	$Z_{ m vap}^{ m sat}$
380	$441.0_{7.9}$	$82.2_{3.1}$	$3.839_{0.090}$	$10.96_{0.34}$	$0.59_{0.01}$
370	$472.7_{5.0}$	$62.7_{2.7}$	$3.164_{0.073}$	$12.83_{0.31}$	$0.657_{0.015}$
360	$498.3_{2.8}$	$48.6_{1.9}$	$2.584_{0.057}$	$14.34_{0.24}$	$0.711_{0.015}$
350	$520.1_{2.4}$	$38.1_{1.3}$	$2.088_{0.045}$	$15.58_{0.19}$	$0.754_{0.011}$
340	$539.4_{2.1}$	$29.88_{0.90}$	$1.667_{0.035}$	$16.65_{0.15}$	$0.79_{0.01}$
330	$556.6_{1.4}$	$23.31_{0.72}$	$1.313_{0.027}$	$17.58_{0.11}$	$0.822_{0.010}$
320	$572.1_{1.3}$	$18.02_{0.60}$	$1.018_{0.019}$	$18.41_{0.11}$	$0.850_{0.014}$
310	$587.6_{1.3}$	$13.76_{0.47}$	$0.776_{0.012}$	$19.20_{0.12}$	$0.876_{0.017}$
300	$603.3_{1.5}$	$10.35_{0.32}$	$0.5799_{0.0068}$	$19.97_{0.13}$	$0.900_{0.019}$
290	$617.9_{2.2}$	$7.65_{0.20}$	$0.4240_{0.0040}$	$20.67_{0.15}$	$0.921_{0.020}$

Table S66: GCMC-MBAR results for 1-butyne with the MiPPE force field. Subscripts correspond to the 95% confidence interval computed with bootstrap re-sampling.

$T^{\mathrm{sat}}\left(\mathbf{K}\right)$	$ ho_{ m liq}^{ m sat}$ (kg/m ³)	$ ho_{ m vap}^{ m sat}$ (kg/m ³)	$P_{\mathrm{vap}}^{\mathrm{sat}}$ (MPa)	$\Delta H_{\rm v}$ (kJ/mol)	$Z_{ m vap}^{ m sat}$
410	$445.1_{5.3}$	76_{12}	$2.95_{0.10}$	$12.82_{0.72}$	$0.620_{0.056}$
400	$472.3_{3.4}$	$59.2_{6.8}$	$2.464_{0.050}$	$14.61_{0.60}$	$0.677_{0.054}$
390	$495.0_{2.6}$	$47.1_{2.3}$	$2.038_{0.030}$	$16.08_{0.32}$	$0.722_{0.027}$
380	$515.5_{2.0}$	$37.54_{0.86}$	$1.669_{0.023}$	$17.37_{0.16}$	$0.76_{0.01}$
370	$534.5_{1.3}$	$29.90_{0.70}$	$1.351_{0.018}$	$18.53_{0.13}$	$0.79_{0.01}$
360	$552.0_{1.6}$	$23.69_{0.62}$	$1.081_{0.013}$	$19.57_{0.16}$	$0.824_{0.013}$
350	$567.8_{1.9}$	$18.62_{0.51}$	$0.8524_{0.0086}$	$20.50_{0.18}$	$0.851_{0.017}$
340	$582.2_{1.1}$	$14.49_{0.38}$	$0.6623_{0.0060}$	$21.34_{0.13}$	$0.874_{0.019}$
330	$595.8_{1.1}$	$11.15_{0.24}$	$0.5061_{0.0049}$	$22.112_{0.082}$	$0.895_{0.019}$
320	$610.6_{2.8}$	$8.45_{0.14}$	$0.3795_{0.0049}$	$22.905_{0.095}$	$0.913_{0.019}$
310	$624.6_{1.8}$	$6.284_{0.087}$	$0.2782_{0.0051}$	$23.650_{0.059}$	$0.929_{0.022}$

Table S67: GCMC-MBAR results for 2-butyne with the MiPPE force field. Subscripts correspond to the 95% confidence interval computed with bootstrap re-sampling.

T ^{sat} (K)	$ ho_{ m liq}^{ m sat}$ (kg/m ³)	$ ho_{ m vap}^{ m sat}$ (kg/m ³)	$P_{\mathrm{vap}}^{\mathrm{sat}}$ (MPa)	$\Delta H_{\rm v}$ (kJ/mol)	$Z_{ m vap}^{ m sat}$
450	$431.8_{7.4}$	$93.5_{4.3}$	$3.624_{0.050}$	$11.93_{0.26}$	$0.561_{0.018}$
440	$466.0_{5.5}$	$74.1_{3.5}$	$3.073_{0.028}$	$14.00_{0.24}$	$0.613_{0.024}$
430	$491.6_{2.0}$	$59.1_{1.9}$	$2.587_{0.016}$	$15.71_{0.17}$	$0.662_{0.020}$
420	$512.10_{0.77}$	$47.58_{0.69}$	$2.163_{0.014}$	$17.114_{0.094}$	$0.704_{0.010}$
410	$530.5_{1.1}$	$38.42_{0.30}$	$1.795_{0.013}$	$18.346_{0.054}$	$0.74_{0.01}$
400	$548.28_{0.94}$	$30.99_{0.31}$	$1.476_{0.011}$	$19.487_{0.051}$	$0.77_{0.01}$
390	$565.05_{0.94}$	$24.89_{0.27}$	$1.2013_{0.0089}$	$20.533_{0.061}$	$0.81_{0.01}$
380	$580.6_{1.1}$	$19.89_{0.25}$	$0.9674_{0.0068}$	$21.483_{0.073}$	$0.83_{0.01}$
370	$594.97_{0.83}$	$15.78_{0.25}$	$0.7697_{0.0050}$	$22.349_{0.074}$	$0.858_{0.011}$
360	$608.65_{0.59}$	$12.41_{0.22}$	$0.6041_{0.0038}$	$23.157_{0.070}$	$0.880_{0.017}$
350	$621.69_{0.66}$	$9.66_{0.19}$	$0.4672_{0.0041}$	$23.912_{0.091}$	$0.899_{0.024}$
340	$633.85_{0.59}$	$7.42_{0.16}$	$0.3552_{0.0052}$	$24.60_{0.12}$	$0.916_{0.033}$
330	$646.13_{0.73}$	$5.62_{0.13}$	$0.2651_{0.0064}$	$25.26_{0.16}$	$0.930_{0.044}$

Table S68: GCMC-MBAR results for 1-pentyne with the MiPPE force field. Subscripts correspond to the 95% confidence interval computed with bootstrap re-sampling.

$T^{\mathrm{sat}}(\mathbf{K})$	$ ho_{ m liq}^{ m sat}$ (kg/m ³)	$ ho_{ m vap}^{ m sat}$ (kg/m ³)	$P_{\mathrm{vap}}^{\mathrm{sat}}$ (MPa)	$\Delta H_{\rm v}$ (kJ/mol)	$Z_{ m vap}^{ m sat}$
450	$433.7_{2.3}$	$85.6_{2.5}$	$2.732_{0.022}$	$13.15_{0.18}$	$0.581_{0.014}$
440	$461.7_{1.7}$	$66.9_{2.0}$	$2.304_{0.015}$	$15.29_{0.18}$	$0.641_{0.018}$
430	$485.2_{1.5}$	$53.1_{1.2}$	$1.932_{0.012}$	$17.06_{0.16}$	$0.693_{0.016}$
420	$505.4_{1.6}$	$42.65_{0.51}$	$1.608_{0.012}$	$18.54_{0.11}$	$0.735_{0.011}$
410	$523.3_{1.4}$	$34.37_{0.30}$	$1.327_{0.010}$	$19.810_{0.078}$	$0.77_{0.01}$
400	$539.7_{1.2}$	$27.67_{0.31}$	$1.0844_{0.0077}$	$20.949_{0.055}$	$0.80_{0.01}$
390	$555.3_{1.1}$	$22.17_{0.30}$	$0.8770_{0.0052}$	$21.998_{0.041}$	$0.83_{0.01}$
380	$570.2_{1.0}$	$17.64_{0.27}$	$0.7009_{0.0033}$	$22.977_{0.033}$	$0.857_{0.012}$
370	$584.03_{0.90}$	$13.91_{0.25}$	$0.5528_{0.0028}$	$23.874_{0.050}$	$0.880_{0.018}$
360	$596.86_{0.83}$	$10.86_{0.22}$	$0.4300_{0.0040}$	$24.697_{0.083}$	$0.901_{0.026}$
350	$609.71_{0.69}$	$8.37_{0.19}$	$0.3291_{0.0055}$	$25.49_{0.11}$	$0.920_{0.037}$
340	$622.58_{0.99}$	$6.37_{0.15}$	$0.2474_{0.0070}$	$26.27_{0.13}$	$0.936_{0.050}$

Table S69: GCMC-MBAR results for 2-pentyne with the MiPPE force field. Subscripts correspond to the 95% confidence interval computed with bootstrap re-sampling.

T ^{sat} (K)	$ ho_{ m liq}^{ m sat}$ (kg/m ³)	$ ho_{ m vap}^{ m sat}$ (kg/m ³)	$P_{ m vap}^{ m sat}$ (MPa)	$\Delta H_{\rm v}$ (kJ/mol)	$Z_{ m vap}^{ m sat}$
470	$445.8_{3.1}$	$83.4_{6.2}$	$2.77_{0.12}$	$14.09_{0.22}$	$0.578_{0.020}$
460	$473.8_{1.9}$	$65.6_{5.4}$	$2.343_{0.088}$	$16.27_{0.30}$	$0.636_{0.028}$
450	$496.8_{1.0}$	$52.5_{3.7}$	$1.973_{0.064}$	$18.06_{0.28}$	$0.685_{0.026}$
440	$516.64_{0.73}$	$42.4_{2.3}$	$1.650_{0.048}$	$19.56_{0.22}$	$0.725_{0.020}$
430	$534.83_{0.74}$	$34.3_{1.7}$	$1.369_{0.036}$	$20.89_{0.19}$	$0.761_{0.017}$
420	$551.57_{0.81}$	$27.7_{1.4}$	$1.126_{0.025}$	$22.08_{0.19}$	$0.792_{0.022}$
410	$566.89_{0.86}$	$22.3_{1.2}$	$0.917_{0.016}$	$23.16_{0.22}$	$0.821_{0.030}$
400	$581.3_{1.1}$	$17.9_{1.0}$	$0.7394_{0.0080}$	$24.15_{0.26}$	$0.847_{0.038}$
390	$595.3_{1.6}$	$14.24_{0.71}$	$0.5890_{0.0039}$	$25.09_{0.28}$	$0.869_{0.040}$
380	$608.6_{1.7}$	$11.23_{0.40}$	$0.4631_{0.0052}$	$25.95_{0.25}$	$0.889_{0.038}$
370	$621.0_{1.3}$	$8.76_{0.19}$	$0.3587_{0.0066}$	$26.75_{0.19}$	$0.907_{0.032}$
360	$632.99_{0.96}$	$6.75_{0.16}$	$0.2735_{0.0069}$	$27.52_{0.12}$	$0.922_{0.031}$
350	644.7 _{1.0}	$5.12_{0.20}$	$0.2049_{0.0065}$	$28.249_{0.10}$	$0.937_{0.044}$

Table S70: GCMC-MBAR results for 1-hexyne with the MiPPE force field. Subscripts correspond to the 95% confidence interval computed with bootstrap re-sampling.

$T^{\mathrm{sat}}(\mathbf{K})$	$ ho_{ m liq}^{ m sat}$ (kg/m ³)	$ ho_{ m vap}^{ m sat}$ (kg/m ³)	$P_{ m vap}^{ m sat}$ (MPa)	$\Delta H_{\rm v}$ (kJ/mol)	$Z_{ m vap}^{ m sat}$
490	$423.3_{3.5}$	$87.3_{2.1}$	$2.538_{0.068}$	$14.25_{0.14}$	$0.586_{0.010}$
480	$453.3_{2.0}$	$69.9_{1.5}$	$2.170_{0.060}$	$16.54_{0.12}$	$0.639_{0.015}$
470	$477.4_{1.3}$	$56.51_{0.96}$	$1.844_{0.056}$	$18.448_{0.089}$	$0.686_{0.016}$
460	$497.3_{1.4}$	$46.06_{0.95}$	$1.556_{0.051}$	$20.041_{0.074}$	$0.726_{0.011}$
450	$514.8_{1.3}$	$37.6_{1.3}$	$1.304_{0.044}$	$21.428_{0.10}$	$0.76_{0.01}$
440	$531.5_{1.2}$	$30.7_{1.7}$	$1.084_{0.035}$	$22.71_{0.16}$	$0.792_{0.017}$
430	$547.4_{1.2}$	$25.0_{1.7}$	$0.893_{0.024}$	$23.91_{0.22}$	$0.820_{0.032}$
420	$561.77_{0.87}$	$20.3_{1.5}$	$0.728_{0.013}$	$24.98_{0.23}$	$0.845_{0.042}$
410	$575.17_{0.62}$	$16.34_{0.99}$	$0.5875_{0.0050}$	$25.97_{0.20}$	$0.867_{0.043}$
400	$588.08_{0.75}$	$13.04_{0.55}$	$0.4682_{0.0027}$	$26.90_{0.15}$	$0.887_{0.038}$
390	$599.80_{0.63}$	$10.31_{0.28}$	$0.3684_{0.0047}$	$27.75_{0.11}$	$0.905_{0.033}$
380	$610.32_{0.79}$	$8.06_{0.17}$	$0.2858_{0.0061}$	$28.507_{0.080}$	$0.922_{0.036}$
370	$621.3_{2.9}$	$6.23_{0.13}$	$0.2185_{0.0072}$	$29.267_{0.086}$	$0.937_{0.048}$
360	$634.3_{3.1}$	$4.74_{0.11}$	$0.1640_{0.0083}$	$30.118_{0.078}$	$0.950_{0.067}$

Table S71: GCMC-MBAR results for 2-hexyne with the MiPPE force field. Subscripts correspond to the 95% confidence interval computed with bootstrap re-sampling.

T ^{sat} (K)	$ ho_{ m liq}^{ m sat}$ (kg/m ³)	$ ho_{ m vap}^{ m sat}$ (kg/m ³)	$P_{ m vap}^{ m sat}$ (MPa)	$\Delta H_{\rm v}$ (kJ/mol)	$Z_{ m vap}^{ m sat}$
500	$438.2_{2.9}$	$85.9_{4.0}$	$2.495_{0.026}$	$14.93_{0.36}$	$0.574_{0.024}$
490	$464.9_{1.8}$	$67.7_{2.5}$	$2.131_{0.016}$	$17.31_{0.29}$	$0.635_{0.021}$
480	$486.7_{1.5}$	$54.7_{1.3}$	$1.811_{0.011}$	$19.18_{0.19}$	$0.682_{0.016}$
470	$505.2_{1.7}$	$44.67_{0.74}$	$1.5302_{0.0087}$	$20.71_{0.14}$	$0.720_{0.012}$
460	$522.5_{2.3}$	$36.61_{0.52}$	$1.2839_{0.0074}$	$22.09_{0.14}$	$0.753_{0.011}$
450	$539.3_{2.5}$	$29.96_{0.40}$	$1.0686_{0.0062}$	$23.39_{0.15}$	$0.783_{0.010}$
440	$555.2_{1.8}$	$24.43_{0.31}$	$0.8815_{0.0050}$	$24.60_{0.11}$	$0.81_{0.01}$
430	$569.62_{0.68}$	$19.82_{0.28}$	$0.7201_{0.0040}$	$25.678_{0.066}$	$0.835_{0.010}$
420	$583.3_{1.4}$	$15.98_{0.26}$	$0.5821_{0.0034}$	$26.69_{0.11}$	$0.857_{0.014}$
410	$597.0_{1.4}$	$12.77_{0.22}$	$0.4651_{0.0035}$	$27.67_{0.12}$	$0.877_{0.017}$
400	$609.9_{1.1}$	$10.11_{0.16}$	$0.3669_{0.0039}$	$28.59_{0.11}$	$0.896_{0.020}$
390	$621.7_{1.4}$	$7.92_{0.14}$	$0.2857_{0.0045}$	$29.42_{0.14}$	$0.914_{0.026}$
380	$633.2_{1.2}$	$6.12_{0.16}$	$0.2190_{0.0050}$	$30.23_{0.16}$	$0.930_{0.040}$
370	$644.01_{0.40}$	$4.67_{0.18}$	$0.1653_{0.0059}$	$30.98_{0.19}$	$0.944_{0.063}$

Table S72: GCMC-MBAR results for 1-heptyne with the MiPPE force field. Subscripts correspond to the 95% confidence interval computed with bootstrap re-sampling.

T ^{sat} (K)	$ ho_{ m liq}^{ m sat}$ (kg/m ³)	$ ho_{ m vap}^{ m sat}$ (kg/m ³)	$P_{\mathrm{vap}}^{\mathrm{sat}}$ (MPa)	$\Delta H_{\rm v}$ (kJ/mol)	$Z_{ m vap}^{ m sat}$
520	$427.5_{6.0}$	$82.9_{6.4}$	$2.218_{0.071}$	$16.05_{0.64}$	$0.595_{0.026}$
510	$454.3_{2.5}$	$66.9_{4.8}$	$1.906_{0.055}$	$18.37_{0.49}$	$0.646_{0.027}$
500	$476.5_{1.4}$	$54.5_{3.3}$	$1.629_{0.041}$	$20.34_{0.35}$	$0.691_{0.024}$
490	$495.7_{1.4}$	$44.8_{2.4}$	$1.384_{0.030}$	$22.02_{0.25}$	$0.730_{0.023}$
480	$512.9_{1.6}$	$36.9_{1.8}$	$1.168_{0.020}$	$23.51_{0.18}$	$0.764_{0.024}$
470	$528.7_{2.0}$	$30.3_{1.4}$	$0.979_{0.012}$	$24.85_{0.13}$	$0.794_{0.026}$
460	$543.2_{1.9}$	$24.91_{0.95}$	$0.8138_{0.0072}$	$26.066_{0.092}$	$0.821_{0.027}$
450	$556.9_{1.5}$	$20.37_{0.57}$	$0.6705_{0.0058}$	$27.199_{0.070}$	$0.846_{0.025}$
440	$570.2_{1.0}$	$16.57_{0.25}$	$0.5472_{0.0063}$	$28.279_{0.062}$	$0.868_{0.019}$
430	$583.08_{0.58}$	$13.38_{0.11}$	$0.4419_{0.0062}$	$29.301_{0.062}$	$0.888_{0.012}$
420	$595.19_{0.32}$	$10.71_{0.23}$	$0.3526_{0.0055}$	$30.253_{0.097}$	$0.907_{0.017}$
410	$606.63_{0.36}$	$8.50_{0.30}$	$0.2779_{0.0046}$	$31.14_{0.16}$	$0.923_{0.035}$
400	$617.58_{0.39}$	$6.66_{0.33}$	$0.2160_{0.0048}$	$31.98_{0.23}$	$0.938_{0.058}$
390	$628.63_{0.36}$	$5.16_{0.31}$	$0.1654_{0.0061}$	$32.81_{0.31}$	$0.950_{0.088}$

Table S73: GCMC-MBAR results for 1-octyne with the MiPPE force field. Subscripts correspond to the 95% confidence interval computed with bootstrap re-sampling.

T ^{sat} (K)	$ ho_{ m liq}^{ m sat}$ (kg/m ³)	$ ho_{ m vap}^{ m sat}$ (kg/m ³)	$P_{\mathrm{vap}}^{\mathrm{sat}}$ (MPa)	$\Delta H_{\rm v}$ (kJ/mol)	$Z_{ m vap}^{ m sat}$
550	$419.4_{3.6}$	$89.5_{1.2}$	$2.075_{0.015}$	$16.27_{0.24}$	$0.56_{0.01}$
540	$445.2_{3.0}$	$70.95_{0.88}$	$1.788_{0.015}$	$18.98_{0.20}$	$0.62_{0.01}$
530	$467.6_{2.6}$	$57.19_{0.55}$	$1.535_{0.015}$	$21.30_{0.17}$	$0.67_{0.01}$
520	$487.1_{2.4}$	$46.85_{0.42}$	$1.311_{0.014}$	$23.22_{0.15}$	$0.71_{0.01}$
510	$504.3_{2.0}$	$38.69_{0.48}$	$1.114_{0.012}$	$24.87_{0.13}$	$0.75_{0.01}$
500	$519.8_{1.5}$	$32.01_{0.56}$	$0.9395_{0.0099}$	$26.33_{0.12}$	$0.78_{0.01}$
490	$534.3_{1.2}$	$26.45_{0.57}$	$0.7869_{0.0075}$	$27.66_{0.13}$	$0.805_{0.010}$
480	$548.2_{1.2}$	$21.77_{0.52}$	$0.6539_{0.0053}$	$28.92_{0.15}$	$0.829_{0.014}$
470	$561.6_{1.2}$	$17.83_{0.40}$	$0.5385_{0.0038}$	$30.10_{0.15}$	$0.852_{0.016}$
460	$574.15_{0.95}$	$14.52_{0.26}$	$0.4392_{0.0033}$	$31.21_{0.13}$	$0.872_{0.016}$
450	$586.02_{0.57}$	$11.73_{0.12}$	$0.3546_{0.0033}$	$32.245_{0.084}$	$0.890_{0.012}$
440	$597.51_{0.35}$	$9.404_{0.077}$	$0.2830_{0.0032}$	$33.229_{0.046}$	$0.91_{0.01}$
430	$608.64_{0.40}$	$7.46_{0.15}$	$0.2231_{0.0029}$	$34.171_{0.089}$	$0.921_{0.019}$
420	$619.31_{0.42}$	$5.86_{0.20}$	$0.1736_{0.0027}$	$35.06_{0.16}$	$0.935_{0.039}$
410	$630.00_{0.38}$	$4.55_{0.22}$	$0.1330_{0.0032}$	$35.94_{0.24}$	$0.946_{0.067}$

Table S74: GCMC-MBAR results for 1-nonyne with the MiPPE force field. Subscripts correspond to the 95% confidence interval computed with bootstrap re-sampling.

$T^{\mathrm{sat}}(\mathbf{K})$	$ ho_{ m liq}^{ m sat}$ (kg/m ³)	$ ho_{ m vap}^{ m sat}$ (kg/m ³)	$P_{ m vap}^{ m sat}$ (MPa)	$\Delta H_{\rm v}$ (kJ/mol)	$Z_{ m vap}^{ m sat}$
570	427.1 _{1.2}	$80.5_{1.0}$	$1.776_{0.015}$	18.58 _{0.17}	$0.58_{0.01}$
560	$450.9_{1.3}$	$64.43_{0.86}$	$1.531_{0.013}$	$21.28_{0.20}$	$0.63_{0.01}$
550	$471.7_{1.6}$	$52.31_{0.73}$	$1.315_{0.010}$	$23.58_{0.20}$	$0.68_{0.01}$
540	$489.9_{1.5}$	$43.02_{0.62}$	$1.1239_{0.0080}$	$25.52_{0.17}$	$0.72_{0.01}$
530	$506.3_{1.1}$	$35.61_{0.52}$	$0.9552_{0.0059}$	$27.21_{0.13}$	$0.76_{0.01}$
520	$521.47_{0.66}$	$29.51_{0.42}$	$0.8067_{0.0041}$	$28.739_{0.093}$	$0.79_{0.01}$
510	$535.75_{0.67}$	$24.42_{0.33}$	$0.6762_{0.0026}$	$30.149_{0.083}$	$0.81_{0.01}$
500	$549.10_{0.85}$	$20.14_{0.26}$	$0.5626_{0.0015}$	$31.452_{0.094}$	$0.83_{0.01}$
490	$561.65_{0.81}$	$16.54_{0.20}$	$0.46410_{0.00097}$	$32.666_{0.094}$	$0.856_{0.010}$
480	$573.68_{0.62}$	$13.50_{0.15}$	$0.3792_{0.0010}$	$33.811_{0.080}$	$0.875_{0.011}$
470	$585.26_{0.49}$	$10.94_{0.11}$	$0.3068_{0.0014}$	$34.896_{0.067}$	$0.892_{0.012}$
460	$596.35_{0.58}$	$8.794_{0.096}$	$0.2455_{0.0017}$	$35.924_{0.069}$	$0.907_{0.015}$
450	$607.27_{0.71}$	$7.003_{0.091}$	$0.1942_{0.0020}$	$36.924_{0.081}$	$0.921_{0.019}$
440	$618.21_{0.61}$	$5.516_{0.091}$	$0.1516_{0.0023}$	$37.91_{0.10}$	$0.933_{0.027}$
430	$628.74_{0.51}$	$4.292_{0.090}$	$0.1166_{0.0026}$	$38.85_{0.14}$	$0.944_{0.037}$
420	$638.50_{0.50}$	$3.296_{0.086}$	$0.0885_{0.0030}$	$39.72_{0.18}$	$0.955_{0.052}$

S9 Simulation state points

S9.1 Cyclohexane

Table S75: State points simulated for cyclohexane with the MiPPE force field (second iteration, $\theta^{(2)}$ $\lambda_{\rm CH_2}=16$).

T(K)	μ (K)	L (nm)
450	-4370	3.0
500	-4370	3.0
550	-4370	3.0
500	-4135	3.0
460	-4025	3.0
410	-3890	3.0
360	-3790	3.0

Table S76: State points simulated for cyclohexane with the TraPPE force field (zeroth iteration, $\theta^{(0)}$).

T (K)	μ (K)	L (nm)
450	-4350	3.0
500	-4350	3.0
550	-4350	3.0
500	-4120	3.0
460	-3977	3.0
410	-3790	3.0
350	-3562	3.0

Table S77: State points simulated for cyclohexane with the first iteration $(\theta^{(1)})$ $\lambda_{\rm CH_2}=14$ force field.

T(K)	μ (K)	L (nm)
450	-4389	3.0
500	-4389	3.0
550	-4389	3.0
500	-4164	3.0
460	-4033	3.0
410	-3891	3.0
360	-3780	3.0

Table S78: State points simulated for cyclohexane with the first iteration $(\theta^{(1)})$ $\lambda_{\rm CH_2}=16$ force field.

T (K)	μ (K)	L (nm)
450	-4367	3.0
500	-4367	3.0
550	-4367	3.0
500	-4149	3.0
460	-4024	3.0
410	-3893	3.0
360	-3792	3.0

Table S79: State points simulated for cyclohexane with the first iteration $(\theta^{(1)})$ $\lambda_{\rm CH_2}=18$ force field.

T	'(K)	μ (K)	L (nm)
4	450	-4370	3.0
1	500	-4370	3.0
[550	-4370	3.0
1	500	-4158	3.0
4	460	-4037	3.0
4	410	-3912	3.0
	360	-3825	3.0

Table S80: State points simulated for cyclohexane with the first iteration $(\theta^{\langle 1 \rangle}) \lambda_{\rm CH_2} = 20$ force field.

T (K)	μ (K)	L (nm)
450	-4386	3.0
500	-4386	3.0
550	-4386	3.0
500	-4178	3.0
460	-4062	3.0
410	-3946	3.0
360	-3866	3.0

Table S81: State points simulated to test finite-size effects for cyclohexane with the MiPPE force field.

T (K)	μ (K)	L (nm)
450	-4370	3.5
510	-4370	3.5
550	-4370	3.5
510	-4177	3.5
470	-4048	3.5
430	-3936	3.5
400	-3865	3.5
370	-3806	3.5
350	-3774	3.5

Table S82: State points simulated to validate TAMie for cyclohexane.

T (K)	μ (K)	L (nm)
450	-4358	3.5
510	-4358	3.5
550	-4358	3.5
510	-4165	3.5
470	-4036	3.5
430	-3923	3.5
400	-3852	3.5
370	-3793	3.5
350	-3762	3.5

S9.2 Branched alkanes

Table S83: State points simulated for 2-methylpropane with the TraPPE force field.

T (K)	μ (K)	L (nm)
350	-3120	3.0
380	-3120	3.0
405	-3117	3.0
380	-2980	3.0
350	-2880	3.0
320	-2790	3.0
290	-2705	3.0
260	-2645	3.0
230	-2600	3.0
200	-2570	3.0

Table S84: State points simulated for 2,2-dimethylpropane with the TraPPE force field.

T (K)	μ (K)	L (nm)
380	-3405	3.0
410	-3405	3.0
440	-3405	3.0
410	-3250	3.0
380	-3140	3.0
350	-3037	3.0
330	-2970	3.0
300	-2900	3.0
270	-2820	3.0

Table S85: State points simulated for 2,2-dimethylbutane with the TraPPE force field.

T (K)	μ (K)	L (nm)
420	-3860	3.5
450	-3860	3.5
480	-3860	3.5
450	-3719	3.5
420	-3600	3.5
400	-3524	3.5
380	-3450	3.5
360	-3368	3.5
340	-3288	3.5
310	-3280	3.5

Table S86: State points simulated for 2,3-dimethylbutane with the TraPPE force field.

T (K)	μ (K)	L (nm)
440	-4015	3.0
470	-4015	3.0
500	-4011	3.0
470	-3845	3.0
440	-3735	3.0
410	-3635	3.0
380	-3555	3.0
350	-3480	3.0
320	-3415	3.0

Table S87: State points simulated for 3,3-dimethylhexane with the TraPPE force field.

T (K)	μ (K)	L (nm)
500	-4670	3.5
530	-4670	3.5
560	-4670	3.5
520	-4476	3.5
490	-4370	3.5
460	-4268	3.5
430	-4164	3.5
400	-4039	3.5
370	-3925	3.5

Table S88: State points simulated for 3-methyl-3-ethylpentane with the TraPPE force field.

T (K)	μ (K)	L (nm)
500	-4785	4.0
550	-4785	4.0
580	-4785	4.0
550	-4636	4.0
520	-4520	4.0
490	-4400	4.0
460	-4280	4.0
430	-4160	4.0
410	-4080	4.0
390	-3990	4.0

Table S89: State points simulated for 2,3,4-trimethylpentane with the TraPPE force field.

T(K)	μ (K)	L (nm)
480	-4740	3.5
520	-4740	3.5
565	-4735	3.5
530	-4549	3.5
500	-4436	3.5
470	-4337	3.5
440	-4241	3.5
410	-4182	3.5
380	-4090	3.5
350	-4020	3.5

Table S90: State points simulated for 2,2,4-trimethylpentane with the TraPPE force field.

T (K)	μ (K)	L (nm)
480	-4600	4.0
530	-4600	4.0
560	-4600	4.0
530	-4450	4.0
500	-4330	4.0
470	-4210	4.0
440	-4090	4.0
410	-3960	4.0
380	-3840	4.0

Table S91: State points simulated for 2-methylpropane with the MiPPE-gen force field.

T (K)	μ (K)	L (nm)
350	-3150	3.0
380	-3150	3.0
410	-3145	3.0
380	-3010	3.0
350	-2910	3.0
320	-2830	3.0
290	-2760	3.0
260	-2700	3.0
230	-2670	3.0
200	-2640	3.0

Table S92: State points simulated for 2,2-dimethylpropane with the MiPPE-gen force field.

T (K)	μ (K)	L (nm)
368	-3344	3.0
398	-3344	3.0
430	-3400	3.0
398	-3216	3.0
372	-3124	3.0
346	-3032	3.0
326	-2961	3.0
299	-2865	3.0
270	-2759	3.0

Table S93: State points simulated for 2,2-dimethylbutane with the MiPPE-gen force field.

T (K)	μ (K)	L (nm)
415	-3873	3.5
445	-3873	3.5
480	-3895	3.5
450	-3756	3.5
420	-3654	3.5
400	-3588	3.5
380	-3521	3.5
360	-3454	3.5
340	-3384	3.5
310	-3380	3.5

Table S94: State points simulated for 2,3-dimethylbutane with the MiPPE-gen force field.

T (K)	μ (K)	<i>L</i> (nm)
440	-4010	3.0
470	-4010	3.0
500	-4009	3.0
470	-3860	3.0
440	-3760	3.0
410	-3670	3.0
380	-3600	3.0
350	-3530	3.0
320	-3480	3.0

Table S95: State points simulated for 2,3,4-trimethylpentane with the MiPPE-gen force field.

T(K)	μ (K)	L (nm)
480	-4720	3.5
520	-4720	3.5
565	-4713	3.5
530	-4540	3.5
500	-4360	3.5
470	-4355	3.5
440	-4275	3.5
410	-4205	3.5
380	-4165	3.5
350	-4115	3.5

Table S96: State points simulated for 2,2,4-trimethylpentane with the MiPPE-gen force field.

T (K)	μ (K)	L (nm)
470	-4570	4.0
520	-4570	4.0
550	-4570	4.0
520	-4420	4.0
490	-4300	4.0
460	-4170	4.0
430	-4050	4.0
400	-3920	4.0
370	-3790	4.0